The Dissertation Committee for Ji Hee Song Certifies that this is the approved version of the following dissertation:

Land Use Forecasting in Regional Air Quality Modeling

Committee:

David Allen, Supervisor

Elena McDonald-Buller, Co-Supervisor

Howard Liljestrand

Richard Corsi

Zong-liang Yang

Jeffrey Siegel

Land Use Forecasting in Regional Air Quality Modeling

by

Ji Hee Song, B.S.; M.S.

Dissertation

Presented to the Faculty of the Graduate School of

The University of Texas at Austin

in Partial Fulfillment

of the Requirements

for the Degree of

Doctor of Philosophy

The University of Texas at Austin

May 2007

Dedication

To my husband Namhong Min and my parents Jaechul Song and Hyunjeong Park-Song

Acknowledgements

I would like to give my sincere gratitude to my advisor Dr. David T. Allen for his advice, guidance, and support. I am also deeply grateful for the support of my co-advisor Dr. Elena McDonald-Buller.

A special thank to Dr. Yosuke Kimura for his wonderful help, which made my work possible. I extend my gratitude to my friends at center for energy and environmental resources.

I deeply thank my parents and my younger brother for their love, encouragement, and support. Finally, a very special thank to my dearest husband for all his love, care, understanding, and encouragement.

Land Use Forecasting in Regional Air Quality Modeling

Publication No._____

Ji Hee Song, Ph.D.

The University of Texas at Austin, 2007

Supervisor: David Allen

Co-Supervisor: Elena McDonald-Buller

When estimating the impacts of air pollutant control measures on future air quality, it is typically presumed that land covers remain constant. However, changes in land cover can have an impact on air pollutant concentrations. This work develops and applies modeling methodologies for land cover and regional air quality interactions, using regions in and around central and eastern Texas as case studies. Changes in land cover considered in this work are driven by urban development and inter-annual variability in climate. Urbanization, associated with changes in biogenic emissions and air pollutant dry deposition, leads to changes in daily maximum ozone concentration, that range from -0.94 to 0.12 ppb for the Austin area. In comparison, the effects of the same urban development led to changes in anthropogenic emissions that led to changes ranging from -7.0 to -1.3 ppb in ozone concentrations for the Austin area. Inter-annual variation in climate led much larger changes in daily maximum ozone concentrations than changes due to urbanization. Changes in daily maximum ozone concentrations, due to inter-

annual variation in biogenic emissions associated with inter-annual variability in climate, ranged from -5.9 to 9.7 ppb for the Austin area and 0.0 to 18 ppb for the Houston area.

Table of Contents

List of Tables

List of Figures

Chapter 1: Introduction

Changes in land use/land cover affect regional air quality by influencing surface albedo, the removal of air pollutants from the atmosphere through dry or wet deposition, the emissions of biogenic volatile organic compounds (BVOCs) from soil and vegetation, and through a variety of indirect mechanisms. These changes in land cover are driven by changes in climate, urbanization, and other factors. The overall goal of this thesis is to develop mechanisms for estimating changes in land cover and to incorporate these changes in land cover into air quality models.

Air quality models, such as the Comprehensive Air Quality Model with Extensions (CAMx) and the Community Multiscale Air Quality Model (CMAQ), are essential tools for assessing the impacts of urban development and climate change on future air quality. Robust forecasts of land use, land cover, and anthropogenic and biogenic emissions are, in turn, essential components of air quality model predictions. Land cover – air quality interactions are mapped conceptually in Figure 1-1.

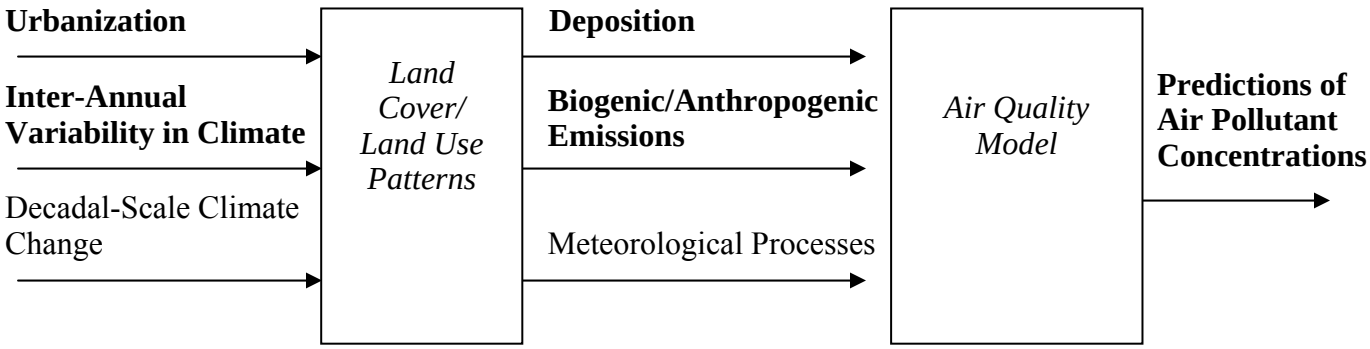

Figure 1-1. Conceptual Framework for Land Use/Air Quality Interactions. Note that the bolded letters indicate the pathways that will be examined in this study

The objective of this work will be to develop and apply modeling methodologies for selected interactions illustrated in Figure 1-1. This work will specifically focus on methods for estimating changes in land cover due to urbanization and climate. Land use and land cover induced changes in anthropogenic and biogenic emissions and air pollutant deposition will be examined and will be used to predict changes in air quality, specifically ozone concentrations. The pathways that will be examined in this work are bolded in Figure 1-1.

Chapter 2 describes in more detail (1) the drivers for land cover changes that are important in air quality modeling, (2) the mechanisms through which land cover changes influence air quality, focusing on deposition velocities and emissions, and (3) the modeling tools used in assessing the impacts that changes in biogenic emissions and deposition rates have on air quality. The remaining chapters will examine selected pathways in the system shown in Figure 1-1. For example, Chapter 3 will report on the effect of urbanization on land cover, using Austin as a case study, and the effects of land cover changes on deposition velocities, biogenic emissions, and ozone concentrations. Chapter 4 will describe the effects of land cover changes on anthropogenic emissions (including non-road mobile source emissions and area source emissions), and the effects of those changes on ozone concentrations. These results will be contrasted with the changes in predicted air quality due to biogenic emissions and dry deposition associated with the same land cover changes. Chapter 5 will describe the effect of inter-annual variability in climate on land covers, using Texas as a case study, and the effects of those land cover changes on biogenic emissions, and ozone concentrations. Finally, Chapter 6 will provide summarize the work that will complete this thesis.

Chapter 2: Background

The primary hypothesis examined in this work is that land cover changes, driven by a variety of factors, can influence regional air quality. This chapter will document that land cover changes can be extensive, and that these changes in land cover can influence parameters important in controlling regional air quality. The review of these topics will not be exhaustive, but rather will seek to document that changes in land use/land cover and their impacts on regional air quality are pervasive. Subsequent chapters will describe in more detail the interactions of land use/land cover with regional air quality in Texas, which is the focus of this thesis.

2.1 Land Use and Land Cover Change

Typical land cover changes are caused by activities such as urbanization, and also by phenomena such as long term climate changes and inter-annual variability in weather. Urbanization impacts the urban and rural environment in many ways. The most obvious impact is the permanent loss to the rural land base when land is converted from rural to urban uses. A total of 11 million acres was developed in the United States, with 7 million acres located in metropolitan areas, between 1992 and 1997 (Natural Resources Inventory, 1997). Changes in the classification land cover due to development are shown in Figure 2-1 for the United States. The most significant changes occurred from development of forested areas, followed by cropland, pastureland and rangeland.

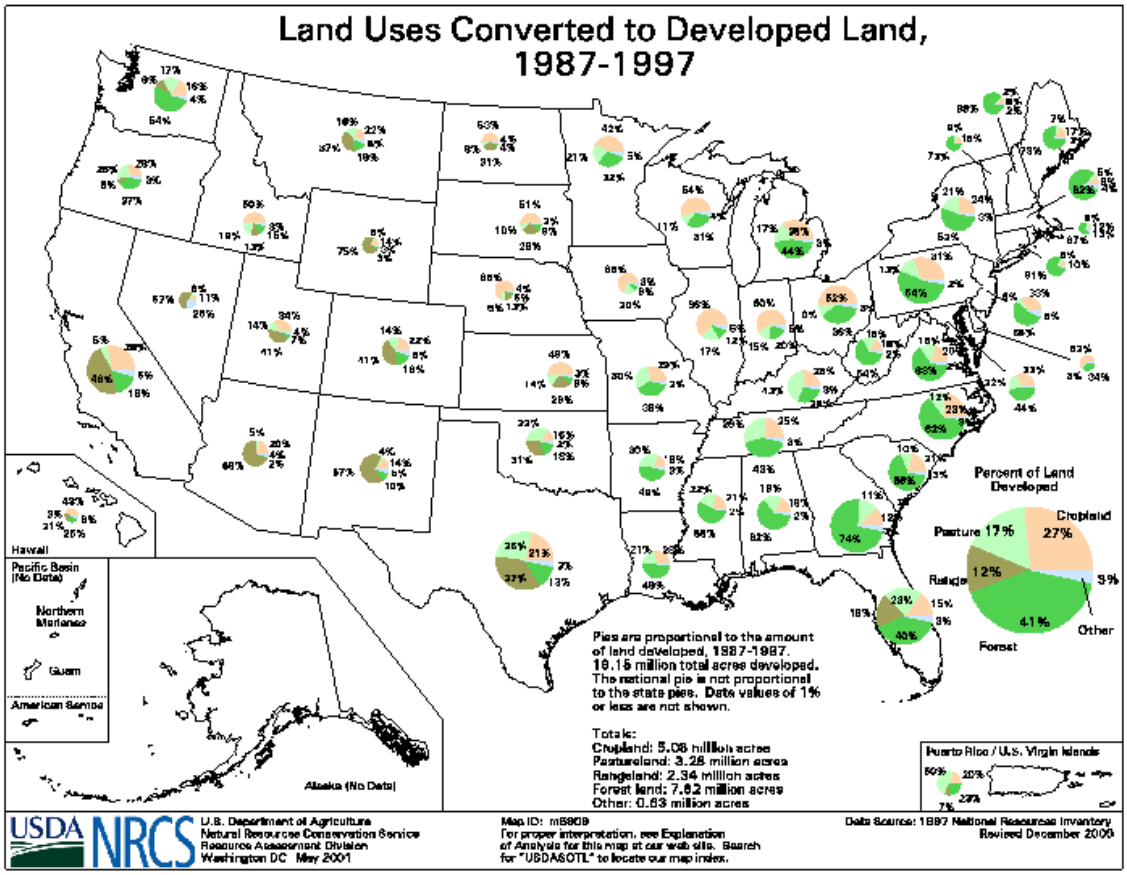

Figure 2-1. Land development patterns for each state and the nation. *Source*: National Resources Inventory (1997)

A number of studies have been conducted on the potential effects of climate change on land cover. These efforts have largely focused on agricultural land on both global and regional scales (Alexandrov *et al*., 2002; Chang, 2002; Kane *et al*., 1992; Theurillat and Guisan, 2001). Changes in temperature and precipitation affect surface and subsurface soil properties such as moisture and temperature, which, in turn, influence potential vegetation production rates (Foster, 1989). Responses to climate change by land cover vary both temporally and spatially (Parry, 2000; Olesen and Bindi, 2002).

Gulden *et al*. (2007) showed the relative contribution of inter-annual variations in weather to inter-annual variability in biogenic emissions. They estimated the historical inter-annual variations in BVOC emissions over the period from 1979 to 2002 due to changes in leaf area index (LAI) using a regional land-surface model. These results will be described in more detail in later chapter, but Figures 2-2 and 2-3, illustrate the main findings. Both LAI and biogenic emissions show large inter-annual variations during past 20 years. As shown in Figure 2-3, annual variations in BVOC fluxes due to changes in land cover from longer-term climate change overwhelm inter-annual variations. These results demonstrate that long term changes in land cover, induced by climate, will likely have a large impact of emissions, and consequently, air quality.

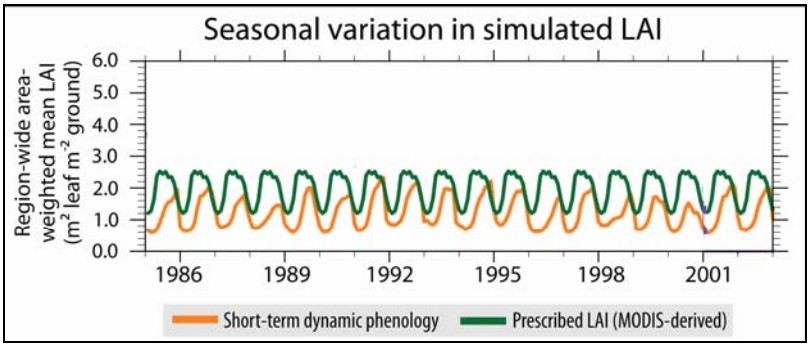

Figure 2-2. Comparison of simulated LAI accounting for the variability in environmental conditions (dynamic phenology scheme) and MODIS derived LAI which remains constant inter-annually

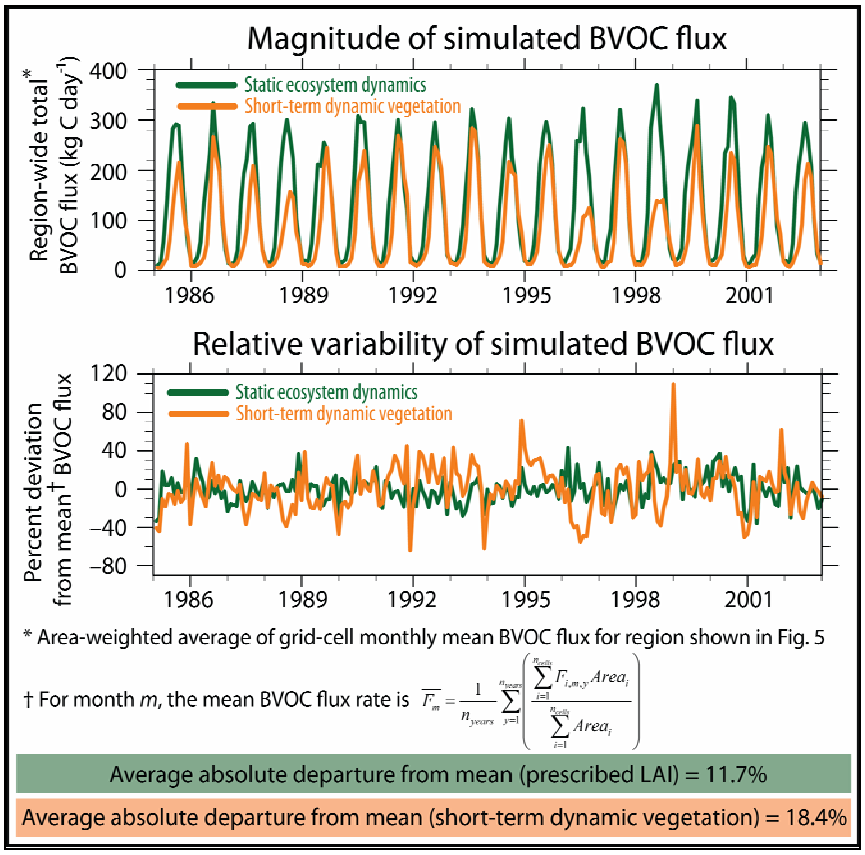

Figure 2-3. Comparison of simulated biogenic emission fluxes over Eastern Texas with inter-annually constant LAI and with inter-annually varying LAI. *Note*: 1998 was particularly dry and hot in Texas due to strong El Niño conditions

2.2 IMPACTS OF LAND COVER CHANGES ON PARAMETER INFLUENCING REGIONAL AIR QUALITY

Air quality is influenced by dry deposition processes, biogenic emissions and surface albedo, that are all a function of land cover type. Dry deposition, the transport of air pollutants to the surface of earth in the absence of precipitation processes, is an important loss mechanism for many reactive and soluble air pollutants. The dry deposition model used in most air quality simulations (Wesely, 1989; Walmsley and Wesely, 1996) calculates deposition fluxes from surface layer concentrations and dry deposition velocities. Dry deposition velocities reflect a series of mass transfer resistances to deposition. These resistances are due to turbulent transport to the surface of earth, molecular diffusion across a quasi-laminar sub-layer, and surface uptake. Dry deposition to different land cover types is dominated by different resistances with different magnitudes and diurnal patterns.

BVOC emissions from ecosystems are highly dependent on plant species and density. Benjamin *et al*. (1996) showed that the predicted biogenic emissions varied by as much as four orders of magnitude depending on the plant species. For example, vegetation changes from grassland to thorn woodland in a sub-tropical area increased isoprene emissions by a factor of three; whereas the replacement of grassland to cropland showed less than a 25% change in emissions (Guenther *et al*., 1999). Purves *et al*. (2004) showed that an increase in the population of sweetgum in the southeastern United States has resulted in large increases in isoprene emissions.

Albedo is a function of absorbed solar radiation at the surface and can be determined using a surface energy balance. The surface albedo varies depending on the soil/vegetation type, the density, texture, and structure of the surface, and the season of the year (Gao *et al*., 2005). Betts and Ball (1997) and others (Culf *et al*., 1995; Fuller

and Ottke, 2002) have calculated surface albedos for different vegetation types and seasonal conditions. For example, in summer (the season that is important for ozone formation), the albedo was found to be 0.16 for forested areas and 0.20 for grassland (Betts and Ball, 1997). A number of studies have demonstrated the relationship between changes in land cover and surface albedo due to anthropogenic influences (Betts, 2000; Giambelluca *et al*., 1997; Henderson-Sellers and Wilson, 1983; Mika *et al*., 2001; Myhre and Myhre, 2003). The early studies of Henderson-Sellers and Wilson (1983) showed that human activities have increased surface albedo by changing vegetation covers, with the most significant changes due to deforestation for agricultural activities. Desertification from shrub land and dam construction was found to be another important cause for human-induced vegetation changes. In a recent study, Matthews *et al*. (2004) estimated global changes in surface albedo over the last 300 years focusing on the effects of land cover change. Increases in surface albedo have resulted in a decrease in precipitation and a global cooling of -0.13 ^{o}C.

2.3 THESIS SCOPE

These, and other complex impacts of land cover on air quality are rarely included in regional air quality models. The overall goal of this thesis is to couple models of climate, land use, biogenic emissions, and air quality to predict future air quality trends. Not all of the large number of potential interactions could be examined within the scope of this thesis, so the thesis focuses on land cover – air quality interactions that have been hypothesized to have significant impact on air quality in Texas. Specifically, this thesis assess how changes in emissions and deposition velocities due to urbanization and future climate changes are predicted to impact air pollutant concentrations, with a specific focus on ozone concentrations.

2.4 REFERENCES

Alexandrov, V., Eitzinger, J., Cajic, V., Oberforster, M. (2002) "Potential impact of climate change on selected agricultural crops in north-eastern Austria." *Global Change Biology* **8**(4), 372-389.

Benjamin, M.T., Sudol, M., Bloch, L., Winer, A.M. (1996) "Low-emitting urban forests: A taxonomic methodology for assigning Isoprene and Monoterpene emission rates." *Atmospheric Environment* **30**(9), 1437-1452.

Betts, R.A. (2000) "Offset of the potential carbon sink from boreal forestation by decreases in surface albedo." *Nature* **408**(6809), 187-190.

Betts, A.K., Ball, J.H. (1997) "Albedo over the boreal forest." *Journal of Geophysical Research-Atmospheres* **102**(D24), 28901-28909.

Chang, C.C. (2002) "The potential impact of climate change on Taiwan's agriculture." *Agricultural Economics* **27**(1), 51-64.

Culf, A.D., Fisch, G., Hodnett, M.G. (1995) "The albedo of Amazonian forest and ranch land." *Journal of Climate* **8**, 1544-1554.

Foster, H.L. (1989) "The influence of soil and climatic factors on groundnut production on alluvial soils in peninsular Malaysia." *Oleagineux* **44**(2), 105-111.

Fuller, D.O., Ottke, C. (2002) "Land cover, rainfall and land-surface albedo in west Africa." *Climate Change* **54**, 181-204.

Gao, F., Schaaf, C.B., Strahler, A.H., Roesch, A., Lucht, W., Dickinson, R. (2005) "MODIS bidirectional reflectance distribution function and albedo Climate Modeling Grid products and the variability of albedo for major global vegetation types." *Journal of Geophysical Research-Atmospheres* **110**(D1): Art. No. D01104.

Giambelluca, T.W., Holscher, D., Bastos, T.X., Frazao, R.R., Nullet, M.A., Ziegler, A.D. (1997) "Observations of albedo and radiation balance over postforest land surfaces in the eastern Amazon Basin." *Journal of Climate* **10**, 919-928.

Gulden, L.E., Yang, Z.L. Niu, G-.Y. (2007) "Interannual variation in biogenic emissions on a regional scale." Submitted to *Journal of Geophysical Research-Atmospheres* in 2007.

Guenther, A., Archer, S., Greenberg, J., Harley, P., Helmig, D., Klinger, L., Vierling, L., Wildermuth, M., Zimmerman, P., Zitzer, S. (1999) "Biogenic hydrocarbon emissions and landcover/climate change in a subtropical savanna." *Physics and*

Chemistry of the Earth Part B-Hydrology Oceans and Atmosphere **24**(6), 659-667.

Henderson-Sellers, A., Wilson, M.F. (1983) "Surface albedo data for climatic modeling." *Reviews of Geophysics* **21**(8), 1743-1778.

Kane, S., Reilly, J., Tobey, J. (1992) "An empirical-study of the economic-effects of climate change on world agriculture." *Climatic Change* **21**(1), 17-35.

Matthews, H.D., Weaver, A.J., Meissner, K.J., Gillett, N.P., Eby, M. (2004) "Natural and anthropogenic climate change: incorporating historical land cover change, vegetation dynamics and the global carbon cycle." *Climate Dynamics* **22**(5), 461-479.

Mika, J., Horvath, S., Makra, L. (2001) "Impact of documented land use changes on the surface albedo and evapotranspiration in a plain watershed." *Physics and chemistry of the Earth B-Hydrology Oceans and Atmosphere* **26**(7-8), 601-606.

Myhre, G., Myhre, A. (2003) "Uncertainties in radiative forcing due to surface albedo changes caused by land-use changes." *Journal of Climate* **16**, 1511-1524.

Natural Resources Inventory (1997) "Land uses converted to developed land, 1987-1997." Available at http://www.nrcs.usda.gov/technical/land/meta/m5909 .html.

Olesen, J.E., Bindi, M. (2002) "Consequences of climate change for europe agricultural productivity, land use and policy." *European Journal of Agronomy* **16**(4), 239-262.

Parry, M.L. (2000) "Assessment of potential effects and adaptations for climate change in Europe." In: M.L. Parry, Editor, The Europe ACACIA Project, Jackson Environment Institute, University of East Anglia, Norwich, UK.

Purves, D.W., Caspersen, J.P., Moorcroft, P.R., Hurtt, G.C., Pacala, S.W. (2004) "Human-induced changes in US biogenic volatile organic compound emissions: evidence from long-term forest inventory data." *Global Change Biology* **10**(10), 1737-1755.

Theurillat, J.P., Guisan, A. (2001) "Potential impact of climate change on vegetation in the European Alps: A review." *Climatic Change* **50**(1-2), 77-109.

Wesely, M.L. (1989) "Parameterization of surface resistances to gaseous dry deposition in regional-scale numerical-models." *Atmospheric Environment* **23**(6), 1293-1304.

Walmsley, J.L., Wesely, M.L. (1996) “Modification of coded parameterizations of surface resistances to gaseous dry deposition.” *Atmospheric Environment* **30**(7), 1181-1188.

Chapter 3: Impacts of Urbanization on Biogenic Emissions and Air Pollutant Deposition

3.1 INTRODUCTION

The objectives of this study are to couple representations of future land use, reflecting varying urban development scenarios, to air quality models, and to assess the effects of changes in land use to air quality. Changes in land use, including human-induced changes, are known to affect biogenic emissions, air pollutant deposition, and regional air quality, as described in the previous chapter, but the magnitude of these effects are not well understood. The work presented in this Chapter will examine the response of biogenic emissions, air pollutant deposition velocities, and overall regional air quality, as represented by ozone concentrations, to land use development. Austin, Texas will serve as the case study area. The anthropogenic land use datasets that have been employed in the study were developed through a regional visioning initiative, Envision Central Texas (ECT). Different scenarios representing the response of land use to urban development policies will consider the issues of land use planning as well as tree preservation.

The case study region is shown in Figure 3-1. The focus of the analysis will be on the 5-county Capital Area Metropolitan Statistical Area (MSA) consisting of Bastrop, Caldwell, Hays, Travis and Williamson counties. The population of the MSA is approximately 1.4 million, and is concentrated in Travis and Williamson counties. The area is growing rapidly; the population of Williamson County increased by 79% between 1990 and 2000. Over that period, Williamson County was the second fastest growing county in Texas and the 19th fastest growing county in the country. Williamson (5th), Hays (26th), Bastrop (30th), and Caldwell (51st) counties were among the 100 fastest

growing counties by percent change in the country, while Travis (32nd) County was one of 100 fastest growing counties by numeric change in the country between 2000 and 2001.

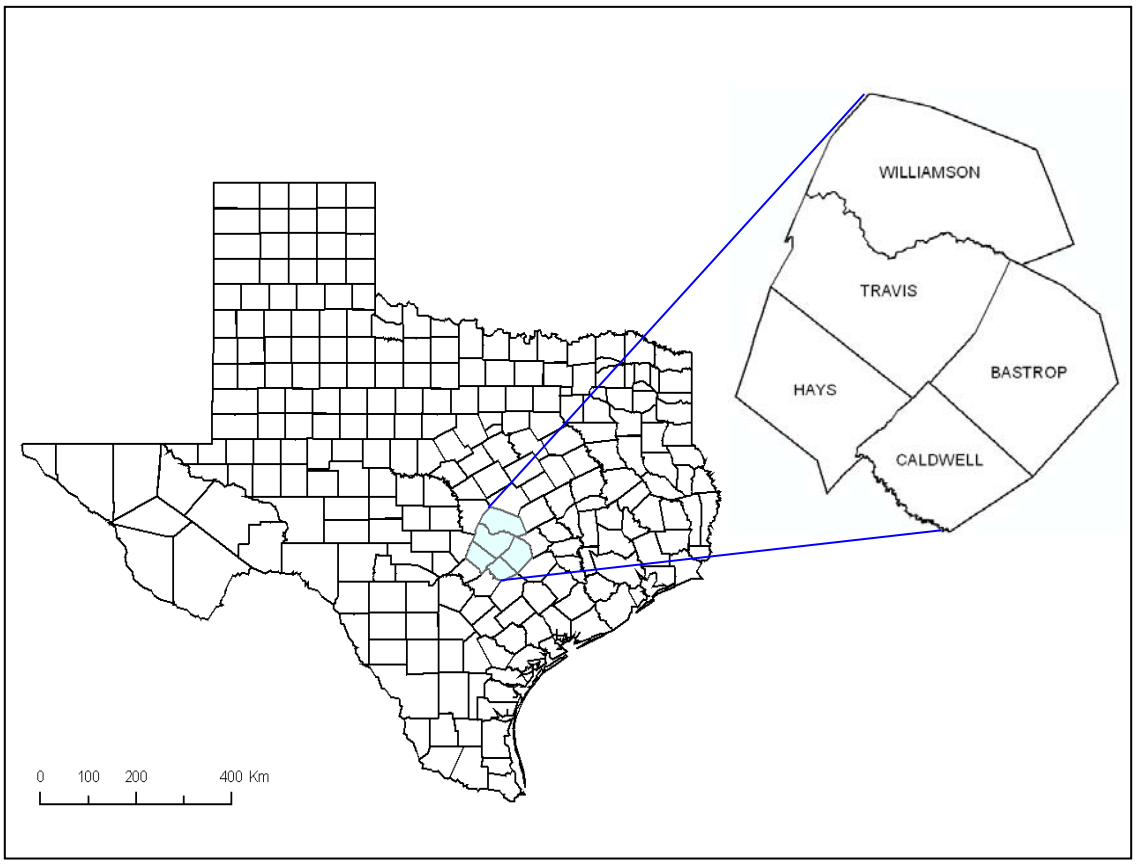

Figure 3-1. Location of the 5 county study area in Texas

Growth scenarios for the region have been developed through Envision Central Texas (ECT), which began in 2001. Figure 3-2 shows 2001 Landsat satellite imagery which distinguishes developed areas from undeveloped areas. This dataset served as the primary reference to examine how urban development changes with a doubling of population under different scenarios.

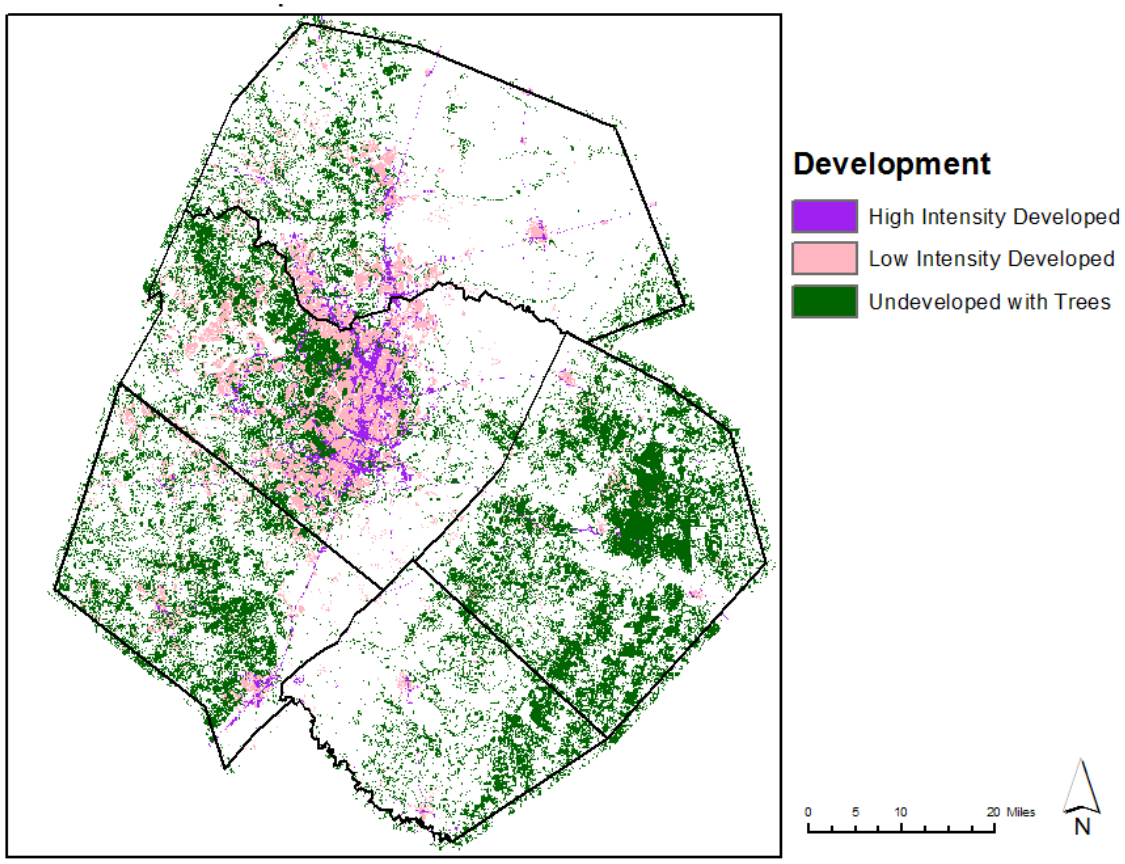

Figure 3-2. 2001 Landsat satellite image showing urban development and undeveloped land with tree cover

The ECT process engaged state and local government, business, environmental, and community development organizations, and elected leaders from the five counties. Based on information discussed in public workshops held in late 2002, the ECT process projected a set of four possible growth scenarios, which represent a range of growth patterns (Additional details of the ECT Scenarios are available at the ECT web site: http://www.envisioncentraltexas.org). All of the Scenarios are based on the same assumption: a doubling of population within 20 to 40 years, and introducing the same number of new jobs. However, the Scenarios assume very different types of growth. ECT Scenario A assumes a typical urban sprawl pattern which is consistent with recent land development patterns, consuming the greatest amount of undeveloped land; Scenario B concentrates growth within 1 mile of transportation corridors; Scenario C assumes new development in new and existing towns throughout the region instead of contiguous corridor development; Scenario D assumes increasing population density in existing towns and cities, consuming the least amount of land. Figure 3-3 shows how those land use types are projected to change relative to 2001 land use patterns for each of the scenarios. Note that land use is how land is used by people (*e.g.*, agricultural, residential, industrial), and land cover is how a land surface is naturally covered (*e.g.*, forest, water, soil).

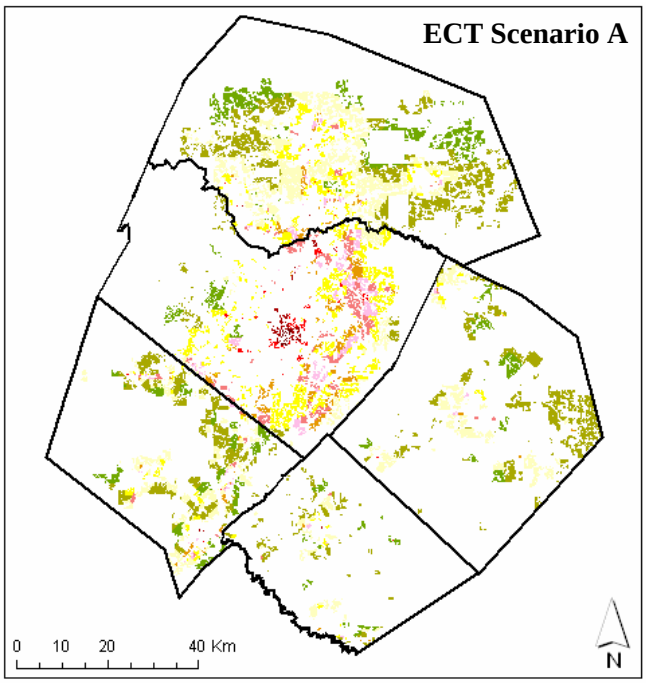

Development Type of ECT Scenario A

- Downtown
- City
- Town
- Residential Subdivision
- Large Lot
- Rural
- Conservation Rural
- Activity Center
- Highway Commercial
- Industrial / Office Park

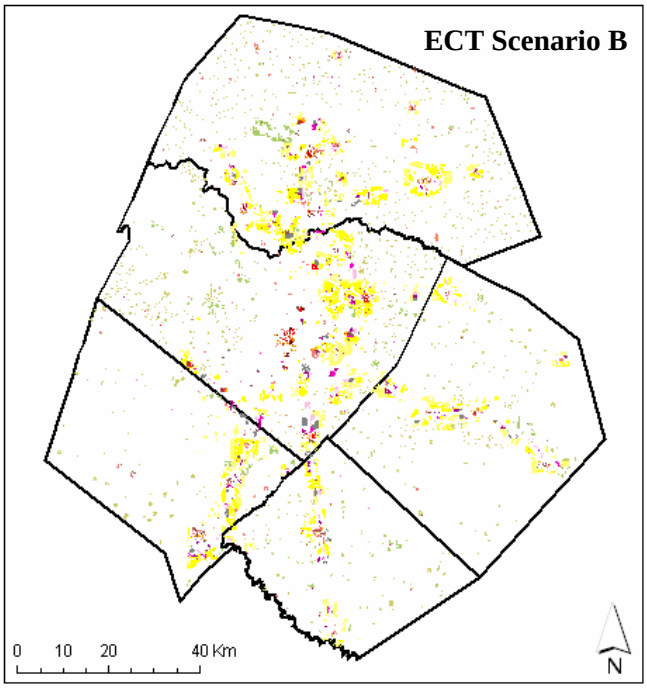

Development Type of ECT Scenario B

- Downtown
- Downtown Commercial
- Downtown Residential
- City
- City Neighborhood
- Town
- Residential Subdivision
- Large Lot
- Rural
- Conservation Rural
- City Commercial
- New Town
- Activity Center
- Highway Commercial
- Office Park
- Industrial

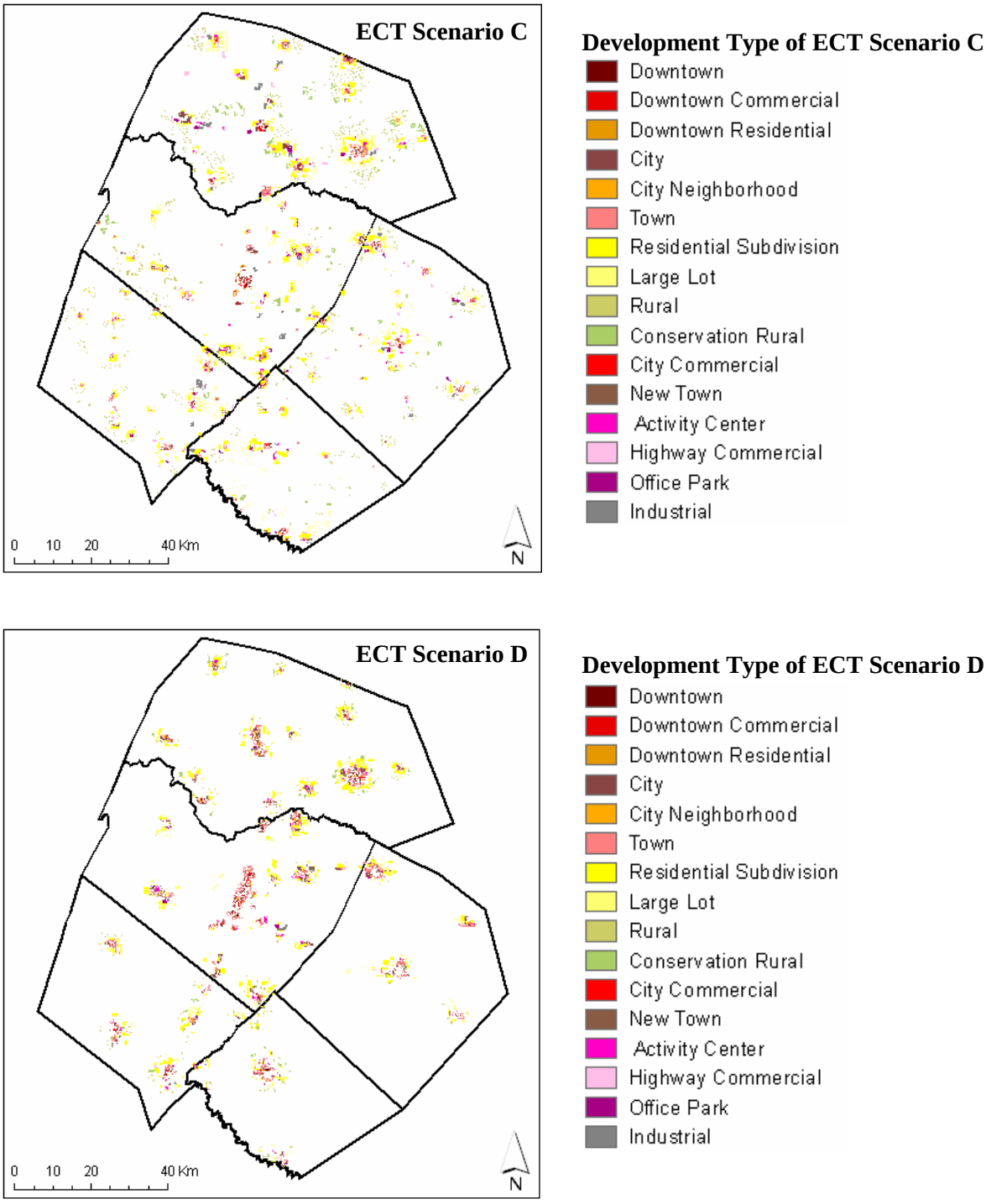

Figure 3-3. ECT Scenarios: maps indicating land use changes that will occur for each of the growth scenarios. Area with no color will not have any new development

These alternative land use scenarios, all associated with a doubling of population, have the potential to have different impacts on air pollutant concentrations. The two types of air quality impacts, tied to land cover changes, that will be examined in this work are the effects on biogenic hydrocarbon emissions and the impacts on deposition velocities.

As discussed in Chapter 1, biogenic emissions are highly dependent on land use/land cover type and spatial distribution. In central Texas, biogenic emissions are a dominant source of reactive hydrocarbon emissions (Wiedinmyer *et al*., 2001), and therefore changes in biogenic emissions have the potential to significantly impact air quality. Similarly, dry deposition, which is the dominant loss mechanism for air pollutants in central Texas, is also a strong function of land use/land cover type. As described in more detail in the Methods section of this chapter, the dry deposition model used in most air quality simulations (Wesely, 1989; Walmsley and Wesely, 1996) calculates deposition rates by estimating a series of mass transfer resistances to deposition. These resistances are due to aerodynamic transport, diffusion across a quasi-laminar sub-layer, and surface uptake. When the land cover is classified as urban or barren, the deposition rate is controlled by aerodynamic transport and diffusion across the quasi-laminar sub-layer. Deposition rates for other land cover categories are dominated by the resistances due to surface uptake. Because different resistances can dominate, deposition rates for different land cover types can have different magnitudes and diurnal patterns. For example, dry deposition velocities for forest land covers are a factor of 2-2.5 higher than those of urban and barren land during daytime; in contrast, dry deposition velocities of forest land covers are generally smaller than those of urban and barren categories in the early morning and late night.

Thus, changes in biogenic emissions and air pollutant deposition rates, due to land cover changes, are expected to have both significant and complex impacts on air pollutant concentrations. The goal of this work will be to evaluate, for each of the four ECT scenarios, the impacts of land cover changes on air pollutant concentrations (particularly ozone). The influences of biogenic emissions and deposition velocities will be considered both separately, and in tandem, and the overall effects of land cover changes will be compared to the effects of typical air pollutant control strategies.

3.2 METHODOLOGY

3.2.1 Biogenic Emission Estimation

Guenther *et al*. (1993) developed the model to estimate isoprene emissions from plant canopies, called the Global Biosphere Emissions and Interactions System (GloBEIS). Guenther *et al*. (1993) assumed that emission activity is influenced by the light and temperature for a variety of plants. Guenther *et al*. (1999) modified the algorithms to account for leaf age and phenology. GloBEIS estimates foliar emissions as follows:

$$F = \varepsilon \cdot D_p \cdot D_f \cdot \gamma_T \cdot \gamma_L \cdot \gamma_A \cdot \rho$$

where F is the emission flux (μg C m^{-2} h^{-1}), ε is the ecosystem-specific emission factor (μg C g^{-1} h^{-1}) at a standard leaf temperature (T_S) of 303.15K and standard photosynthetically active radiation (PAR) flux of 1000 μmol m^{-2} s^{-1}, D_p is the annual peak foliar biomass density (g dry mass of foliage per m^2 of land surface area), D_f is the foliage fraction (the ratio of the foliage at a specific time of year to the peak foliage

during the year), γ_T, γ_L, and γ_A are dimensionless scalars that describe the response of emission to diurnal variations in leaf temperature, incident sunlight, and leaf age, respectively, and ρ is an escape efficiency factor that represents the fraction of gas emitted by the canopy that is released into the above-canopy atmosphere. For isoprene, emission, temperature, light, and leaf age dependence factors are given by

$$\gamma_T = \frac{\exp\left(\frac{C_{T1}(T - T_s)}{RT_sT}\right)}{0.961 + \exp\left(\frac{C_{T2}(T - T_M)}{RT_sT}\right)},$$

$$\gamma_L = \frac{\alpha C_{L1} PAR}{\sqrt{1 + \alpha^2 PAR^2}},$$

$$\text{and} \quad \gamma_A = A_1 \Delta D_f + A_2 (1 - \Delta D_f)$$

where T is current leaf temperature (K), R is the gas constant (8.314 J K^{-1} mol^{-1}), C_{T1} (95,000 J mol^{-1}), C_{T2} (230,000 J mol^{-1}), T_M (314K), α (0.0027), and C_{L1} (1.066) are empirical coefficients derived from non-linear best fit procedures using emission rate measurements (Guenther *et al*., 1993). Additionally, A_1 and A_2 are empirical coefficients to represent typical vegetation; A_1 is the average emission activity of young and old leaves (0.33) and A_2 is the fraction of mature foliage present during the month of peak foliar density (0.95) (Guenther *et al*., 1999).

The Global Biogenic Emissions and Interactions System (GloBEIS) was used to develop the emission inventory (Yarwood *et al*., 1999a, b). GloBEIS requires data on temperature, photosynthetically active radiation (PAR), wind speed, humidity, and land

use/land cover (LULC) to estimate biogenic emissions. All the simulations reported in this work used the GloBEIS 3.1 model.

Vizuete *et al*. (2002) interpolated hourly ambient surface temperatures measured by National Weather Service (NWS) and other weather stations throughout southeast Texas. Estimates of PAR flux were based on calculations done by the University of Maryland and the National Oceanic and Atmospheric Administration (NOAA) for the Global Energy and Water Cycle Experiment (GEWEX) Continent Scale International Project (GCIP). NOAA used a modified version of the GEWEX surface radiation budget (SRB) algorithm (version 1.1) to calculate radiation flux fields from Geostationary Operational Environmental Satellite (GOES-8) data (TCEQ, 2003). Wind speed and humidity estimates were derived from simulations using the MM5 meteorological model. MM5 is the fifth generation NCAR/Penn State mesoscale regional climate model.

The LULC input data required by GloBEIS 3.1 were derived from two different datasets. The first dataset was developed by Wiedinmyer *et al*. (2000, 2001) and incorporated data from different sources such as the Texas Parks and Wildlife Department, various Councils of Government (COG) in the eastern Texas, the U.S. Department of Agriculture (USDA), and field survey. This dataset encompasses most of Texas and available at a 1-km resolution (Figure 3-4); The LULC database contains emission factor data for 156 different vegetation types, including 41 species (*e.g.*, Quercus alba), 80 genera (*e.g.*, Quercus), and 35 land cover types (*e.g.*, Pecan Elm forest). Each classification is assigned a vegetation species, leaf biomass, and density distribution (Wiedinmyer *et al*., 2001). In this study, the 1-km data were aggregated to a 4-km resolution used in the photochemical modeling.

The second LULC database was derived from the ECT Scenarios. These scenarios used only 10 or 16 land use classes (10 land use types for Scenario A and 16 for other scenarios); the land use classifications included information on pervious ground cover but relatively little information on vegetation types. The ECT Scenario land uses, therefore, were overlaid on the Basecase land covers developed by Wiedinmyer *et al*. (2000, 2001) to understand how development would impact land cover at the species and genus level.

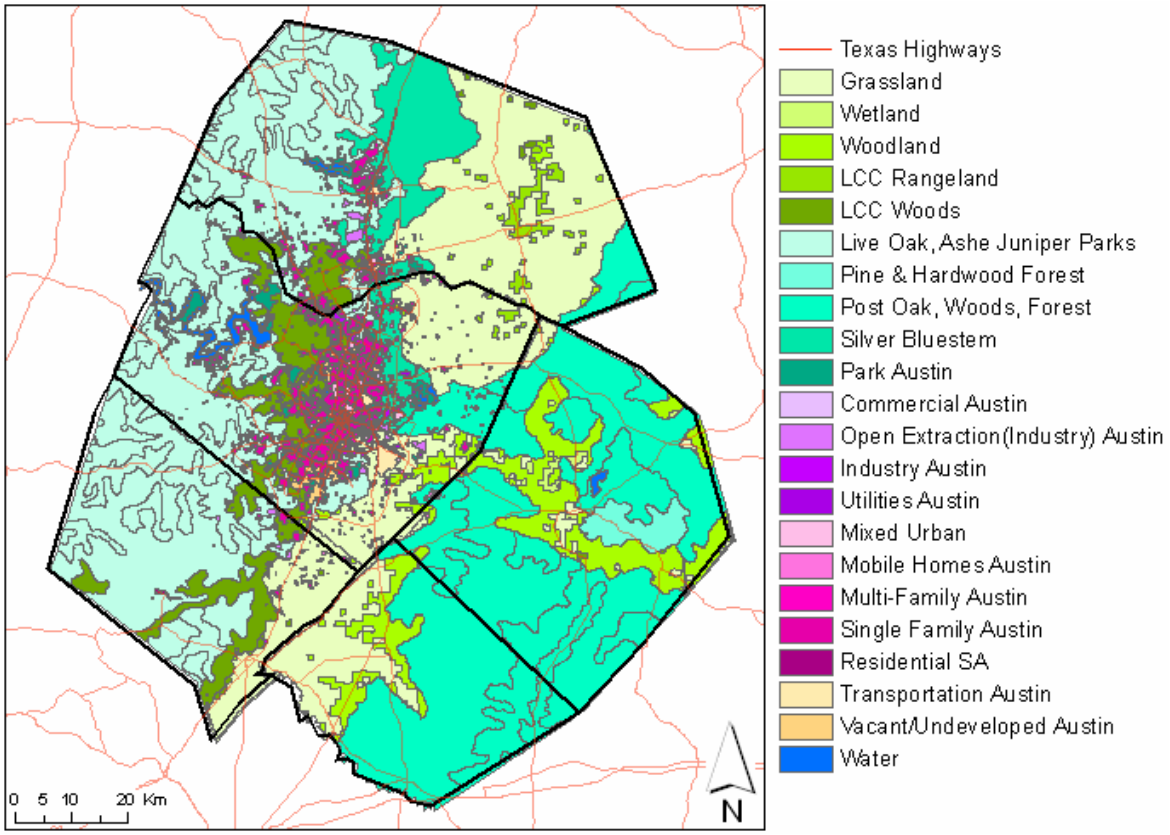

Figure 3-4. Basecase land cover derived by Wiedinmyer *et al*. (2001)

When ECT Scenarios are overlaid on the Basecase land covers, a mapping can be made between the original vegetation types and the new land cover classes, for the regions where future development is expected. For these areas, ECT planners and Parmenter and Kim (2005, Personal communication) have estimated the fraction of pervious cover for each development type. This fraction of pervious cover is then used to calculate the fraction of the original trees remaining in that area. For example, areas which are designated to develop as "Downtown" are assumed to have 2.3% pervious ground cover and will therefore keep 2.3% of original vegetation types. The rest of the area is assumed to have no vegetation. Table 3-1 shows the percentage of vegetation remaining for each development type from ECT Scenario A. Table 3-2 reports the fraction of vegetation remaining for each development type from ECT Scenarios B, C, and D.

Table 3-1. Fraction of trees remaining for each development type for ECT Scenario A

Development type from ECT Scenario A		Fraction of trees remaining
1	Downtown	0.023
2	City	0.146
3	Town	0.171
4	Residential Subdivision	0.363
5	Large lot	0.493
6	Rural	0.763
7	Conservation Rural	0.827
8	Activity Center	0.042
9	Highway Commercial	0.023
10	Industrial/ Office Park	0.144

Table 3-2. Fraction of trees remaining for each development type for ECT Scenarios B, C, and D

Development type from ECT Scenario B,C,D		Fraction of trees remaining
1	Downtown	0.023
2	Downtown Commercial	0.000
3	Downtown Residential	0.055
4	City	0.146
5	City Neighborhood	0.193
6	Town	0.171
7	Residential Subdivision	0.363
8	Large Lot	0.492
9	Rural Housing	0.763
10	Conservation Rural	0.827
11	City Commercial	0.011
12	New Town	0.148
13	Activity Center	0.041
14	Highway Commercial	0.023
16	Office Park	0.144
17	Industrial	0.025

This impact of development on tree cover was assessed by comparing 1995 and 2002 Austin orthophotos in selected low density or high density areas in the Austin Metropolitan area. Figure 3-5 shows the difference in tree coverage for low density residential area before and after development (Parmenter and Kim, 2005; Personal communication). As shown in Figure 3-4, the fraction of trees remaining for each development type tends to follow average treed area remaining after each development (Table 3-1 and 3-2). Additional examples are provided in Appendix A.

(a) 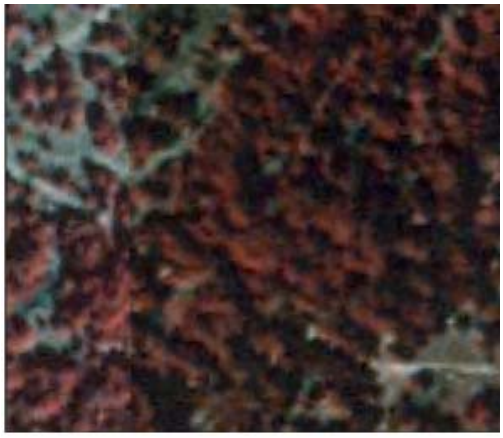

Tree coverage: 233,000 ft^2

(b) 

Tree coverage: 82,000 ft^2

$$\text{Fraction of trees remaining} = \frac{\text{Tree cover after development}}{\text{Tree cover before development}} = \frac{82000}{233000} = 35\%$$

Figure 3-5. Orthophotos for low density residential area in the Austin Metropolitan area; (a) Treed area before development in 1995 orthophotos, and (b) Treed area after development in 2002 orthophotos

3.2.2 Estimating Dry Deposition Rates

Dry deposition estimation methods in CAMx are based on the work of Wesely *et al*. (1989) and Walmsley and Wesely (1996) which is the most commonly used approach in urban and regional-scale photochemical models. In this algorithm, dry deposition rates are influenced by resistances due to three mechanisms; aerodynamic transport, diffusion across a quasi-laminar sub-layer, and surface uptake (McDonald-Buller *et al*., 2001).

The dry deposition flux is found as:

$$F_c = V_d \cdot C_z$$

where F_c is the dry deposition flux of the gas of interest, V_d is the dry deposition velocity, and C_z is the concentration or mixing ratio at the mid-point of first vertical layer height in CAMx (20m in CAMx version 4.03). For gases, the dry deposition velocity is calculated as follows:

$$V_d = \frac{1}{r_a + r_d + r_s}$$

where r_a is the aerodynamic resistance above the surface, r_d is the deposition layer (or quasi-laminar sub-layer) resistance and r_s is the bulk surface (or canopy) resistance (Wesely, 1989). r_a and r_d are expressed as follows:

$$r_a = \frac{1}{\kappa \cdot u_*}\left[\ln\left(\frac{\Delta z}{z_o}\right) - \phi_h\right]$$

$$r_d = \frac{2S_c^{2/3}}{\kappa \cdot u_*}$$

where u_* is friction velocity (m s^{-1}), κ is von Karman constant (value of 0.4, dimensionless), Δz is the lowest model layer midpoint height which has the value of 20 m, z_o is land use-dependent aerodynamic surface roughness length (m) shown in Table 3-3, Φ_h is the stability correction function for trace gases, S_c is the Schmidt number or the ratio of kinematic viscosity of air to species molecular diffusivity.

Table 3-3. Surface roughness length, z_o (m) for 11 CAMx land use/land cover categories used in calculating deposition rates

	Land use/land cover type	Abbreviation	z_o (m)
1	Urban land	Urban	3
2	Agricultural land	Agri	0.25
3	Range land	Rang	0.05
4	Deciduous forest	Dfor	1
5	Coniferous forest	Cfor	1
6	Mixed Forest including wetland	Mfor	1
7	Water, both salt and fresh	Water	0.0001
8	Barren land, mostly desert	Barr	0.002
9	Non-forested wetland	Wetland	0.15
10	Mixed Agricultural and Range land	AgRn	0.1
11	Rocky open areas with low-growing shrubs	Rocky	0.1

Source: CAMx User's Guide (2004)

Bulk surface (or canopy) resistance is expressed as several serial and parallel resistances that are influenced by land cover type.

$$r_s = \frac{1}{\frac{1}{r_{st} + r_m} + \frac{1}{r_{uc}} + \frac{1}{r_{dc} + r_{lc}} + \frac{1}{r_{ac} + r_{gs}}}$$

where the first serial resistance set represents the pathway into stomatal and mesophyllic portions of active plants, the second is the pathway into the upper canopy, the third is the pathway into the lower canopy, and the fourth is the pathway to the ground surface. The assumed values of baseline resistances for estimating resistances are shown in Table 3-4. It is important to understand that these baseline resistances were assumed to represent very broad land use categories, not specific to characteristics of each land use type.

Table 3-4. Baseline resistance (s m^{-1}) for the calculations of Bulk Surface Resistance (r_s) from Wesely which are developed based on data collected in northeastern United States. Value of '9999' indicates that there is no air-surface exchange through that resistance pathway

	Land use/land cover type										
Resistance component	1	2	3	4	5	6	7	8	9	10	11
Seasonal Category 1: Midsummer with lush vegetation											
r_j	9999	60	120	70	130	100	9999	9999	80	100	150
r_{lu}	9999	2000	2000	2000	2000	2000	9999	9999	2500	2000	4000
r_{lcs}	100	200	100	2000	2000	2000	0	0	300	150	200
r_{lco}	400	150	350	500	500	100	0	1000	0	220	400
r_{ac}	300	150	200	200	200	300	2000	400	1000	180	200
r_{gss}	9999	2000	2000	2000	2000	2000	9999	9999	2500	2000	4000
r_{gso}	9999	1000	1000	1000	1000	1000	9999	9999	1000	1000	1000
Seasonal Category 2: Autumn with unharvested cropland											
r_j	9999	9999	9999	9999	250	500	9999	9999	9999	9999	9999
r_{lu}	9999	9000	9000	9000	4000	8000	9999	9999	9000	9000	9000
r_{lcs}	9999	9000	9000	9000	2000	4000	9999	9999	9000	9000	9000
r_{lco}	9999	400	400	400	1000	600	9999	9999	400	400	400
r_{ac}	100	150	100	1500	2000	1700	0.001	0.001	200	120	140
r_{gss}	400	200	350	500	500	100	0.001	1000	0.001	300	400
r_{gso}	300	150	200	200	200	300	2000	400	800	180	200

Note: r_j is baseline minimum stomatal resistance; r_{lu} is baseline upper canopy resistance; r_{lcs} is baseline SO_2 lower canopy resistance; r_{lco} is baseline O_3 lower canopy resistance; r_{ac} is baseline canopy height/density resistance; r_{gss} is baseline SO_2 ground surface resistance; and r_{gso} is baseline O_3 ground surface resistance

Source: Wesely (1989)

The stomatal resistance is estimated as:

$$r_{st} = diffrat \times r_j \times \left(1 + \left(\frac{200}{solflux + 0.1}\right)^2\right) \times \left(\frac{400}{t_s(40 - t_s)}\right)$$

where *diffrat* is ratio of molecular diffusivity of water to the molecular diffusivity of the species of interest (NO: 1.29; NO_2: 1.60; and O_3: 1.63), r_j is the baseline minimum stomatal resistance (s m^{-1}), *solflux* is the solar irradiation flux (W m^{-2}), and t_s is the surface air temperature (^oC).

The mesophyll resistance, r_m, the leaf cuticular resistance in healthy vegetation, r_{uc}, the resistance to buoyant convection, r_{dc}, the resistance of exposed surfaces in lower canopy, r_{lc}, the baseline canopy height/density resistance, r_{ac}, and is the resistance of ground surface, r_{gs}, are calculated as:

$$r_m = \left(\frac{Henry_i}{3000} + 100 \cdot f_o^{\,i}\right)^{-1}$$

$$r_{uc} = \frac{r_{lu}}{\frac{Henry_i}{Henry_{SO2}} + f_o^{\,i}}$$

$$r_{dc} = 100 \cdot \left(1 + \frac{1000}{solflux + 10}\right)$$

$$r_{lc} = \left(\frac{Henry_i}{Henry_{SO2} \cdot r_{lcs}} + \frac{f_o^{\,i}}{r_{lco}}\right)^{-1}$$

$$r_{gs} = \left(\frac{Henry_i}{Henry_{SO2} \cdot r_{gss}} + \frac{f_o^{\ i}}{r_{gso}} \right)^{-1}$$

where $Henry_i$ is the Henry's law constant for each species *i*, $Henry_{SO2}$ is the Henry's law constant for SO_2, and f_o^i is normalized reactivity parameter for each species *i*.

All the resistances are set to be in the range of 1 and 10^5 s m^{-1}. If the calculated value of any resistance is less than 1 or greater than 10^5 s m^{-1}, the model sets these values to 1 and 10^5 s m^{-1}, respectively. For example, whenever the surface air temperature is above 40 or below 0 ^oC, the transfer through stomata is stopped. Therefore, the stomatal resistance is set to be very large value, 10^5 s m^{-1}, indicating little surface air exchange.

To estimate deposition rates, CAMx land use files assign the areal fractional distribution (0 to 1) of eleven land use categories (Table 3) in each individual grid cell. In this work, Basecase LULCs were mapped to one of the eleven land use/land cover categories used by the dry deposition module in CAMx (McDonald-Buller *et al*., 2001). For the ECT Scenarios, the areal percentage of remaining trees for each development type (from Table 1 and 2) remained as the Basecase land cover, however, the rest of the area, *i.e.*, the areal fraction of newly developed land, was classified as urban.

Figure 3-6 shows differences in areal coverage for CAMx land use/land cover category between ECT Scenario A and the Basecase. The changes in land cover categories not shown, such as Agricultural, Coniferous forest/wetland, Water, Barren land, Non-forested wetlands, and Rocky, were negligible.

(a)

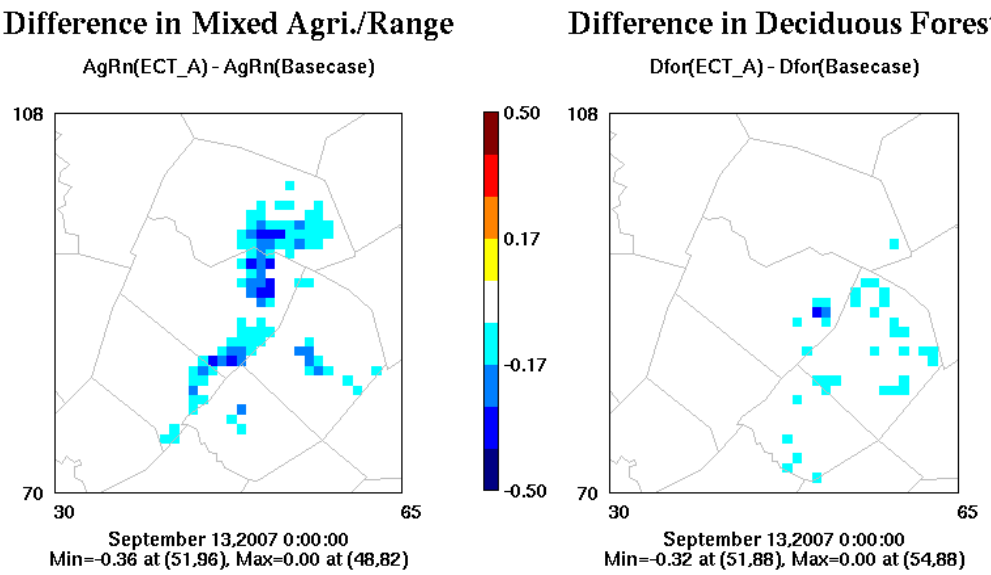
Difference in Mixed Agri./Range
AgRn(ECT_A) - AgRn(Basecase)
108
70
30
65
September 13,2007 0:00:00
Min=-0.36 at (51,96), Max=0.00 at (48,82)
0.50
0.17
-0.17
-0.50
Difference in Deciduous Forest
Dfor(ECT_A) - Dfor(Basecase)
108
70
30
65
September 13,2007 0:00:00
Min=-0.32 at (51,88), Max=0.00 at (54,88)

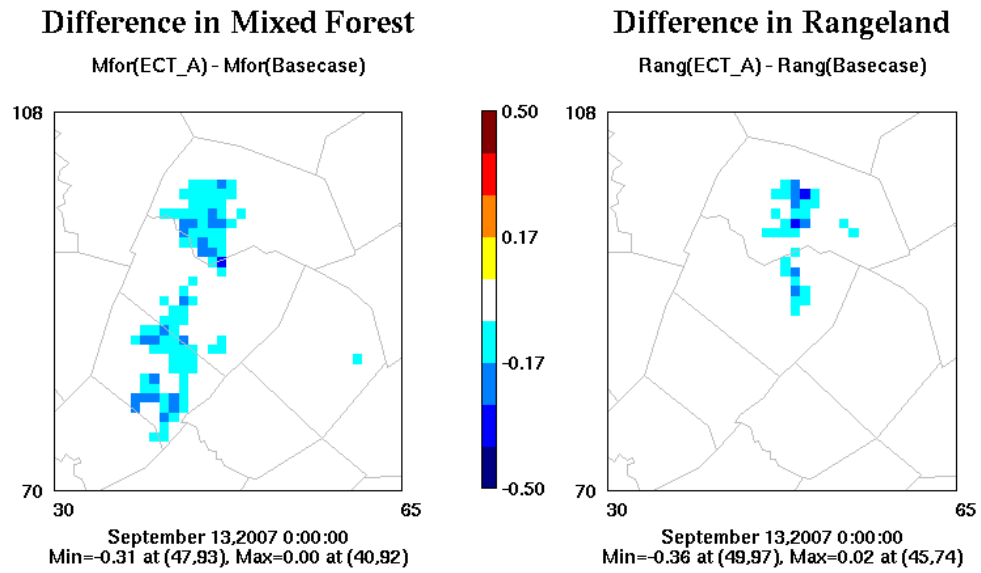
Difference in Mixed Forest
Mfor(ECT_A) - Mfor(Basecase)
108
70
30
65
September 13,2007 0:00:00
Min=-0.31 at (47,93), Max=0.00 at (40,92)
0.50
0.17
-0.17
-0.50
Difference in Rangeland
Rang(ECT_A) - Rang(Basecase)
108
70
30
65
September 13,2007 0:00:00
Min=-0.36 at (49,97), Max=0.02 at (45,74)

(b)

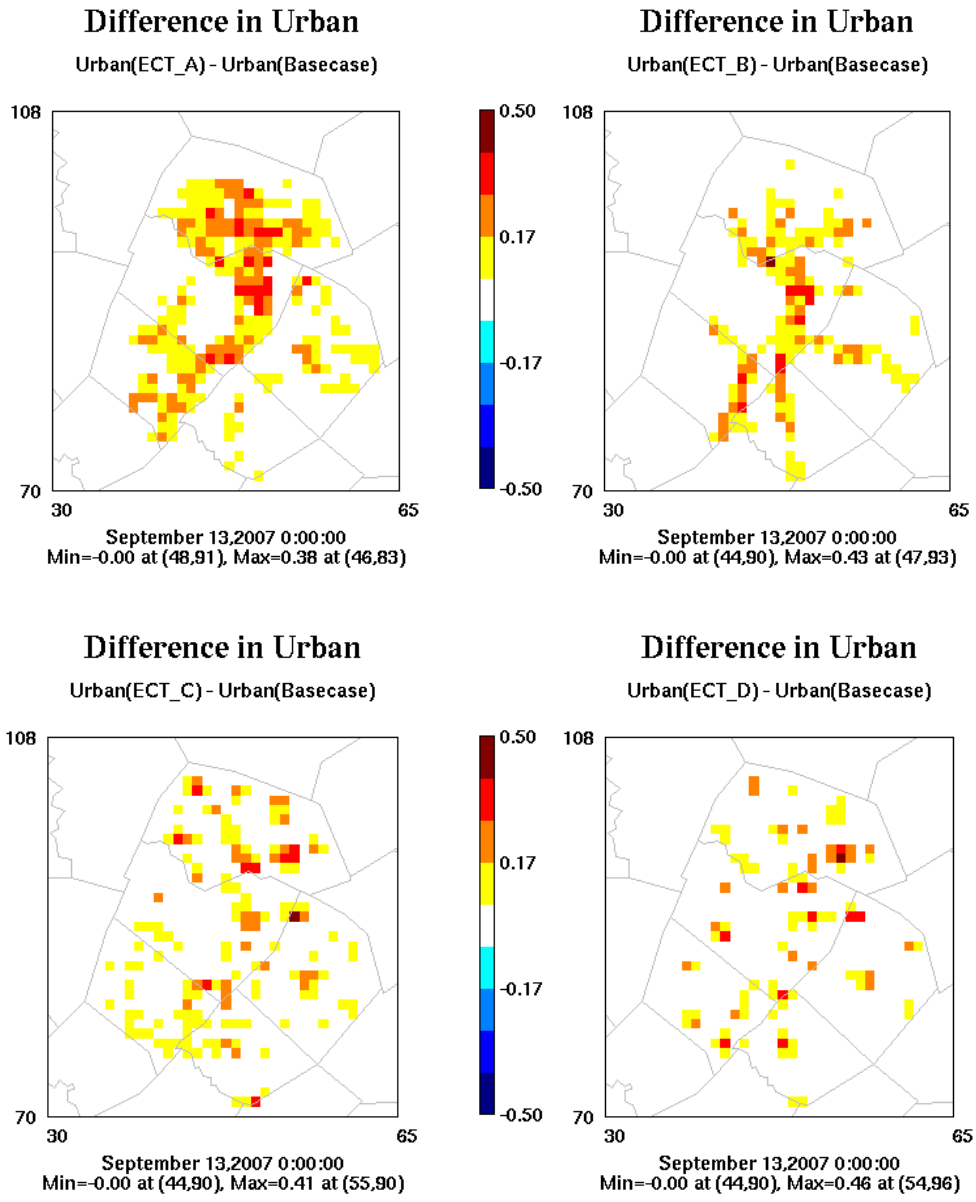

Figure 3-6. Areal fraction difference in (a) CAMx land cover areal fraction between ECT Scenario A and the Basecase; (b) Areal fraction for the Urban land cover category between the various ECT Sceanrios and the Basecase. A value of 1.0 indicates a 100% increase in the corresponding land cover category, while a value of -1.0 indicates a 100% decrease in the corresponding land cover category. *Note*: the changes in other categories, such as Agricultural, Coniferous forest/wetland, Water, Barren land, Non-forested wetlands, were Rocky, are negligible

3.2.3 Photochemical Modeling

Concentrations of air pollutants were predicted using the Comprehensive Air Quality Model, with extensions (CAMx; Environ, 2005). This model is used by the State of Texas in developing air quality management plans. CAMx and similar eulerian photochemical grid models simulate emission, advection, dispersion, chemical transformation and physical removal of air pollutants in the framework of a 3-dimensional grid. The modeling episode is from September 13th to September 20th, 1999, representing the meteorology for typical ozone exceedance days. This modeling episode has been used in by the Austin Metropolitan area and the State of Texas in the evaluation of emission control strategies. The analyses were part of the development of an Early Action Compact for attaining the National Ambient Air Quality Standard for ozone, with concentrations averaged over 8 hours (CAPCO, 2004a). As shown in Figure 3-7, three nested regional and urban scale domains were used; the Regional domain (36km), East Texas subdomain (12km), and Austin subdomain (4km). Details of the model development for Austin Metropolitan area are provided in "Development of the September 13-20, 1999 Base Case Photochemical Model for Austin's Early Action Compact", submitted by The Capital Area Planning Council to the Texas Commission on Environmental Quality and the U.S. Environmental Protection Agency, March 2004 (CAPCO, 2004b).

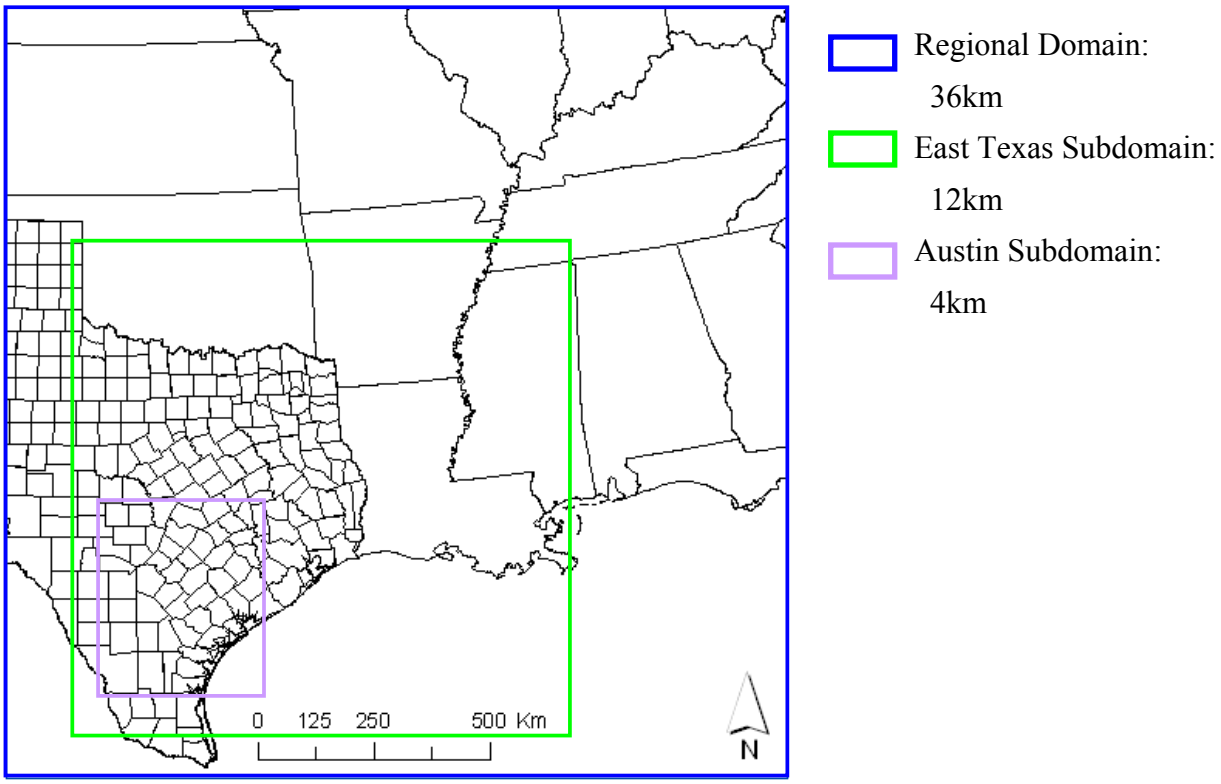

Figure 3-7. Air quality modeling domain: The domain's horizontal structure consists a coarse grid regional domain (36km by 36km resolution) and three nested fine grid subdomains; an East Texas subdomain (12km by 12km), Houston/Galveston-Beaumont/Port Arthur subdomain (4km by 4km), and Austin subdomain (4km by 4km)

Wind field inputs were estimated by the Texas Commission on Environmental Quality (TCEQ) using the MM5 meteorological model. In accordance with US EPA guidance, MOBILE6.2 was used to develop 1999 and 2007 onroad mobile source emissions, and US EPA's NONROAD 2005 model was used to develop nonroad mobile source emissions for both years. Development of biogenic emission inventories was described in Section 3.2.1. Modeling was conducted using the September 13-20, 1999 CAMx modeling episode with Austin's predicted 2007 emission inventory which will show the area is in attainment or non-attainment with the 8-hour NAAQS.

3.3 RESULTS

Predictions of isoprene emissions and 1-hour averaged ozone concentrations using the new land use/land cover dataset, referred as ECT Scenarios, were compared to predictions based on the original land cover dataset, referred as the Basecase. Since the first two days of the modeled episode, September 13th and 14th, were used for model 'spin-up', results of these days are not included.

3.3.1 Contribution of Biogenic Emissions to O_3 Concentration Changes

The difference in predicted daily isoprene emissions during episode days are presented in Table 3-5. The differences in land use/land cover led to 1 to 6% reductions in daily biogenic emissions in the 5-county area that includes Austin. ECT Scenario A showed the largest differences, as compared to the Basecase. If the percentage change in biogenic emissions is restricted to grid cells that experienced land cover changes, the percentage reductions are larger, ranging from 5 to 11%, as shown in Table 3-6. ECT Scenario A shows the largest reductions.

Table 3-5. Percent decrease in isoprene emissions, compared to Basecase emissions, using different ECT Scenarios for the 5 county MSA (Austin area)

	Units	Date in September, 1999								
		13	14	15	16	17	18	19	20	**Avg.**
Basecase	Mmoles day^{-1}	1.5	2.1	1.8	1.5	1.9	2.2	3.0	1.9	**2.0**
ECT Scenario A	%	5.4	5.5	5.4	5.3	5.3	5.4	5.5	5.2	**5.4**
ECT Scenario B	%	2.6	2.6	2.6	2.6	2.6	2.6	2.6	2.5	**2.6**
ECT Scenario C	%	2.6	2.7	2.6	2.9	2.6	2.6	2.6	2.5	**2.6**
ECT Scenario D	%	1.6	1.6	1.5	1.5	1.3	1.5	1.6	1.5	**1.5**

Note: % difference is defined as $\frac{\text{Basecase ISOP emiss} - \text{Scenario ISOP emiss}}{\text{Basecase ISOP emiss}} \times 100$

Table 3-6. Percent decrease in isoprene emissions in cells that have LULC changes, compared to Basecase emissions, using different ECT Scenarios for the 5 county MSA (Austin area)

	Units	Date in September, 1999								
		13	14	15	16	17	18	19	20	**Avg.**
ECT Scenario A	%	10.4	10.2	10.3	10.1	10.4	10.7	10.8	10.8	**10.5**
ECT Scenario B	%	4.5	4.4	4.8	4.1	4.5	4.6	4.7	4.7	**4.5**
ECT Scenario C	%	6.4	6.0	6.4	5.7	6.0	6.1	5.9	6.2	**6.1**
ECT Scenario D	%	7.2	7.8	8.4	7.5	7.4	7.3	7.7	7.6	**7.6**

Note: % difference is defined as $\frac{\text{Basecase ISOP emiss} - \text{Scenario ISOP emiss}}{\text{Basecase ISOP emiss}} \times 100$

The spatial distribution of changes in isoprene emissions, in the 5-county MSA, on September 20, 1999, is shown in Figure 3-8. Isoprene emissions decrease in locations where land covers have become more urban.

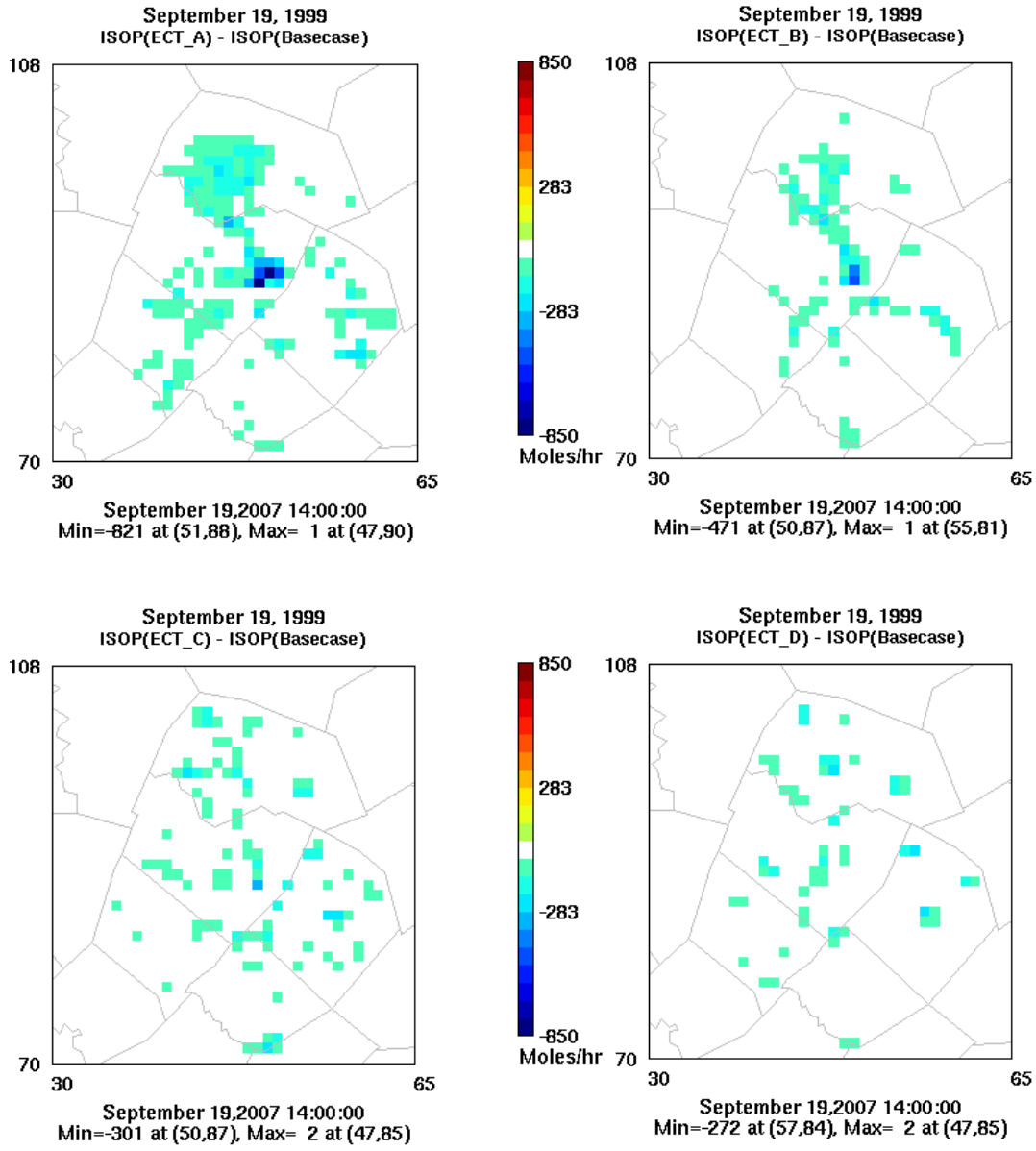

Figure 3-8. Difference in isoprene emissions between ECT Scenarios and the Basecase

The reductions in biogenic emissions led to reductions in maximum ozone concentrations (Figure 3-9). Reductions in daily maximum ozone concentrations, due to decreases in biogenic emissions associated with increased urbanization, ranged from 0.024 to 0.99 ppb, with typically values of 0.26 ppb for the Austin area.

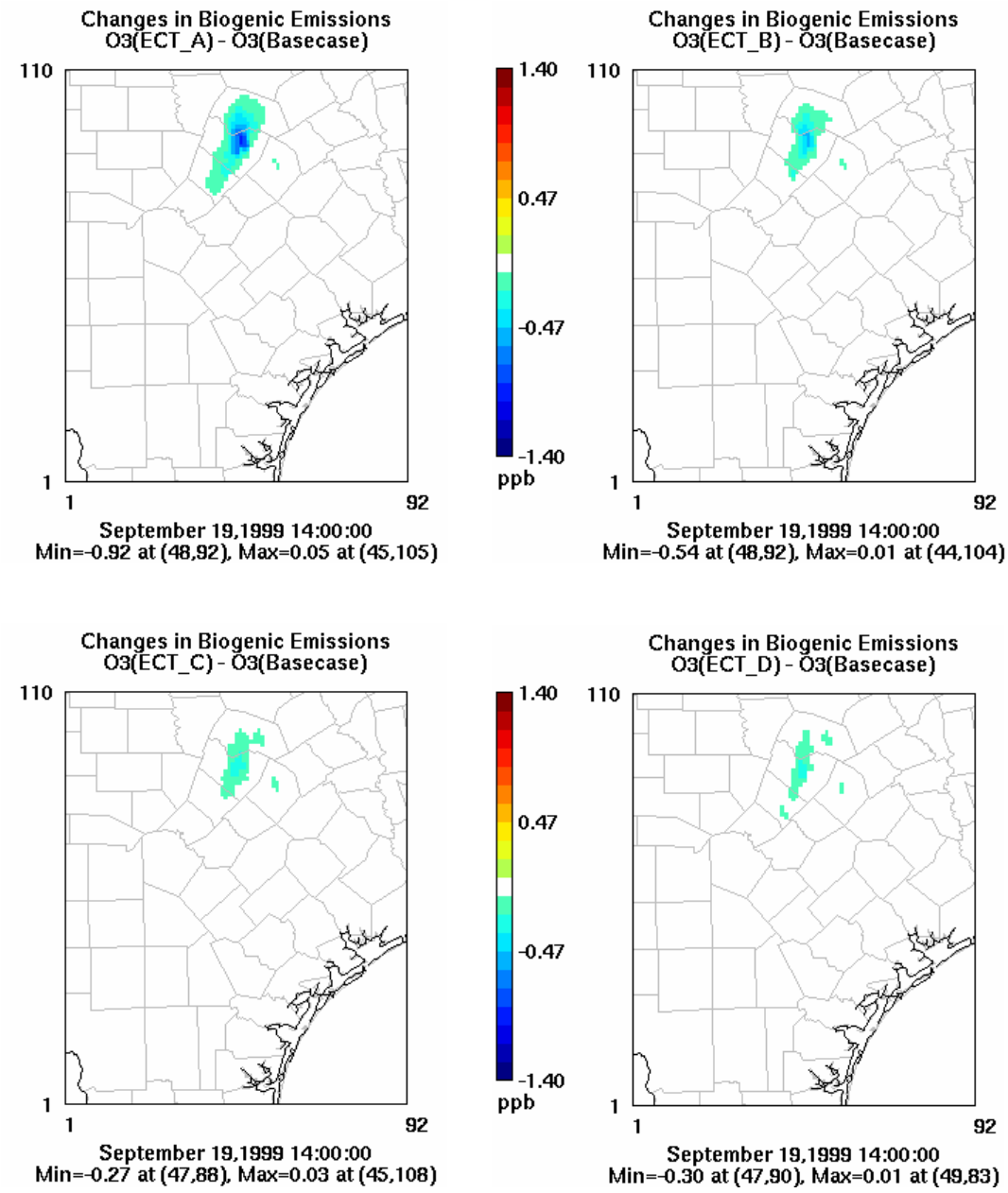

Figure 3-9. Difference in ozone concentrations between ECT Scenarios and the Basecase due to changes in biogenic emissions

3.3.2 Contribution of Dry Deposition to O_3 Concentration Changes

The corresponding differences in deposition velocities due to development led to decreases in ozone concentrations of up to 1.4 ppb. Maximum decreases occurred during early morning and late night hours. In contrast, changes in deposition velocities led to increases in daytime ozone concentrations. Maximum increases in daytime ozone concentrations due to changes in deposition velocities were 0.53 ppb. Figure 3-10 shows the spatial distribution of changes in estimated ozone concentrations, compared to the Basecase, due to changes in deposition velocities.

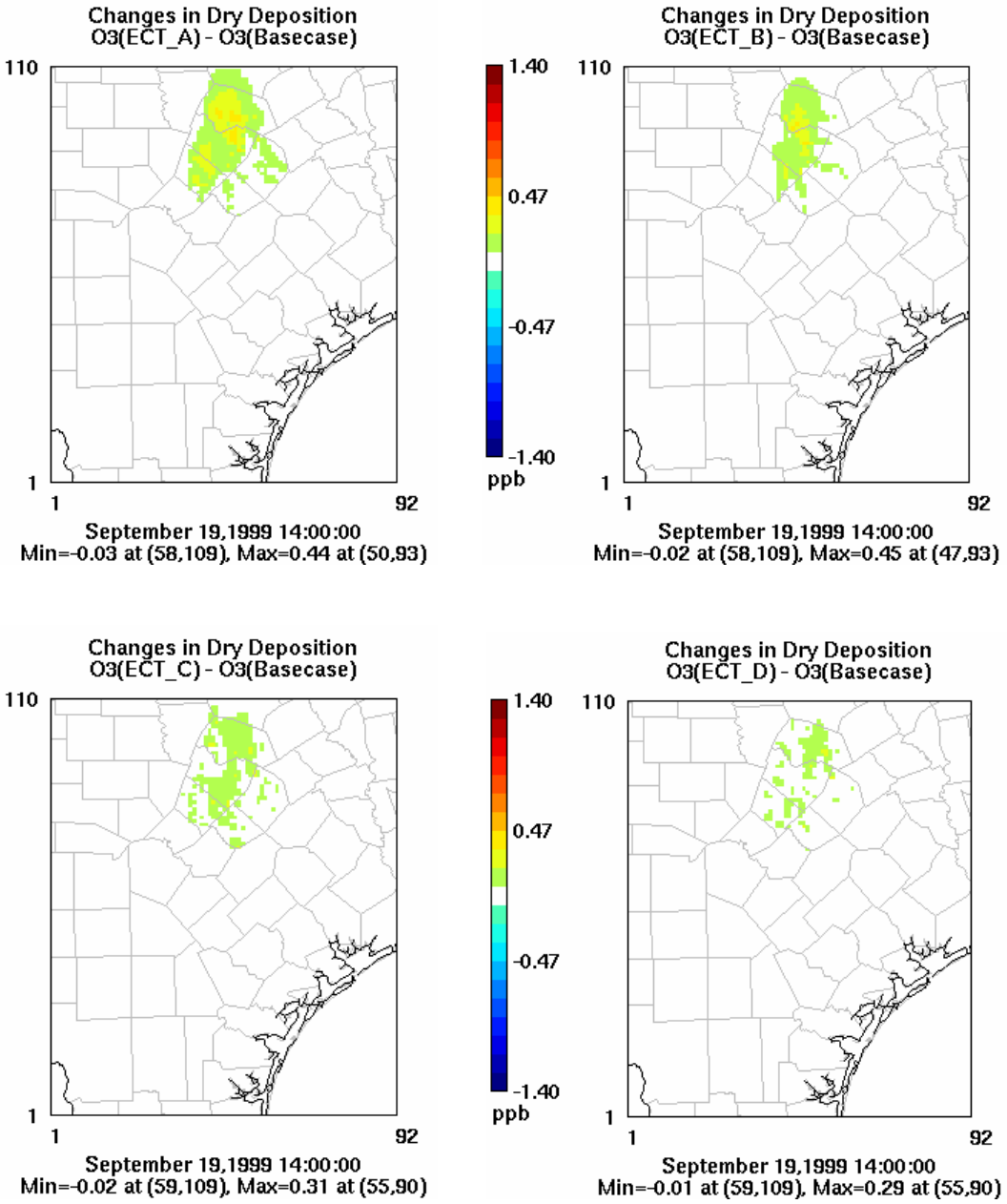

Figure 3-10. Difference in ozone concentrations between ECT Scenarios and Basecase due to changes in dry deposition

3.3.3 Combined Contribution of Biogenic Emissions and Dry Deposition to O_3 Concentration Changes

Combined, the effects of land cover changes on biogenic emissions and deposition velocities result in afternoon increases in ozone concentrations of up to 0.31 ppb (Figure 3-11), but decreases in ozone concentrations of approximately 1.4 ppb at the locations where peak ozone concentrations are predicted to occur in the afternoon.

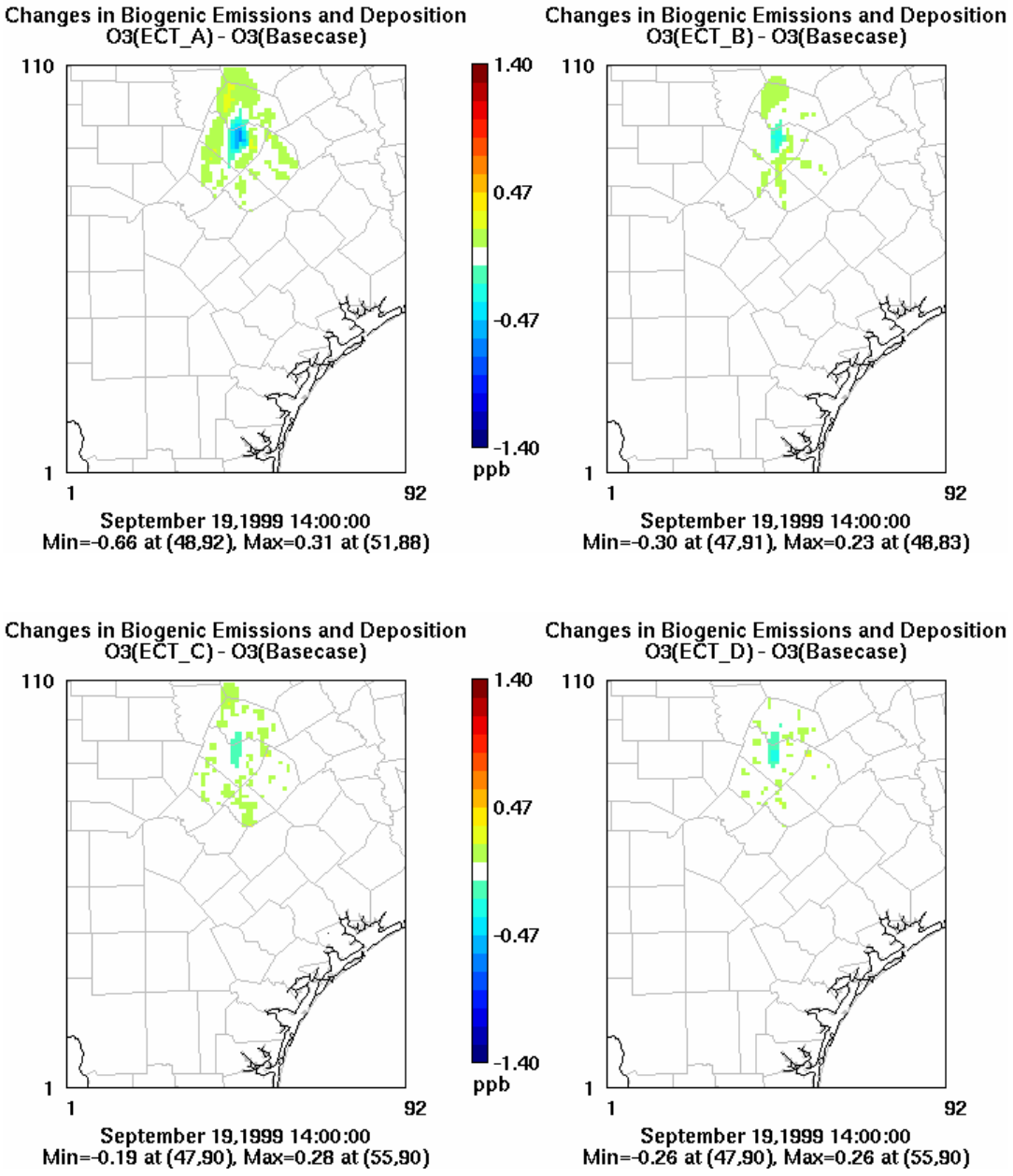

Figure 3-11. Difference in ozone concentrations between ECT Scenarios and Basecase with changes in both emissions and dry deposition

These impacts are comparable in magnitude to emission control strategies adopted as part of Austin's Early Action Compact. To put these results in context, reducing 50% of anthropogenic NOx emissions leads to a decrease in maximum 8 hour ozone concentrations of 5 ppb on high ozone days. Additionally, reducing 50% of anthropogenic VOC emissions leads to a decrease in maximum 8 hour ozone concentrations of 1 to 2 ppb (CAPCO, 2004a).

3.4 REFERENCES

The Capital Area Planning Council (CAPCO). "Photochemical modeling for Austin's Early Action Compact: Analysis of emission control strategies for ozone precursor." Submitted to U.S. EPA and TCEQ in March 2004a. Available at http://www.capco.state.tx.us/CAPCOairquality/Documents/eac_basecase_milestone_controlstrategy_03252004.pdf.

ENVIRON International Corporation "Users Guide to the Comprehensive Air Quality. Model with Extensions (CAMx) version 4.03." Available at http://www.camx.com, 2005.

Guenther, A. B., Zimmerman, P. R., Harley, P. C., Monson, R. K., Fall, R. (1993) "Isoprene and monoterpene emission rate variability: Model evaluations and sensitivity analyses." *Journal of Geophysical Research* **98**(D7), 12609-12617.

Guenther, A., Archer, S., Greenberg, J., Harley, P., Helmig, D., Klinger, L., Vierling, L., Wildermuth, M., Zimmerman, P., Zitzer, S. (1999) "Biogenic hydrocarbon emissions and landcover/climate change in a subtropical savanna." *Physics and Chemistry of the Earth Part B-Hydrology Oceans and Atmosphere* **24**(6), 659-667.

McDonald-Buller, E., Eusebi, A., Russel, M., Quigley, C., Hill, A., Allen, D. "Impacts of regional control strategies on air quality in eastern and central Texas." The Texas Natural Resources Conservation Commission Contract No. 988077600. 12100 Park 35 Circle, Austin, TX, 1999.

McDonald-Buller, E., Wiedinmyer, C., Kimura, Y., Allen, D. (2001) "Effects of land use data on dry deposition in a regional photochemical model for eastern Texas." *Journal of the Air and Waste Management Association* **51**(8), 1211-1218.

Parmenter, B., Kim, J.O. (2005) Personal communication.

Texas Commission on Environmental Quality (TCEQ). Houston/Galveston Air Quality Science Evaluation. Air Quality Modeling Files. CAMx Modeling Files. Files last updated December 2003. Available at http://www.tceq.state.tx.us.

Vizuete, W., Junquera, V., McDonald-Buller, E., McGaughey, G., Yarwood, G., Allen, D. (2002) "Effects of temperature and land use on predictions of biogenic emissions in Eastern Texas, USA." *Atmospheric Environment* **36**(20), 3321-3337.

Wesely, M.L. (1989) "Parameterization of surface resistances to gaseous dry deposition in regional-scale numerical-models." *Atmospheric Environment* **23**(6), 1293-1304.

Walmsley, J.L., Wesely, M.L. (1996) "Modification of coded parametrizations of surface resistances to gaseous dry deposition." *Atmospheric Environment* **30**(7), 1181-1188.

Wiedinmyer, C., Strange, I.W., Estes, M., Yarwood, G., Allen, D. (2000) "Biogenic hydrocarbon emission estimates for north central Texas." *Atmospheric Environment* **34**(20), 3419-3435.

Wiedinmyer, C., Guenther, A., Estes, M., Strange, I. W., Yarwood, G., Allen, D. T. (2001) "A land use database and examples of biogenic isoprene emission estimates for the state of Texas, USA." *Atmospheric Environment* **35**(36), 6465-6477.

Yarwood, G., Wilson, G., Shepard, S., Guenther, A. "User's guide to the Global Biosphere Emissions and Interactions System – Version 3.1." 101 Rowland Way, Suite 220, Novato, California. Available at http://www.globeis.com, 1999a.

Yarwood, G., Wilson, G., Emery, C., Guenther, A. "Development of the GloBEIS – A state of the science biogenics emissions modeling system." Final Report to the Texas Natural Resource Conservation Commission, 12100 Park 35 Circle, Austin, Texas 78753, 1999b.

Chapter 4: Impacts of Urbanization on Anthropogenic Emissions

4.1 INTRODUCTION

Urban development impacts predictions of air quality and human exposure through the spatial and temporal allocation of biogenic and anthropogenic emissions and other mechanisms. Anthropogenic emission inventories are typically classified into four sectors:

1. Point sources: stationary commercial or industrial operations that emit more than state or federal threshold limits of ozone precursors.
2. Area sources: stationary point sources that are too small (individual emission levels fall below thresholds for point sources) or numerous to be surveyed and characterized individually, including solvent utilization, stationary source fuel combustion, industrial processes, storage and transport, waste disposal and recycling. Emission from these sources are estimated collectively and spatially allocated according to surrogates such a population or income.
3. On-road mobile sources: regulated vehicle types including light-duty gasoline vehicles, light-duty gasoline trucks, light-duty diesel vehicles, heavy-duty diesel vehicles, and motorcycles that operate on public highways and roadways.
4. Non-road mobile sources: mobile sources operating off public roadways including locomotives, aircraft, recreational boats, lawn and garden equipment, agricultural equipment, and small engines used in industrial and construction operations.

Changes in population, demographic, and employment patterns have complex influences on emission forecasts. Population increases typically introduce more housing units (both single-family and multi-family homes) and industrial/commercial buildings to a community which may lead to increases in activity and emissions associated with sources such as lawn and garden equipment and dry cleaners, but activity and emissions associated with farming and agricultural equipment may decrease as the land use changes. Projections of emissions from point and area sources are typically developed through the application of socioeconomic growth factors and models of economic activity dynamics. Models such as the Economic Growth Analysis System (EGAS), which is based on Regional Economic Models, Inc. (REMI) and Bureau of Economic Analysis (BEA) forecasts, have been used to generate growth factors for area and point sources, in the absence of factors generated from local economic and demographic activity data. Projections of emissions from mobile sources are based on engine technology, fleet turnover, and activity or vehicle miles traveled (VMT).

McDonald-Buller *et al*. (2005) examined the relative impacts of urbanization on air quality due to changes in the transportation network for each of the ECT scenarios, and the methodology is described in Appendix B. This chapter examines the effects of urbanization on non-road mobile source and area source emissions, compares the changes in air quality due to these sources with those due to changes in the transportation network, and contrasts the relative air quality impacts due to changes in biogenic emissions and dry deposition, discussed in the previous chapter, with those due to anthropogenic emissions. Because the assessment of future energy needs in Texas is on-going, forecasts of point source emissions were not addressed within the framework of this project.

4.2 COUNTY-LEVEL NON-ROAD MOBILE AND AREA SOURCE EMISSION INVENTORY DEVELOPMENT

This study required the development of non-road mobile and area source emissions for the Base Case modeling episode and for four future 2030 ECT scenarios. The results for the ECT scenarios are contrasted with a Base Case that included 2007 emission inventories for anthropogenic sources, emission controls adopted for Austin's Early Action Compact, and a biogenic emissions inventory and dry deposition estimates based on a land cover/land use database developed by Wiedinmyer *et al*. (2000, 2001). The photochemical modeling for the Base Case and all of the ECT scenarios used meteorology from a September 13-20, 1999 historical ozone episode that was used for Austin's Early Action Compact. Only the emission inventories changed between scenarios, no changes were made to the meteorological modeling and other inputs to the air quality model.

4.2.1 Non-Road Mobile Sources

4.2.1.1 Emissions Modeling Methodology

The non-road mobile source emission inventory for the 5-county Austin area was developed primarily from the EPA's NONROAD Mobile Model version 2005 (NONROAD 2005) with the exception of emissions from locomotive, aircraft, military service operations, and gas cans. In 2003, EPA allowed the use of the draft NONROAD model version 2002a for development of non-road emission inventories supporting State Implementation Plans (SIPs). The model was updated in 2004 to incorporate Tier 4 non-road diesel engine standards and other standards. The model was recently updated to NONROAD 2005. Compared to the draft NONROAD 2004 model, several emission categories were added or updated (*e.g.*, new evaporative categories were added), along

with spatial allocations (*e.g.*, allocations were updated using 2002 population and household estimates from the U.S. Census Bureau) for the 2005 version of the model. Details on the development of the NONROAD model can be found at EPA website (http://www.epa.gov/OMSWWW/nonrdmdl.htm). The NONROAD 2005 model can be used to calculate past, present, and future emissions in locations throughout the United States. In estimating future emission inventories, growth and scrappage rates for equipment are applied. In the model, exhaust emissions are estimated as follows:

$$E_{Exhaust} = EF_{Exhaust} \cdot A \cdot L \cdot P \cdot N$$

where $E_{Exhaust}$ is the exhaust emission inventory (tons day^{-1}), $EF_{Exhaust}$ is the emission factor (tons hp^{-1} hr^{-1}), A is the equipment activity (operating hr yr^{-1}), L is the loading factor which is described as average proportion of rated power used during operation (%), P is the average rated power (hp), and N is the equipment population (dimensionless).

In order to calculate and spatially allocate emissions, the NONROAD model requires data on fuel specification, ambient temperature conditions, spatial and temporal allocation, deterioration factors, emissions factors, equipment population, equipment activity, average lifetime, growth factors, and technology types. Non-road emissions are influenced by the composition of the fuel, the effectiveness of existing controls, and ambient temperature conditions. Although Stage II controls used in the model are designed to reduce emissions during refueling due to vapor displacement, EPA currently has no data on the Stage II control effectiveness for non-road equipment. The value of 0% for the control effectiveness was used in this study. Modeling parameters for fuel specification and Stage II control effectiveness are provided in Table 4-1. These values were used for the Base Case and for the ECT scenarios.

Table 4-1. Modeling parameters for fuel specification and Stage II control effectiveness

Parameters	Units	Value
Fuel RVP of gasoline	Psi	7.5
Oxygen weight of gasoline	%	0.0
Gas sulfur	%	0.0166
Diesel sulfur	%	0.0364
CNG/LPG sulfur	%	0.003
Stage II control effectiveness	%	0.0

Source: Pavlovic, 2006; Personal communication

Both weekday and weekend temperature data were calculated from the National Weather Service (NWS) database and from the TCEQ ambient monitoring database (shown in Table 4-2). Maximum, minimum, and average temperatures for weekdays in the model were obtained from weekday temperatures (*i.e.*, from every weekday, every monitoring site) measured during the modeling episode, September 13-19, 1999; while these data for weekends were obtained from measured weekend temperatures during the same period. The temperature data used in the NONROAD model are presented in Tables 4-3 and 4-4.

Table 4-2. Monitoring sites used to create the NONROAD 2005 temperature database

Database	Monitoring site	Site ID
TCEQ	Austin Northwest	C3
	Audubon	C38
	San Marcos Airport Dr.	C62
NWS	Austin-Bergstrom International Airport	13904
	Austin City	13958

Table 4-3. Weekday temperature data used in the NONROAD 2005 model for Austin. These data are minimum, maximum, and average temperatures measured on weekdays during September 13-20, 1999

Parameters	Units	Value
Minimum temperature	°F	54.02
Maximum temperature	°F	100.05
Average temperature	°F	79.12

Table 4-4. Weekend temperature data used in the NONROAD 2005 model for Austin. These data are minimum, maximum, and average temperatures measured on weekends during September 13-20, 1999

Parameters	Units	Value
Minimum temperature	°F	60.12
Maximum temperature	°F	96.15
Average temperature	°F	80.05

For most other modeling parameters, with the exception of equipment population and equipment activity, default values for the temporal allocation of emissions, average equipment lifetime, deterioration factors, emission factors, growth factors, and technology types were derived from national averages. National to county-level spatial allocation factors in the model were adjusted with local data and demographic projections for the ECT scenarios. Development of each modeling parameter is described below.

Default temporal allocations for specific source categories in NONROAD 2005 were obtained by the EPA from available survey data. For categories without available survey data, the temporal allocation was based either on EPA's assessment of typical usage patterns or the temporal activity fractions from the California Air Resources Board (ARB) OFFROAD model (Details are provided in EPA420-P-04-015). An example of the default temporal allocation fraction for residential/commercial lawn and garden equipment is shown in Figure 4-1.

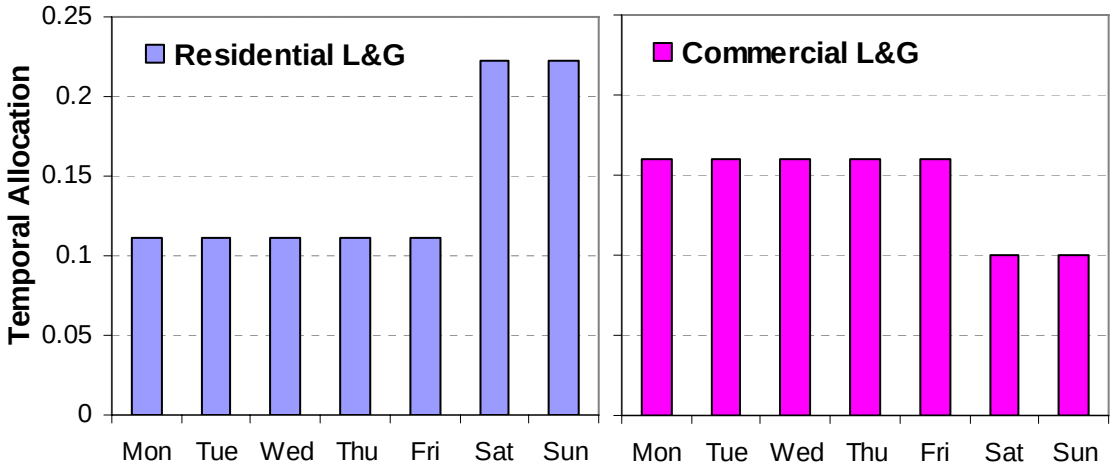

Figure 4-1. Default weekday and weekend activity allocation fraction for residential/commercial lawn and garden equipment. Note that the allocation fraction for lawn and garden equipment was obtained from survey conducted by Systems Applications International, Inc. (SAI) in 1993

Default emission factors in the NONROAD model were primarily based on the EPA's Small Engine Model (EPA420-R-05-019). Emission factors in the NONROAD model are available for different applications and engine sizes, and incorporate emission standards, such as Phase 1 and Phase 2 for spark-ignition engines.

As the lifetime of an engine increases, the engine's exhaust emissions performance may degrade. The term "deterioration factor" refers to the ratio of emissions from a piece of equipment at its median life versus when it is new. This deterioration factor is used to estimate the emission factor for an aged engine as follows:

$$EF_{aged} = EF_{new} \times DF$$

where EF_{aged} is the emission factor for an aged engine, EF_{new} is the emission factor for a new engine, and DF is the deterioration factor. Since the deterioration factor depends on the engine type and the technology type, the deterioration factor is available according to the design of the engine and its emission control technology regardless of its application. Details on the development of the deterioration factor for spark-ignition engine are provided in EPA420-R-05-023.

Default average lifetime estimates in the NONROAD model were originally adopted from the Energy and Environmental Analysis 1997 documentation for the California Air Resources Board (CARB) OFFROAD model with modifications for diesel engines, small gasoline engines, and recreational equipment by EPA (Details are provided in EPA420-P-04-005).

Both equipment population and activity were originally developed by TCEQ and modified by CAPCOG (Pavlovic, 2007). The base year for the equipment population ranged from 1996 to 2000 depending on the engine type. This base year equipment

population is used to estimate future year equipment populations in the NONROAD model. The equipment activity file provides the yearly emission for each engine type.

National growth factors were used to obtain future emission projections for each emission source category with the exception of emissions from airport service operations, military service operations, locomotive service operations, and gas cans. National growth factors are typically derived from actual growth indicators, such as human population or employment, but do not account for state and county-level differences. An example of growth factors for lawn and garden equipment is presented in Figure 4-2.

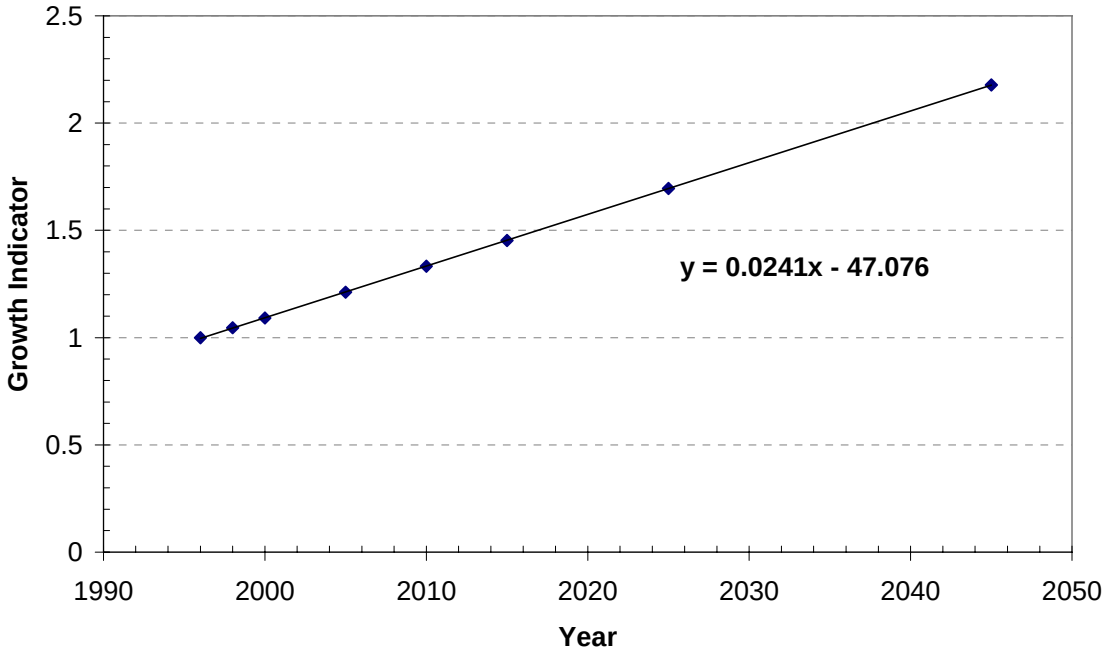

Figure 4-2. Growth factors for total lawn and garden (SIC 0782) which include diesel, gasoline, LPG, and CNG engine types; Base year is 1996

The NONROAD model also accounts for emission standards (or technology types) for each category of new non-road engines. Table 4-5 summarizes adopted emission standards for each non-road equipment category.

Table 4-5. Regulations adopted in NONROAD model

Engine type	Source Category	Control	Engine size	Reduction	Phase-in
Diesel	Agricultural, construction, and industrial equipment	Tier 1	All engine size	NOx by 30%	1996~2000
		Tier 2	All engine size	NOx by 60% from Tier 1 emission levels	2001~2006
		Tier 3	Engine size: 37kW~560kW		2006~2008
		Tier 4	All engine size	PM and NOx by 90%	2008~2015
Small Spark-Ignition	Lawn and garden equipment	Phase 1	Engine size <19kW	HC by 32%	1997~2001
		Phase 2	Engine size <19kW Non-handheld	HC and NOx by 60%	2001~2007
			Engine size <19kW Handheld	HC and NOx by 70%	2002~2007
Large Spark-Ignition	Industrial equipment		Engine size > 19kW	NOx, HC, and CO by 90%	2007~
Special Spark-Ignition	Recreational vehicles		-	HC by 67%, and CO by 28%	2006~

Source: "Reducing Air Pollution from Nonroad Engines" (EPA420-F-03-011, April 2003; http://www.epa.gov/otaq/cleaner-nonroad/f03011.pdf)

NONROAD uses several spatial allocation factors to allocate from state-level equipment populations to county-level equipment populations as shown in Table 4-6. For example, state-level emissions from residential lawn and garden equipment are spatially allocated by the number of single- and double- family households; whereas state-level emissions from commercial lawn and garden equipment are allocated by the number of employees in landscaping services. Spatial allocation factors that were modified for this study are designated by an 'X' in Table 4-6.

Table 4-6. Lists of Spatial allocation factors used to allocate from state-level equipment populations to county-level equipment populations. The 'X' indicates adjusted spatial allocation factors for the Base case and the ECT Scenarios

Category	Description	Modification
AIR	Tons of aircraft NOx	
HOU	Number of single and double (duplex) family housing	X
LSC	Employees in landscape horticulture services	
CON	Dollars spent in construction	
FRM	Harvested cropland in farming industry	
COM	Number of wholesale establishments	
MFG	Employees in manufacturing industry	
LOG	Employees in lumber and wood products	
OIL	Employees engaged in oil and gas extraction	
RVP	Number of camps and recreational vehicle park establishments	
GC	Number of public golf courses	
POP	Human population	X
MIN	Employees engaged in coal mining	
SNM	Snowmobiles: state registration, county snowfall and inverse human population	
SBR	Snowblowers residential	
SBC	Snowblowers commercial	
WIB	Recreational marine state fuel consumption, county water surface area inboard	
WOB	Recreational marine state fuel consumption, county water surface area outboard	
RR	Railroads: tons of locomotive NOx	
txallcon	Diesel construction equipment	

Among the most important spatial allocation factors are human population and number of single- and multi-family households. Because the ECT scenarios are based on a doubling of population relative to 2001 levels, 2001 population and household were used as the basis for future projections. The 2001 demographic data were obtained from the U.S. Census Bureau web site (http://www.census.gov/popest/counties/tables/CO-EST2004-01-48.csv for population and http://www.census.gov/popest/housing/tables/HU-EST2003-04-48.csv for household) for Bastrop, Caldwell, Hays, Travis and Williamson counties as shown in Table 4-7 and Table 4-9.

Household data were developed by Fregonese Calthorpe and obtained from Smart Mobility, Inc. for each ECT scenario (Table 4-7). Average household size by county (*i.e.*, the average number of people living in a one unit household), shown in Table 4-8, was used to estimate the population shown in Table 4-9 for each ECT scenario. Due to differences in the average household size for each county, the total populations for the ECT scenarios are not identical; ECT Scenario C has the largest population in the 5 county Austin area.

Table 4-7. 2001 household and projected household for each ECT scenario by county. The number of households for 2007 (Base Case) were projected from 2001 household data using a national growth factor

Household	2001	ECT A	ECT B	ECT C	ECT D
Bastrop	22,723	52,621	72,309	92,180	72,108
Caldwell	12,188	24,171	41,742	59,652	41,698
Hays	37,946	81,690	84,607	90,271	85,005
Travis	353,272	556,367	507,621	447,476	494,382
Williamson	98,120	215,637	222,604	235,980	226,335
Total	524,249	930,486	928,883	925,559	919,528

Table 4-8. Average household size by county

County	Bastrop	Caldwell	Hays	Travis	Williamson
Average Household Size	2.87	2.98	2.92	2.53	2.88

Table 4-9. 2001 human population and projected human population for each ECT scenario by county

Population	2001 (U.S. Census Bureau)	ECT A	ECT B	ECT C	ECT D
Bastrop	61,480	151,023	207,527	264,555	206,950
Caldwell	33,808	72,029	124,390	177,762	124,261
Hays	104,514	238,536	247,051	263,590	248,215
Travis	842,638	1,407,609	1,284,282	1,132,114	1,250,786
Williamson	276,749	621,035	641,099	679,622	651,846
Total	1,319,189	2,490,231	2,504,349	2,517,644	2,482,059

Because emissions from airport, military, and railroad service operations, and gas cans are not included in the NONROAD model, these categories were estimated separately. Airport and military emissions were acquired from the Alamo Area Council of Governments (AACOG). There is one municipal airport in Austin, the Austin-Bergstrom International Airport (ABIA). AACOG estimated airport emissions from the Emissions and Dispersion Modeling System (EDMS) model, developed by the Federal Aviation Administration (FAA) in cooperation with the U.S. Air Force (USAF). The EDMS model calculates airport emissions from six major sources: aircraft, ground support equipment, service equipment, natural gas burning, parking lots/roadways, fuel storage, and fueling operations, based on information regarding the aircraft/engine/fuel/ground support equipment type, aircraft destination, and the duration of ground support equipment operations. ABIA was originally designed based on forecasts of future aviation demands up to 2020 (http://www.ci.austin.tx.us/austinairport/downloads/chp3mp.pdf). No additional growth was assumed for the current study, but airport activities will likely grow with future passenger demands.

For military service operations, one Army camp in Austin was considered, Camp Mabry, which encompasses approximately 375 acres. A 1999 base year emission inventory for Camp Mabry was developed from information regarding number of operating vehicles, fuel consumption, and natural gas consumption. Aircraft emissions from 107 small public-use airports were also considered. A detailed description of the emission inventory development on the airport and military is provided in the Austin-Round Rock MSA 1999 Ozone Precursor Emissions Inventory (CAPCOG, 2004; http://www.tceq.state.tx.us/assets/public/implementation/air/sip/sipdocs/2004-06-AUS/

04086sipapd_pro.pdf). Due to the uncertainty in future military operations and requirements, no additional growth was assumed for the current study.

Locomotive emissions were estimated based on the TCEQ report (Project #H018.2003, http://www.harc.edu/Projects/AirQuality/Projects/Projects/H018.2003). Locomotive emissions for 2007 and 2030 were generated from 2003 emissions. Similar to airport and military emissions, no growth was assumed for locomotive emissions for the current study. However, it is also important to note that the Trans-Texas Corridor (TTC; http://www.keeptexasmoving.com), a proposed multi-use, statewide transportation network in Texas planning to incorporate freight railways and high-speed commuter railways, may influence locomotive service operations in the State. The current study did account for the implementation of Federal emission controls; control factors of 16.5% and 40.1% reduction for 2007 and 2030, respectively, were applied to NOx emissions in accordance with Federal controls (Figure 4-3; CAPCO, 2004). Note that there are three separate sets of emissions standards for locomotives (effective in the year 2000); the first set of standards (Tier 0) apply to locomotives manufactured from 1973 to 2001; the second set (Tier 1) apply to locomotives manufactured from 2002 to 2004; and the third set (Tier 2) apply to locomotives manufactured in or after 2005 (effective in the year 2005) (EPA, 1997; http://www.epa.gov/otaq/regs/nonroad/locomotv/frm/42097048.pdf).

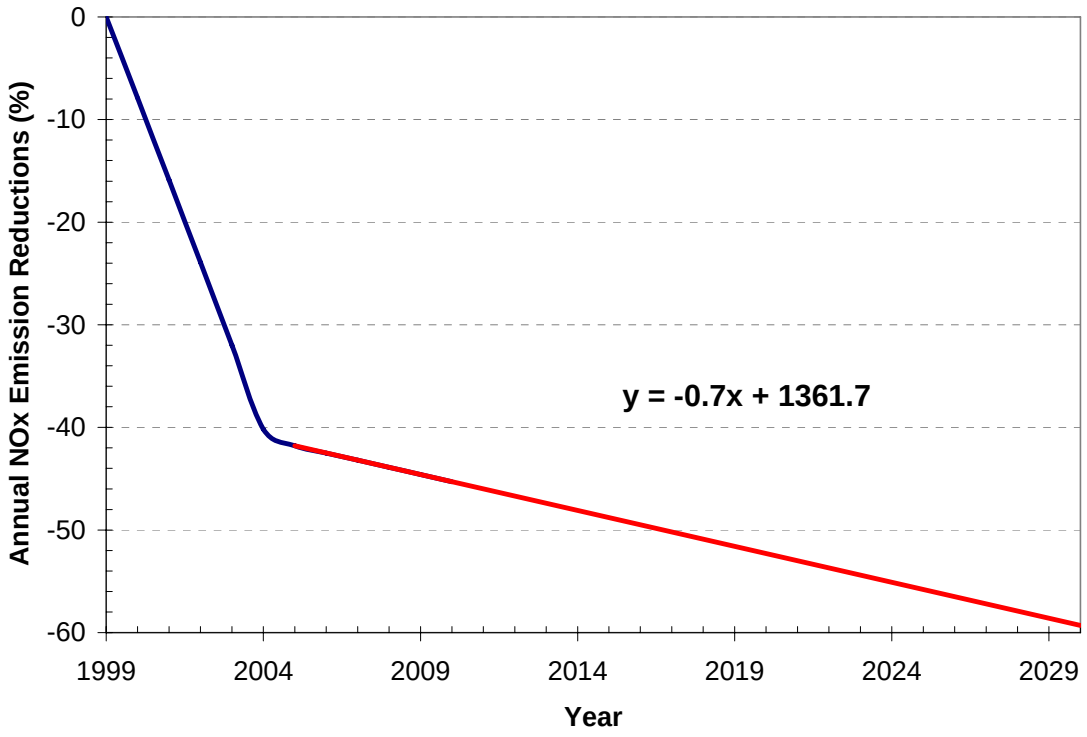

Figure 4-3. Annual NOx reductions for locomotive emissions by incorporating Tier 0, Tier 1, and Tier 2 emission standards (EPA, 1997); Base year is 2003 and further projected to 2030 assuming linear reductions beyond 2005 (http://www.capco.state.tx.us/capcoairquality/CAAP_Apps/App5-2Austin-RR%20Emission%20Reduction%20Strategies.pdf)

Emissions from gas cans were estimated from a study by Eastern Research Group for the TCEQ (Contract #: 582-0-34730-42, http://www.tceq.state.tx.us/assets/public/implementation/air/sip/sipdocs/2004-10-DAL/Appendix%20H.pdf). ERG estimated emissions for 2007 using a survey performed in 2002 of both residential and commercial gas cans. Residential and commercial gas can emissions for 2030 were projected from 2007 emissions using the household trends data. Based on the survey done by NuStats, Inc., several assumptions were made; 1) 72% of total households own residential gas cans, 2) all of residential gas cans were assumed to store gasoline; whereas 94% of

commercial gas cans store gasoline, and the remainder store diesel, 3) control factor of 62.4% reductions with 100% compliance rate were applied to VOC emissions for 2007 and 2030 in order to apply controls adopted in the State as part of the State Implementation Plan (Texas will implement controls on the design of new gas cans to reduce VOC emissions; reference EPA's Regulatory Documentation "Final Rule: Control of Hazardous Air Pollutant from Mobile Sources" February 2007), and 4) the estimated emissions were added to the emissions from the lawn and garden equipment category estimated by the NONROAD model (*i.e.*, residential gas cans were added to residential lawn and garden equipment, and commercial gas cans added to commercial lawn and garden equipment) due to the absence of an appropriate Source Classification Codes (SCC) for gas can category.

4.2.1.2 Non-Road Mobile Source Emission Estimates for the Five-County Austin Area

Predictions of non-road mobile source emissions for the four ECT scenarios were compared to those for the 2007 Base Case. The NONROAD model estimates emissions for six exhaust pollutants; hydrocarbon (HC), NOx, CO, CO_2, SOx, and particulate matter (PM). Hydrocarbons can be further broken down into total hydrocarbons (THC), total organic gases (TOG), non-methane organic gases (NMOG), non-methane hydrocarbons (NMHC), and volatile organic compounds (VOC). Among these exhaust pollutants, the emissions of VOC and NOx were considered in this study.

Weekday emission rates of VOC and NOx in tons per day calculated from the NONROAD 2005 model and from the airport, military, and locomotive operations, and gas cans are provided in Table 4-10.

Table 4-10. Weekday non-road mobile source emissions (tpd) of (a) VOC and (b) NOx for the 2007 Base Case and four ECT Scenarios

(a)

	VOC Emissions (tpd)				
	2007 Base Case	ECT A	ECT B	ECT C	ECT D
Agricultural	0.05	0.03	0.03	0.03	0.03
Commercial	2.05	2.44	2.48	2.48	2.44
Construction and Mining	1.75	1.08	1.08	1.08	1.08
Industrial	0.75	0.08	0.08	0.08	0.08
Lawn and Garden	13.41	16.63	18.37	18.36	16.57
Railway	0.22	0.22	0.22	0.22	0.22
Recreational	2.74	1.73	0.60	0.60	1.73
Airport	0.75	0.75	0.75	0.75	0.75
Military	0.34	0.34	0.34	0.34	0.34
Total	22.06	23.30	23.96	23.94	23.24

(b)

	NOx Emissions (tpd)				
	2007 Base Case	ECT A	ECT B	ECT C	ECT D
Agricultural	0.02	0.01	0.01	0.01	0.01
Commercial	0.53	0.48	0.48	0.48	0.48
Construction and Mining	11.89	2.40	2.39	2.39	2.38
Industrial	2.40	0.44	0.44	0.44	0.44
Lawn and Garden	1.36	1.53	1.69	1.69	1.52
Railway	3.14	2.25	2.25	2.25	2.25
Recreational	0.06	0.05	0.13	0.13	0.06
Airport	1.06	1.06	1.06	1.06	1.06
Military	1.23	1.23	1.23	1.23	1.23
Total	21.69	9.45	9.68	9.68	9.44

Note: ECT scenario emissions are calculated for 2030 future year

For the Base Case, VOC emissions for the five-county Austin area are dominated by emissions from lawn and garden equipment (61%), followed by recreational equipment (12%), and commercial equipment (9%). NOx emissions are dominated by emissions from construction and mining equipment (55%), followed by railway (14%), and industrial equipment (11%). For the ECT Scenarios, emissions from lawn and garden equipment (70%) play a larger role in the total VOC emission inventory; whereas NOx emissions are not dominated by one category. Total VOC emissions for the ECT

scenarios increased slightly relative to the Base Case. ECT Scenario B showed the largest differences in VOC emissions relative to the Base Case. Overall, NOx emissions for the ECT scenarios decreased substantially relative to the Base Case. A summary of VOC and NOx emissions by category and by county is provided in Appendix C.

Emissions from most non-road mobile source categories, with the exception of those from lawn and garden equipment, are less for the ECT scenarios than for the Base Case. The decrease in emissions are due to the phase-in of emission standards, especially for categories associated with industrial and construction/mining equipment; VOC and NOx emissions for those two categories decreased by 38-89% and by 81-82%, respectively. However, VOC and NOx emissions from lawn and garden equipment increased by 15-37% and by 12-24%, respectively. The increase in VOC emissions for lawn and garden equipment was primarily associated with emissions from gas cans, which were projected based on growth in the number of households. NOx emissions from lawn and garden equipment nearly doubled relative the Base Case because emission controls for most of 2-stroke lawn and garden equipment were either unavailable or the same between 2007 and 2030 and emission controls for some 4-stroke lawn and garden equipment, *e.g.*, lawn and garden tractors, were not incorporated into the NONROAD model.

Uncertainties with the future projections do exist. It was assumed that the non-road equipment population follows the national growth rate regardless of the location. If the 5-county Austin area experiences more rapid growth in the next 20 to 40 years, future non-road emissions will be greater than the values shown here. Although the spatial allocations of emissions for each ECT Scenario differ, for example according to population and number of households, equipment population growth rates for each ECT Scenario are the same. One would expect that using national growth rates results in

smaller differences between the ECT Scenarios, but detailed studies of equipment population trends were impractical for this study. It is also important to note that although emission controls for non-road mobile sources were either incorporated within the framework of the NONROAD model itself or applied for other categories that were not estimated by NONROAD model, unanticipated future federal or state emission controls may result in additional reductions.

4.2.2 Area Sources

As described above, area sources include stationary point sources that are too small or numerous to be surveyed and characterized individually. Emissions from these sources are estimated collectively and spatially allocated according to surrogates such a population or income. Because projecting area source emissions on an individual basis is challenging, these emissions are typically projected based on surrogates such as demographic trends, employment trends, or gasoline/oil consumption rates. The emission inventories for this project were adopted from the area source emission inventory developed by the Capital Area Council of Governments (CAPCOG), with assistance from the TCEQ, ERG, and ENVIRON International Corporation, for the Austin area's Early Action Compact. CAPCOG used growth factors, such as human population growth, the gasoline/oil consumption rate, the farm value (in dollars), and employment, to project 1999 area source emissions to obtain an emission inventory for the 2007 attainment year (http://www.tceq.state.tx.us/assets/public/implementation/air/sip/sipdocs/2004-06-AUS/04086sipape_pro.pdf). Federal and state standards were applied to area source emission categories shown in Table 4-11.

Table 4-11. Federal and state regulations adopted to estimate area source emissions

Engine type	Description	Area source Category	VOC Reduction	Phase-in
Federal Rules				
Architectural Coating [1]	Reduction of VOC emissions from architectural coating products	Solvent Utilization	20%	1999~
Auto Body Refinishing [1]	Controlling of VOC emissions from solvent evaporation through reformulation of coatings	Solvent Utilization	37%	2000~
State Rules and Local (5-county Austin) Emission Reduction Strategies				
Degreasing [2]	Controlling of VOC emissions from all new degreasing sources	Solvent Utilization	85%	2001~
Stage I [2]	Prevention of releasing gasoline vapors while gasoline is delivered to a storage tank	Service Stations	95%	Implement no later than 2005
Cutback Asphalt [2]	Restriction of using conventional cutback asphalt containing VOC solvents	Solvent Utilization	80%	2005~

[1] *Source*: "Austin-Round Rock MSA 2007 Future Year Ozone Precursor Modeling Emissions Inventory" (CAPCO, December 2003; http://www.capco.state.tx.us/_;;capcoairquality/DEC_31/AustinMSA_Future%20Year%20Emissions%20Inventory.pdf)

[2] *Source*: "Austin/Round Rock MSA 2007 Emissions Reduction Strategies" (CAPCO, March 2004; http://www.capcog.org/CAPCOairquality/CAAPApps/App5-2Austin-RR%20Emission%20Reduction%20Strategies.pdf)

Emission reductions were estimated by applying rule penetration (RP; the percentage of the area source category that is expected to be complying with the regulation), control efficiency (CE; the percentage of a source category's emissions that are controlled), and rule effectiveness (RE; the uncertainties that affect the actual performance of the control). For example, Stage I Vapor Recovery systems are required for gas stations with 25,000 gallons or greater capacity. These large gas stations represent 64.4% of the total gas stations in the Austin area in 2007. With an emission control efficiency of 95% reduction, the total VOC reduction in 2007 can be estimated as:

$$\text{Stage I VOC Emission Reduction in 2007} = \text{RP} \times \text{CE} \times \text{RE}$$
$$= (64.4\%) \times (95\%) \times (80\%) = 49\%$$

Note that EPA recommends a default value of 0.8 for RE, if the true value of RE is not available.

The 1999 area source emission estimates were developed 1) based on the EPA 1999 NEI Database; *e.g.*, industrial fuel combustion and waste disposal treatment/recovery; 2) by ENVIRON International, under contract to the TCEQ, based on the best available survey data for each area source category; *e.g.*, gasoline service stations and solvent utilization; 3) by allocating statewide consumption with the fraction between statewide and county-level employment (or population); *e.g.*, commercial and industrial LPG consumption; and 4) by multiplying employment/production/usage of each category by emission factors; *e.g.*, solvent degreasing, miscellaneous area source, consumer/commercial products. A detailed description of the development of the 1999 area source emission inventory is provided in Austin-Round Rock MSA 1999 Ozone Precursor Emissions Inventory (CAPCOG, 2004).

Area source emission inventories for each ECT scenario were developed for this study by projecting 2007 Base year area emissions with human population growth. Federal and state emission standards for architectural coating operations, auto-body refinishing, degreasing operations, and Stage I were applied. Weekday area source VOC and NOx emission rates for the Base Case and each ECT Scenario are provided in Table 4-12.

Table 4-12. Weekday area source emissions (tpd) for the 2007 Base Case and projected area source emissions for each ECT scenario: (a) VOC emissions and (b) NOx emissions

(a)

	VOC Emissions (tpd)				
	2007 Base Case	ECT A	ECT B	ECT C	ECT D
Agriculture Production	5.63	12.19	13.77	15.58	13.85
Fuel Storage and Transport	6.93	13.43	13.85	14.32	13.77
Industrial Processes	15.46	33.30	54.81	76.72	54.74
Miscellaneous Area Sources	2.05	4.38	4.96	5.62	4.97
Service Stations	20.84	40.17	40.78	41.55	40.52
Solvent Utilization	48.77	91.17	90.52	89.73	89.63
Stationary Source Fuel Combustion	0.18	0.32	0.31	0.29	0.30
Storage and Transport	0.93	1.82	1.87	1.93	1.86
Waste Disposal, Treatment, and Recovery	9.87	17.50	16.78	15.88	16.48
Total	110.66	214.28	237.64	261.62	236.13

(b)

	NOx Emissions (tpd)				
	2007 Base Case	ECT A	ECT B	ECT C	ECT D
Agriculture Production	5.12	11.05	12.33	13.82	12.41
Fuel Storage and Transport	0.004	0.01	0.01	0.01	0.01
Industrial Processes	0.16	0.38	0.56	0.73	0.55
Miscellaneous Area Sources	0.37	0.77	0.85	0.94	0.85
Stationary Source Fuel Combustion	4.35	8.06	7.99	7.90	7.90
Waste Disposal, Treatment, and Recovery	0.12	0.24	0.27	0.29	0.27
Total	10.12	20.51	22.00	23.70	21.99

Note: ECT scenario emissions are calculated for 2030 future year

For the Base Case, about half of total area source emissions originate from Travis County. In Travis County, VOC emissions are dominated by solvent utilization (*i.e.*, surface coating, degreasing, and dry cleaning) (55%), followed by service stations (20%) and waste disposal, treatment and recovery (14%); while NOx emissions are dominated by stationary source fuel combustion (*i.e.*, commercial, institutional, and residential natural gas: 75%), followed by agriculture production (21%).

Because area source emissions for the ECT Scenarios are projected using human population, they approximately double relative to the Base Case. However, each scenario is based on different spatial development patterns with different fractions of population for each county (*e.g.*, 57% and 45% of the total population live in Travis County for ECT Scenario A and C, respectively). Because ECT Scenario C has the largest total population, the largest differences in emissions relative to the Base Case are observed for ECT Scenario C. For ECT Scenario C, VOC emissions are dominated by solvent utilization (*i.e.*, surface coating, degreasing, and dry cleaning: 34%), followed by industrial processes (29%) and service stations (16%); while NOx emissions are dominated by agriculture production (58%), followed by stationary source fuel combustion (*i.e.*, commercial, institutional, and residential natural gas: 33%). Due to differences in the distribution of the population across each county, other ECT Scenarios do not always follow the same trends as ECT Scenario C. A detailed summary of VOC and NOx emissions from area sources by county is provided in Appendix C.

Similar to emission estimates for non-road mobile sources, uncertainties with the projection exist. There are other growth factors, such as gasoline/oil consumption that will show different growth patterns relative to human population. Unanticipated future federal or state emission controls may also result in additional reductions.

4.3 EMISSIONS PROCESSING FOR PHOTOCHEMICAL MODELING

The non-road mobile source and area source emission inventories described above are estimated as total VOC, NOx, and CO emissions by source category, by county, and by day. However, photochemical models require NOx and chemically speciated VOC emissions at hourly intervals and for each grid cell in the modeling domain. Consequently, county-level non-road mobile source and area source emissions were processed in three steps through the Emissions Preprocessor System 2 software (EPS2) designed by the EPA and Systems Application International to provide emissions in the appropriate format for commonly used photochemical models such as CAMx and the Urban Airshed Model (UAM):

1. Chemical speciation: speciates total VOC emissions to species used in the Carbon Bond Chemical Mechanism version 4 (CB-IV; Gery *et al.*, 1989) in CAMx. The CB-IV mechanism speciates organic compounds into a set of ten components based on their structure; OLE (Olefin), PAR (Paraffin), TOL (Toluene), XYL (Xylene), FORM (Formaldehyde), ALD2 (Higher aldehyde), ETH (Ethene), MEOH (Methanol), ETOH (Ethanol), and ISOP (Isoprene);
2. Temporal allocation: allocates emissions by hourly intervals;
3. Spatial allocation: spatially allocate emissions from a county-level to 4km × 4km modeled grid cells in each county.

Temporal allocation and chemical speciation profiles were assumed not to change for the ECT scenarios relative to the Base Case, the focus of this study, therefore, was on the spatial allocation of the emissions.

4.3.1 Spatial Surrogates for the 2007 Base Year

For both non-road mobile source and area source emission categories, county-level emissions were allocated to each model grid cell according to spatial surrogates. Because spatial surrogates are a strong function of LULC, spatial surrogates for the 2007 Base Case and four ECT scenarios were developed. Although there was an available spatial surrogate profile developed by ENVIRON International (2002) for Austin's Early Action Compact, more recent LULC was used to develop spatial surrogates for the 2007 Base Case for this study.

As shown in Table 4-13, fifteen surrogate categories are recognized by EPS2. In the gridded spatial allocation surrogate input file, the modeling domain definition (minimum easting, minimum northing, maximum easting, and maximum northing in LCP coordinate), size of each grid cell (4km for this study), FIPS code of state or county, the location of each grid cell (in LCP coordinate), and the fraction of each category in county totals (*i.e.*, area of specific grid cell / county area total) are required.

Table 4-13. Land use descriptions and codes recognized by EPS2

Gridcode	EPS2 surrogate
1	County Area
2	Population
3	Households
4	Urban
5	Agriculture
6	Range
7	Deciduous Forest
8	Coniferous Forest
9	Mixed Forest
10	Water
11	Barren
12	Non-forested Wetlands
13	Mixed Agriculture/Range
14	Rocky with Lichens
15	Rural

Population and household distributions were developed based on demographic data from the U.S. Census Bureau's 2000 TIGER/Line®. Webb (2007, Personal communication) combined these population and household data with the grid domain definition using ESRI ArcGIS software, and redistributed using an area weighting to obtain the total population and number of households for each grid cell in the modeling domain.

To develop the surrogate file for other EPS2 surrogate codes (*i.e.*, category 4 through 15), a Base Case LULC database was derived from three different datasets (Parmenter, 2006; Personal communication). The first dataset is a 2003 land use dataset from the City of Austin which encompasses about 4,510,440,200 m^2 in most of Travis County and some of Bastrop, Caldwell, Hays, and Williamson Counties (ftp://coageoid01.ci.austin.tx.us/GIS-Data/Regional/coa_gis.html). This Austin 2003 land use dataset was used as the primary land use dataset. Some of the remaining 5-county area was covered by a CAPCOG developed parcels dataset, which included approximately 620,150,400 m^2 in Bastrop, Caldwell, Hays, and Williamson Counties (http://www.capcog.org/Information_Clearinghouse/geospatial_main.asp). Finally, the area that was not covered by the Austin 2003 land use dataset or by the CAPCOG developed parcels data set was considered undeveloped. Surrogates for the undeveloped area were covered by the USGS 1992 National Land Cover Dataset (http://landcover.usgs.gov/natllandcover.php), which had a spatial resolution of 30 meters. Each dataset is shown in Figure 4-4.

(a)

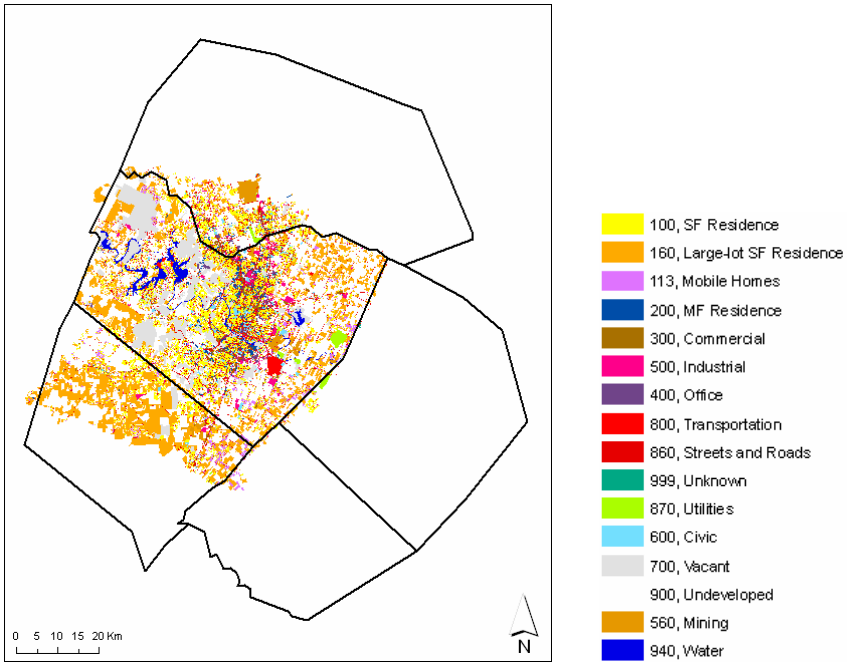
0 5 10 15 20 Km
N
100, SF Residence
160, Large-lot SF Residence
113, Mobile Homes
200, MF Residence
300, Commercial
500, Industrial
400, Office
800, Transportation
860, Streets and Roads
999, Unknown
870, Utilities
600, Civic
700, Vacant
900, Undeveloped
560, Mining
940, Water

(b)

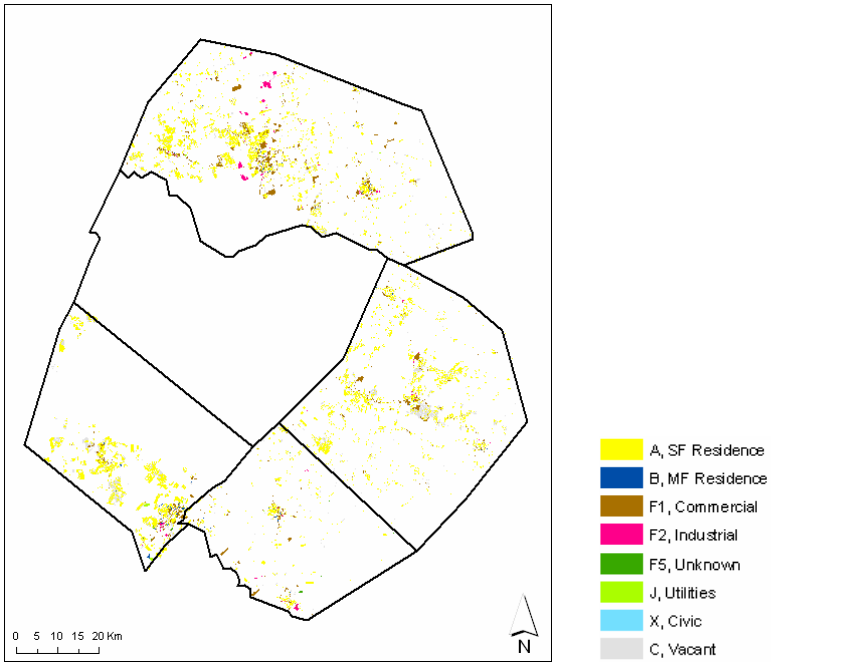
0 5 10 15 20 Km
N
A, SF Residence
B, MF Residence
F1, Commercial
F2, Industrial
F5, Unknown
J, Utilities
X, Civic
C, Vacant

(c)

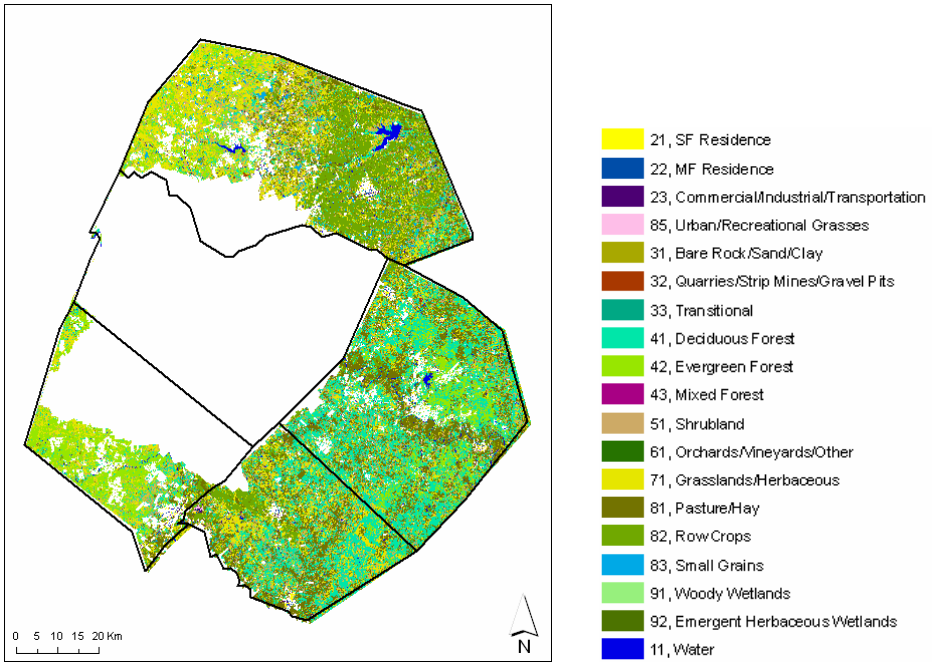

Figure 4-4. LULC datasets with codes and descriptions from (a) City of Austin; (b) CAPCOG; and (c) USGS for 5 counties in Austin, Texas

Since LULC codes from the three datasets were not consistent with each other, they were mapped to the combined LULC categories shown in Table 4-13. The merged base year LULC developed for the five county Austin area is shown in Figure 4-5.

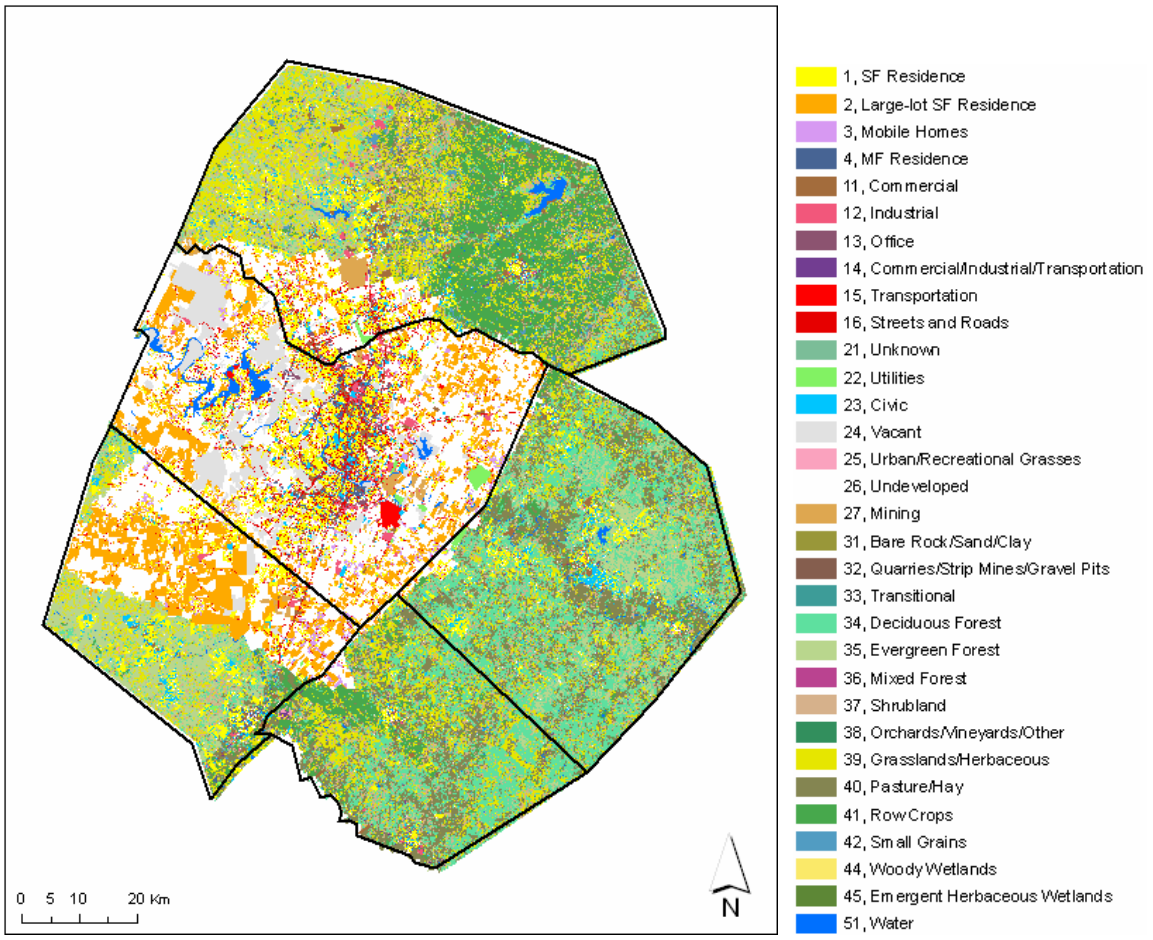

Figure 4-5. Merged LULC with descriptions and codes used to develop spatial surrogates for the five county Austin area

With the use of ArcGIS, the combined LULC dataset was overlaid with county boundary files and the gridded 4km × 4km modeling domain. The area for each polygon in each grid was calculated and the gridded LULC dataset was exported for use as gridded surrogates in the EPS2 framework. The land use codes from exported dataset were assigned to the surrogates recognized by EPS2 as shown in Table 4-14.

Table 4-14. Crosswalk between merged LULC categories and EPS2 surrogates

Combined LULC Category Code	Combined LULC Category Description	EPS2 surrogate
1	Single Family Residence	4
2	Large-lot Single Family Residence	4
3	Mobile Homes	4
4	Multi-family Residence	4
11	Commercial	4
12	Industrial	4
13	Office	4
14	Commercial/Industrial/Transportation	4
15	Transportation	4
16	Streets and Roads	4
21	Unknown	4
22	Utilities	4
23	Civic	4
24	Vacant	4
25	Urban/Recreational Grasses	4
26	Undeveloped	4

Table 4-14. (*Contd.*)

Combined LULC Category Code	Combined LULC Category Description	EPS2 surrogate
27	Mining	11, 15
31	Bare Rock/Sand/Clay	11, 15
32	Quarries/Strip Mines/Gravel Pits	11, 15
33	Transitional	11, 15
34	Deciduous Forest	7, 15
35	Evergreen Forest	8, 15
36	Mixed Forest	9, 15
37	Shrubland	6, 13, 15
38	Orchards/Vineyards/Other	5, 13, 15
39	Grasslands/Herbaceous	6, 13, 15
40	Pasture/Hay	5, 6, 13, 15
41	Row Crops	5, 6, 13, 15
42	Small Grains	5, 6, 13, 15
44	Woody Wetlands	12
45	Emergent Herbaceous Wetlands	12
51	Water	10, 15

Examples of the EPS2 spatial surrogates for the Base Case are shown in Figure 4-6 for the 4km × 4km modeling domain.

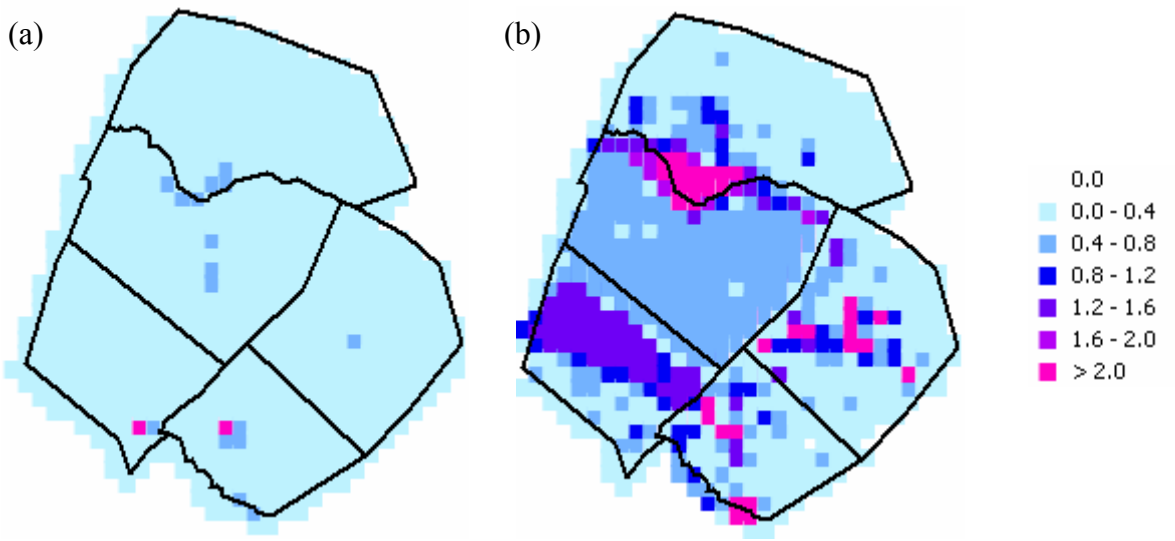

Figure 4-6. Percentage of the EPS2 spatial surrogates; (a) "household" and (b) "urban" for the Base Case

4.3.2 Spatial Surrogates for the 2030 ECT Scenarios

County level households were allocated to each grid cell based on the ECT development patterns from Smart Mobility, Inc. Population was assumed to follow the spatial allocation of households and was estimated using average household size. Both the population and household datasets were combined with the model grid domain and redistributed using an area weighting to obtain total population and number of households for each grid cell.

A future year LULC database was derived for each ECT Scenario. As described in Chapter 3, the ECT scenarios have information on pervious ground cover, but relatively little information on vegetation types. The ECT Scenario land uses, therefore,

were overlaid on the Base Case LULC described in Section 4.3.1. When ECT Scenarios were overlaid on the Base Case LULC, a mapping could be made between the original vegetation types and the new land cover classes, for the regions where future development is expected. For areas undergoing development, the fraction of pervious cover for each development type was used to estimate the fraction of the original trees remaining in the area, as well as the fraction of the area without vegetation. An example of a portion of an EPS2 surrogate file is shown in Figure 4-7.

```
 36000.0 -1404000.  396000.0   -972000        0    4000.0    4000.0
48007          268000  -1304000         0 0.0000440 0.0000000 0.0000000 0.0000000 0.0000360 0.0000090
48007          272000  -1304000         0 0.0058980 0.0001120 0.0000000 0.0000000 0.1000060 0.0213430
48007          272000  -1308000         0 0.0013450 0.0012300 0.0000000 0.0000000 0.0231990 0.0055540
48007          276000  -1300000         0 0.0020910 0.0000000 0.0000000 0.0000000 0.0000000 0.0000450
48007          276000  -1304000         0 0.0113510 0.0000000 0.0000000 0.0000000 0.1180050 0.0362860
48007          276000  -1308000         0 0.0107670 0.0000000 0.0005690 0.0001840 0.0595650 0.0309770
48007          276000  -1312000         0 0.0041400 0.0000000 0.0000000 0.0000000 0.0001020 0.0020710
48007          276000  -1316000         0 0.0000010 0.0000000 0.0000000 0.0000000 0.0000000 0.0000010
48007          280000  -1296000         0 0.0000300 0.0000000 0.0000000 0.0000000 0.0000000 0.0000000
48007          280000  -1300000         0 0.0083210 0.0000000 0.0000000 0.0000000 0.0000000 0.0000000
48007          280000  -1304000         0 0.0114890 0.0000000 0.0000000 0.0000000 0.0167690 0.0046470
48007          280000  -1308000         0 0.0114720 0.0006710 0.0000000 0.0000000 0.0465590 0.0202430
48007          280000  -1312000         0 0.0114540 0.0002790 0.0000000 0.0000000 0.0095840 0.0256600
48007          280000  -1316000         0 0.0076290 0.0235300 0.0000000 0.0000000 0.0118390 0.0173860
48007          280000  -1320000         0 0.0008390 0.0333110 0.0057810 0.0019160 0.0002030 0.0019030
48007          284000  -1280000         0 0.0064840 0.0000000 0.0000000 0.0000000 0.0038580 0.0106010
48007          284000  -1284000         0 0.0029020 0.0000000 0.0000000 0.0000000 0.0163780 0.0079490
48007          284000  -1296000         0 0.0056630 0.0000000 0.0000000 0.0000000 0.0000000 0.0000000
```

Figure 4-7. Gridded spatial allocation surrogate file input to EPS2. The first row has information on the modeling domain definition (minimum easting, minimum northing, maximum easting, and maximum northing in LCP coordinate), zone (0 for this study), and size of each grid cell (4000m for this study). The second row to the end of the file have information on the FIPS code of the state or county, the location of each grid cell (easting and northing coordinate of lower left corner in LCP coordinate), zone, and the fraction of each category with the county (*i.e.*, area in specific grid cell/county area total). Note that LCP is the Lambert Conformal Projection

Examples of the EPS2 spatial surrogates for the ECT scenarios are shown in Figure 4-8.

(a)

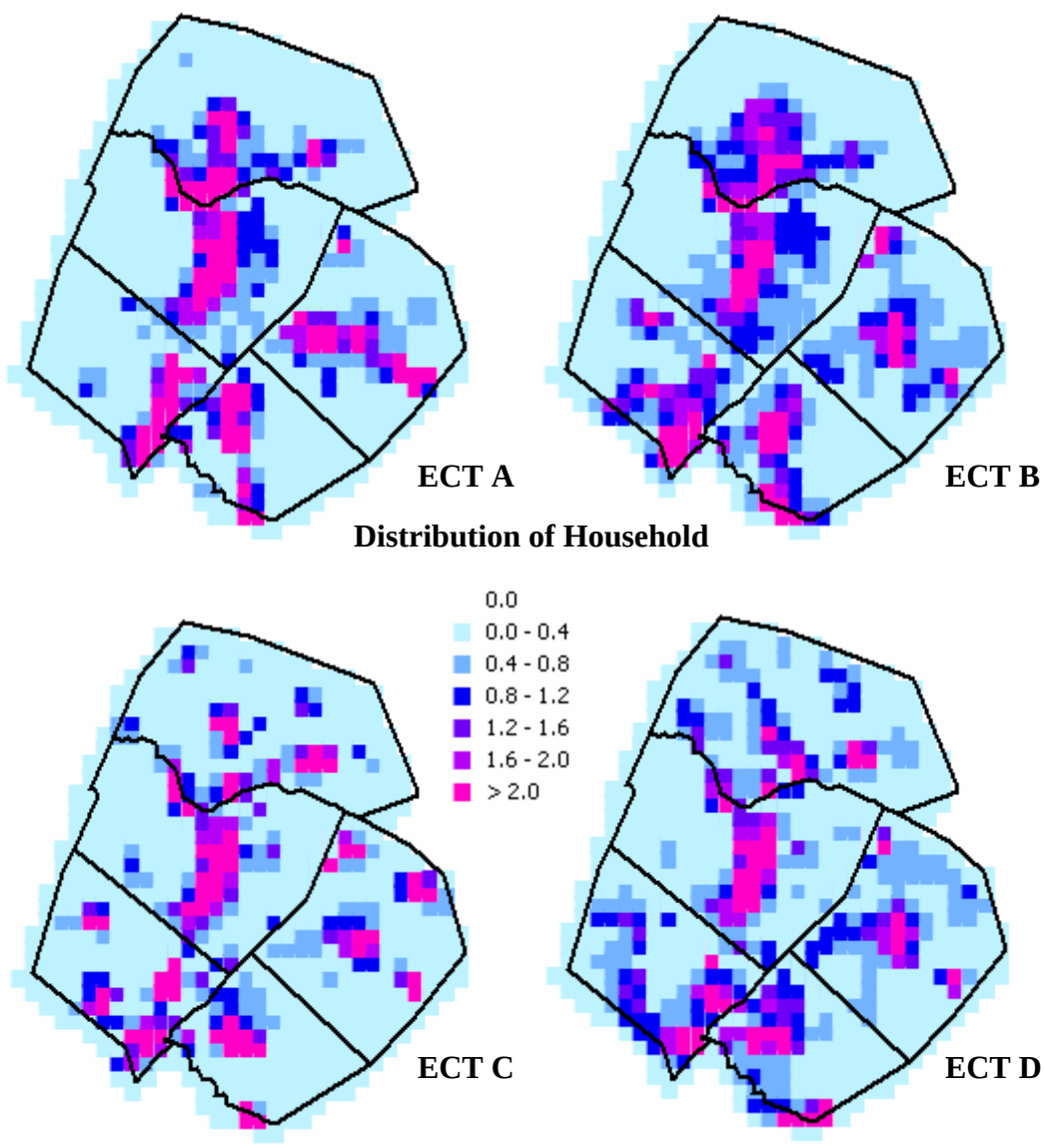
ECT A
ECT B
Distribution of Household
0.0
0.0 - 0.4
0.4 - 0.8
0.8 - 1.2
1.2 - 1.6
1.6 - 2.0
> 2.0
ECT C
ECT D

(b)

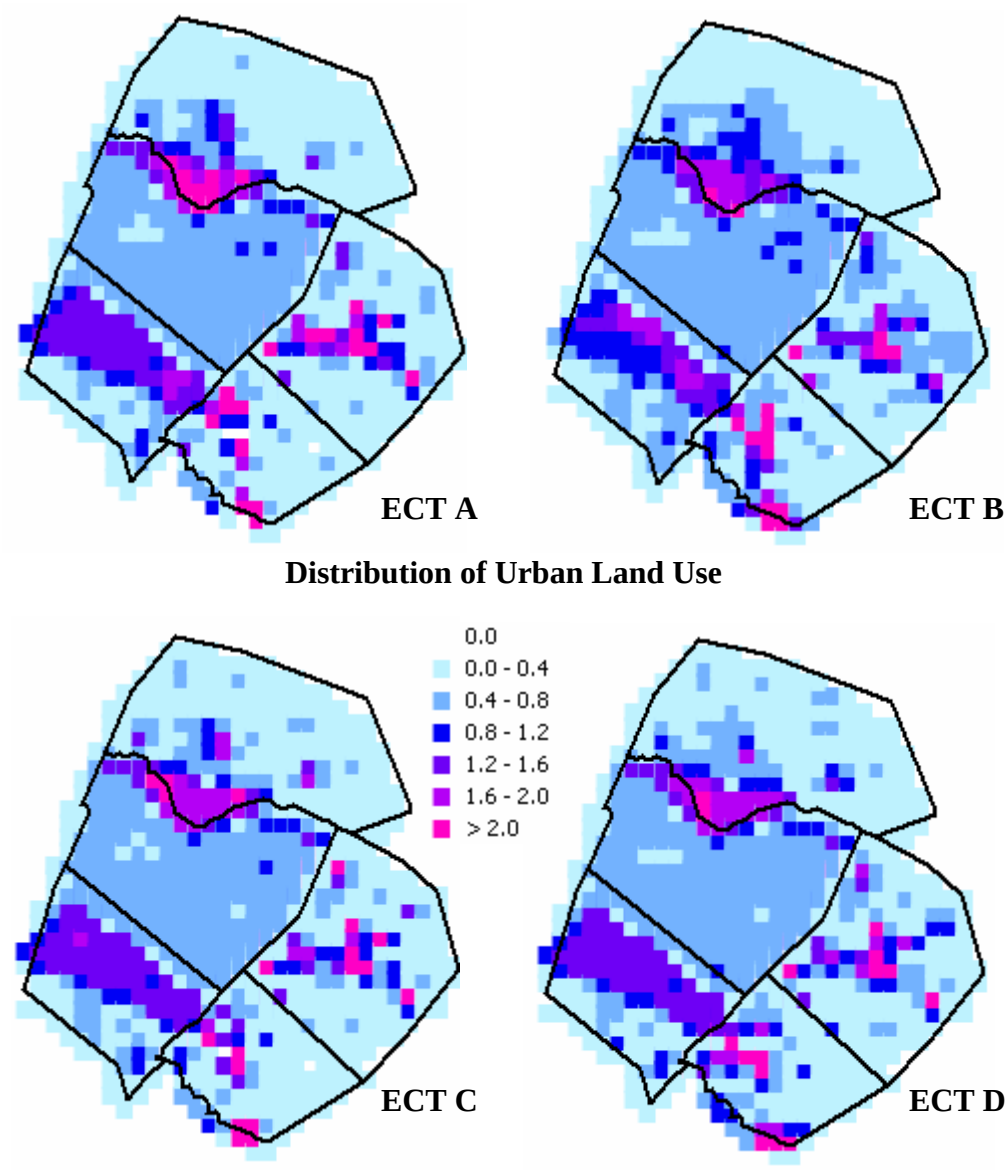

Figure 4-8. Percentages of the EPS2 spatial surrogates: (a) "household" and (b) "urban" for the four ECT scenarios

Once the EPS2 processing was complete, concentrations of air pollutants for each scenario were predicted using the Comprehensive Air Quality Model, with extensions version 4.03 (CAMx; Environ, 2005). Only the emission inventories changed between scenarios, no changes were made to the meteorological modeling and other inputs to the air quality model. Meteorological conditions for the model represented those of a high ozone event during September 13-20, 1999; this episode period was used for air quality modeling and planning for Austin's Early Action Compact as described in the previous chapter. Simulations and their emission inventories are listed in Table 4-15 below. For example, the Base Case is modeled with 2007 emission inventories for anthropogenic sources, and biogenic emissions and dry deposition based on a land cover/land use developed by Widinmyer *et al*. (2000, 2001).

Table 4-15. Matrix of 20 CAMx modeling runs conducted for this study

Scenarios		Bio		Non-road/Area		On-road	
		Wiedinmyer LULC	ECT A-D	2007	ECT A-D	2007	ECT A-D
Basecase		√		√		√	
ECT Bio	(4 runs: ECT A-D)		√	√		√	
ECT Anthro	ECT Non-road/Area (4 runs: ECT A-D)	√			√	√	
	ECT On-Road (4 runs: ECT A-D)	√		√			√
	ECT Mobile/Area (4 runs: ECT A-D)	√			√		√
ECT Combine	(4 runs: ECT A-D)		√		√		√

Note: 'Bio' refers to changes in both biogenic emissions and dry deposition; 'Mobile' refers to changes in both non-road and on-road mobile source emissions; 'Anthro' refers to changes in both 'Mobile' and area source emissions; 'Combine' refers to changes in both 'Bio' and 'Anthro'

4.4 RESULTS

4.4.1 Spatially Allocated Emissions

Spatially allocated non-road and area source emissions, and 1-hour averaged daily maximum ozone concentrations for the four ECT Scenarios were compared to the Base Case. Since September 13th and 14th were used for model initialization, results for these days are not shown. Differences in the spatial distributions of VOC and NOx emissions (gmoles hr^{-1}) from non-road sources in the 5-county MSA for meteorological conditions

on September 20 are shown in Figure 4-9 and Figure 4-10, respectively. As described above, although VOC emissions from most categories decreased, overall VOC emissions for the ECT Scenarios increased slightly relative to the Base Case due to a substantial increase in VOC emissions from lawn and garden equipment. Most equipment associated with VOC emissions, *e.g.*, construction and mining and industrial, are spatially allocated according to the "urban" land use surrogate in EPS2, except for lawn and garden equipment which is allocated by "population". Due to the substantial increase in VOC emissions from lawn and garden equipment, the regions with changes in VOC emissions were consistent with the regions that were allocated according to "population" in EPS2.

Overall NOx emissions for the ECT Scenarios decreased relative to the Base Case. Since most of the NOx emissions are emitted from equipment associated with the "urban" land use spatial surrogate, *e.g.*, construction and mining, and commercial, the reductions in NOx emissions were consistent with the regions that were classified as "urban" in EPS2.

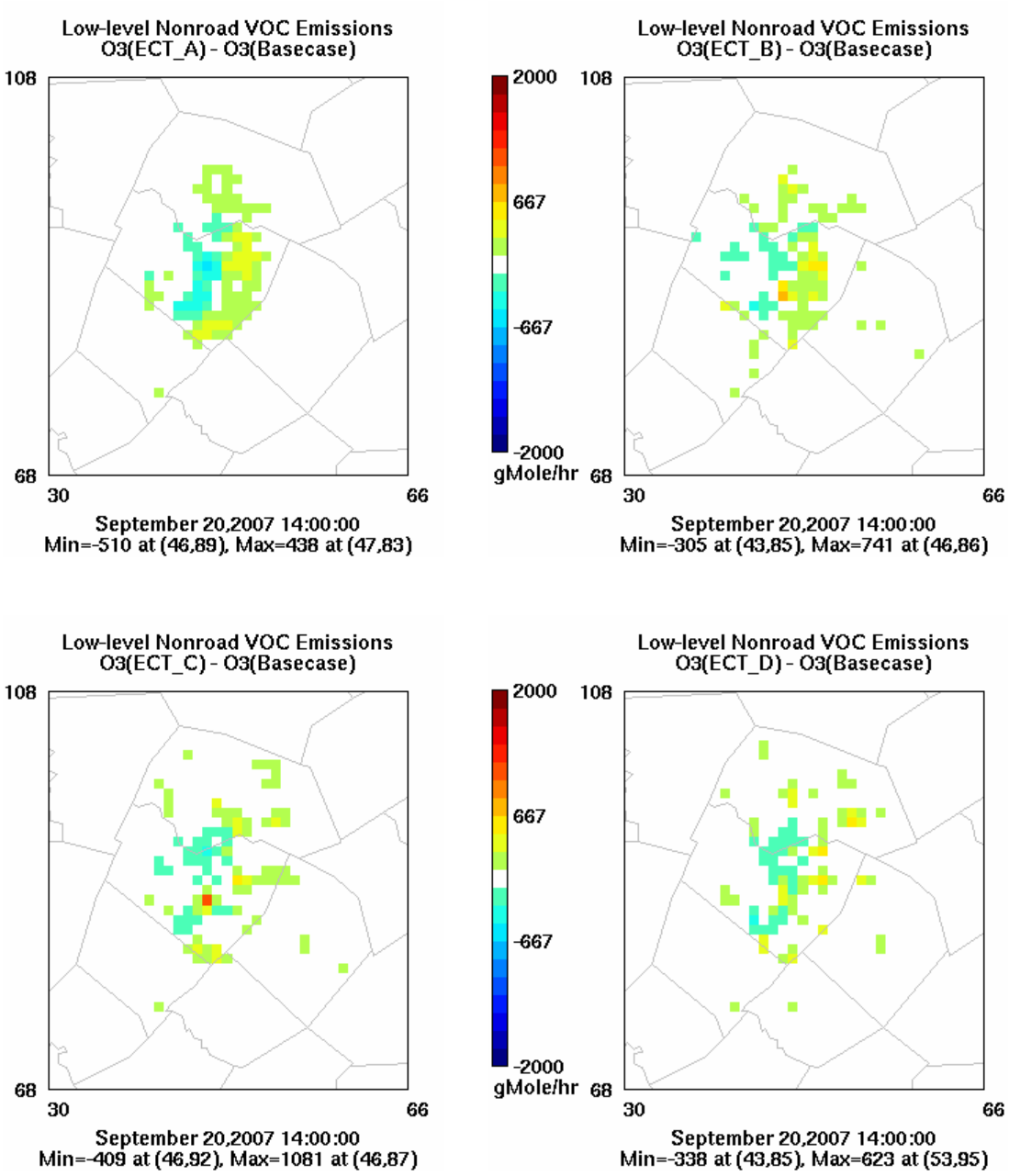

Figure 4-9. Differences in non-road mobile source VOC Emissions between the ECT Scenarios and the Base Case. *Note*: the maximum difference (both increase and decrease) occurred at 0900 (Additional figures for 0900 are provided in Appendix D)

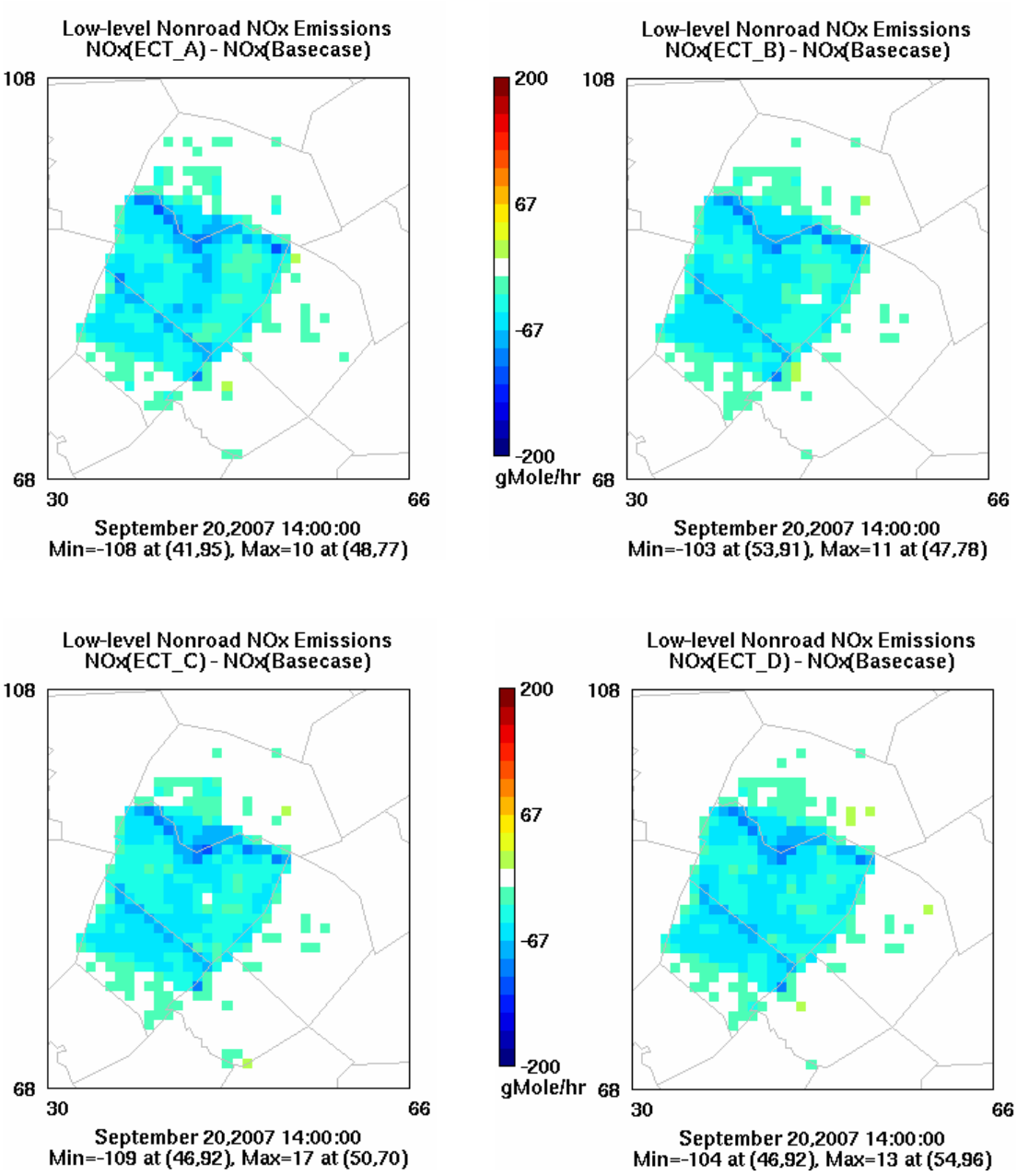

Figure 4-10. Differences in non-road mobile source NOx Emissions between the ECT Scenarios and the Base Case. *Note*: the maximum increase occurred at 0800 (ECT A, B, C, and D) and the maximum decrease at 1200 (ECT C and D) or 1300 (ECT A and B) (Additional figures for 0800, 1200, 1300 are provided in Appendix D)

Differences in the spatial distributions of VOC and NOx emissions (gmoles hr^{-1}) from area sources in the 5-county MSA for meteorological conditions on September 20 are shown in Figure 4-11 and Figure 4-12, respectively. As shown in both figures, VOC and NOx emissions from area sources substantially increased because they were projected according to human population. Most VOC emission categories, *e.g.*, solvent utilization and service stations, are spatially allocated either by "population" or "urban" land use in EPS2. Consequently, regions with changes in VOC emissions were consistent with the regions that were classified as "population" and "urban" in EPS2. Regions with large increases in NOx emissions were located in areas with agriculture, rangeland, deciduous forest, coniferous forest, and mixed agriculture/rangeland. Relative to other counties, Travis County has very little rural area. When spatially allocating emissions for the ECT Scenarios, NOx emission increases from agricultural production were concentrated in small areas, which led to large differences in NOx emissions between the ECT Scenarios and the Base Case in these grid cells.

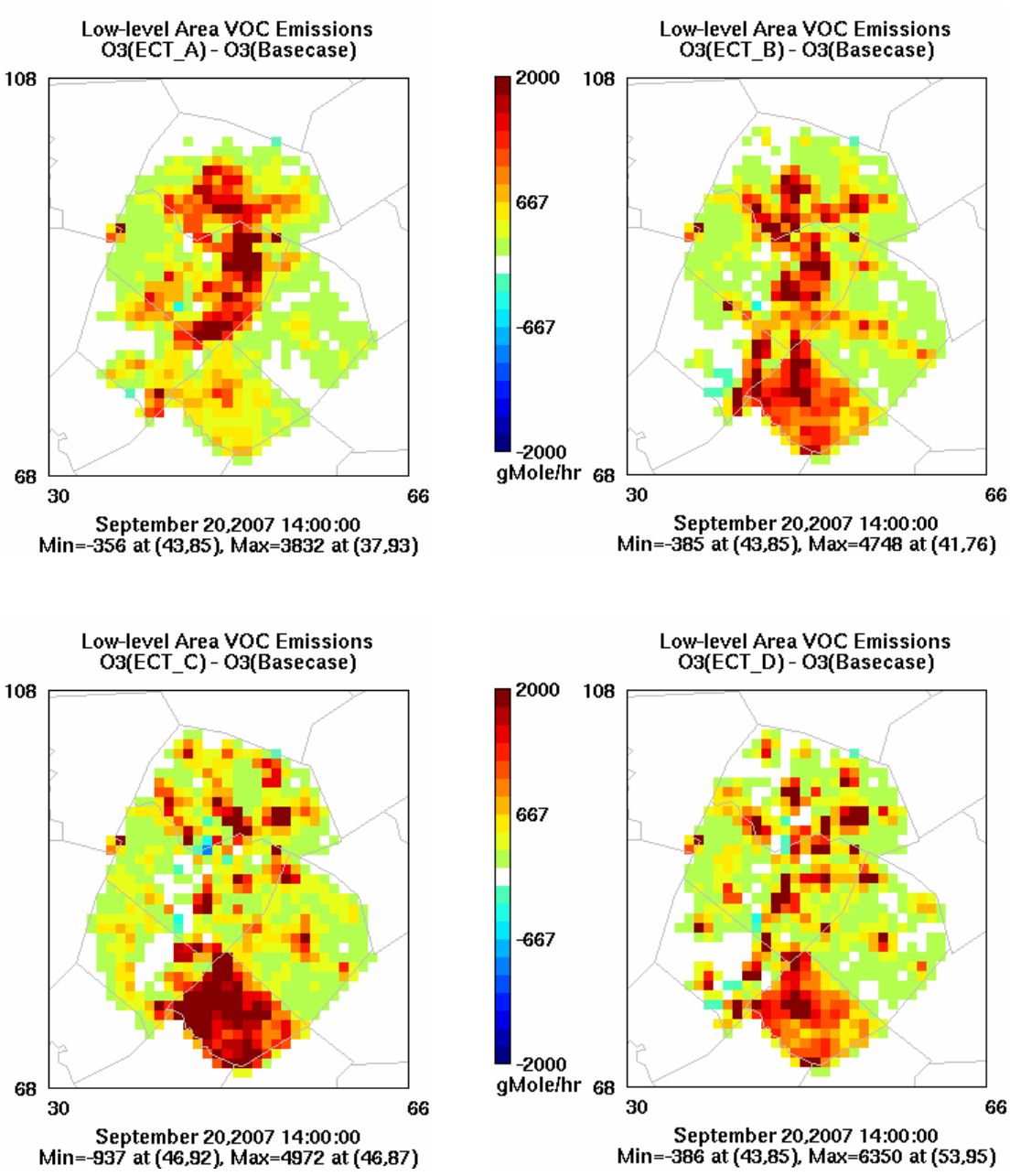

Figure 4-11. Difference in area source VOC Emissions between the ECT Scenarios and the Base Case. *Note*: the maximum increase for the ECT Scenarios with the exception of ECT Scenario A (at 0700) occurred at 1400; the maximum decrease for the ECT Scenarios with the exception of ECT Scenario D (at 1400) occurred at 1600 (Additional figures for 0700 and 1600 are provided in Appendix D)

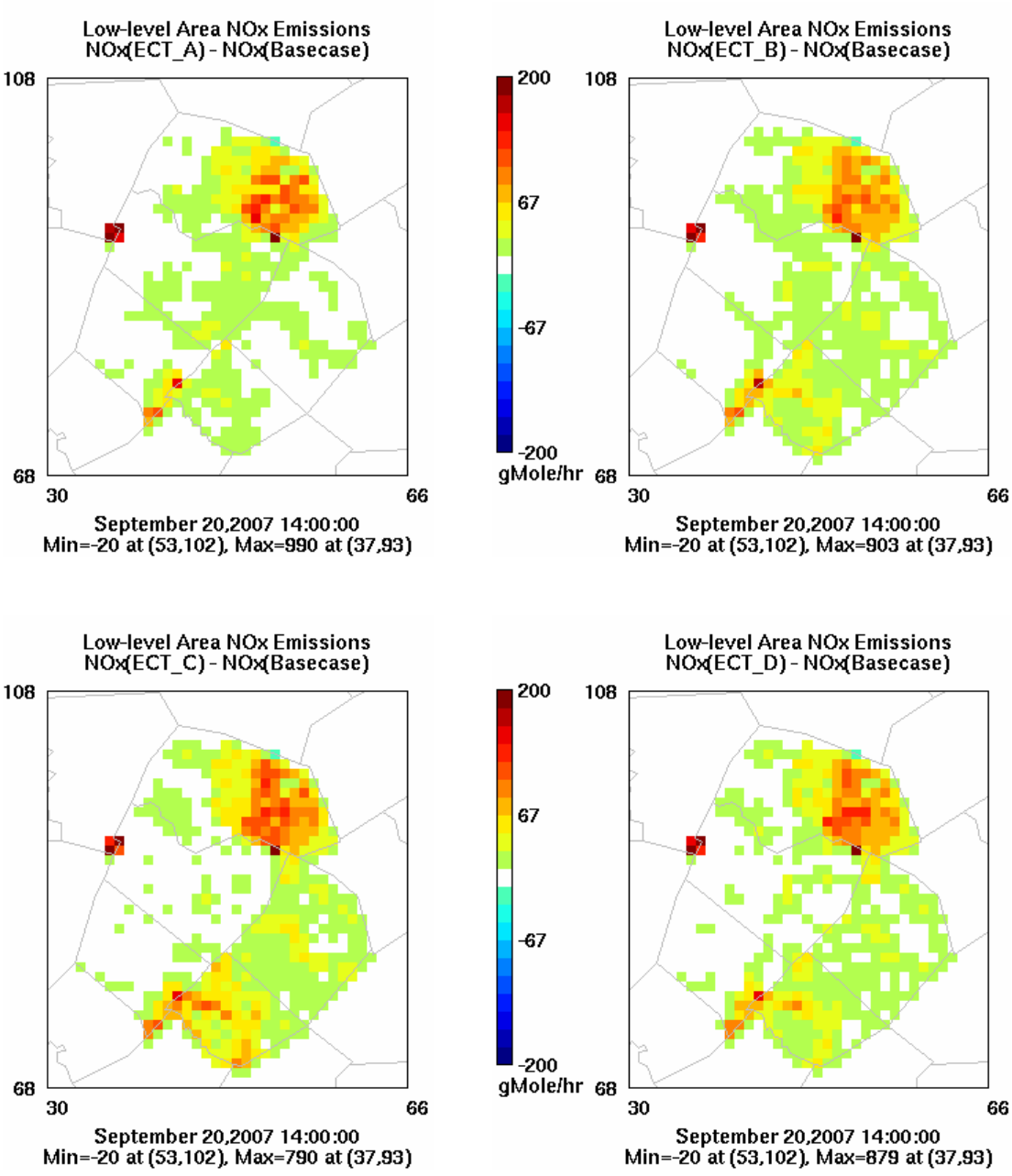

Figure 4-12. Difference in NOx Emissions between the ECT Scenarios and the Basecase. *Note*: The maximum increase occurred at 1600 and increase occurred at 0700 for every ECT Scenarios (Additional figures for 0700 and 1600 are provided in Appendix D)

4.4.2 Air Quality Impacts of Urbanization due to Changes in Non-Road and Area Source Emissions

Predicted 1-hour averaged daily maximum ozone concentrations for the Base Case and differences in the daily maximum ozone concentrations relative to the Base Case due to changes in area and non-road mobile source emissions are presented in Table 4-16. Changes in daily maximum ozone concentrations ranged from -0.13 to 0.77 ppb, with typical values of 0.24 ppb for the Austin area. Although VOC and NOx emissions from area sources doubled and VOC emissions from non-road mobile source slightly increased for the ECT scenarios, changes in maximum daily ozone concentrations were less than 1% due to large reductions in NOx emissions from non-road mobile source. ECT Scenario B showed the largest differences relative to the Base Case. Table 4-17 shows the range of differences in ozone concentrations across the Austin area between the ECT scenarios and the Base Case. The differences in Table 4-17 are not necessarily associated with the area-wide peak predicted ozone concentration, but instead capture the maximum and minimum differences that occur across the region regardless of time of day or magnitude of the ozone concentrations.

Figure 4-13 shows examples of the spatial impacts of changes in non-road and area source emissions from ECT A and ECT D, the two most extreme development scenarios, relative to the Base Case. Changes in non-road and area source emissions result in afternoon increases in ozone concentrations in some grid cells (not necessarily the grid cell with the area-wide maximum ozone concentration) of up to 3.3 ppb. Due to titration of ozone by NOx emissions in the morning, ozone concentrations decreased as much as 7.3 ppb at locations where NOx emissions from area sources increased in northern Travis County for the ECT scenarios. This large decrease in morning ozone concentration was observed throughout the episode period (Table 4-17).

Table 4-16. Daily maximum 1-hour ozone concentration (ppb) for the Basecase and differences in the daily maximum ozone concentrations relative to the Basecase for the ECT Scenarios due to changes in area and non-road mobile source emissions

Scenario	15	16	17	18	19	20
Base Case	81.	72.	86.	86.	90.	91.
ECT A	0.62	0.28	0.11	0.36	0.14	-0.06
ECT B	0.75	0.21	0.31	0.77	0.26	0.33
ECT C	0.52	0.10	-0.09	0.27	-0.04	-0.13
ECT D	0.62	0.21	0.00	0.44	-0.04	-0.13

Table 4-17. Maximum and minimum differences in ozone concentrations (ppb) between the ECT Scenarios and the Basecase across the 5-county Austin area due only to changes in area and non-road mobile source emissions

Range of Differences in Ozone Concentrations Across the Austin Area	
ECT Scenario	'NR+AR'- Base Case
A	4.1 at 1000 on 9/18 -14. at 0800 on 9/18
B	3.8 at 1000 on 9/18 -13. at 0800 on 9/18
C	3.9 at 1400 on 9/18 -11. at 0800 on 9/18
D	4.0 at 0900 on 9/18 -12. at 0800 on 9/18

Note: (1) 'NR+AR' indicates impacts of urbanization due to changes in non-road and area source emissions only

(a)

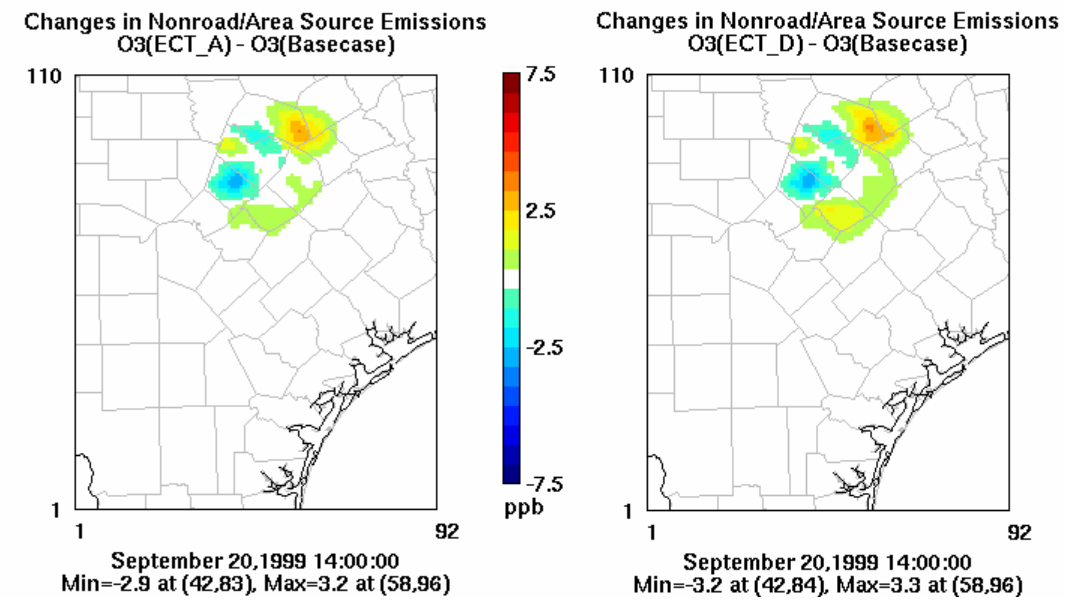

(b)

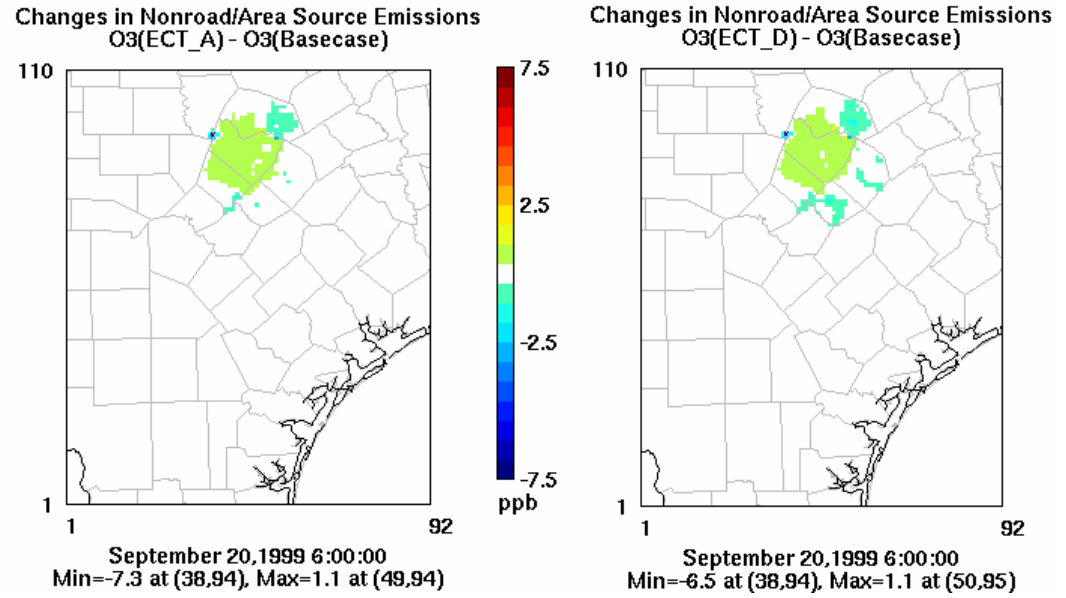

Figure 4-13. Differences in ozone concentrations between ECT A and the Base Case and ECT D and the Base Case at (a) 1400 and (b) 0600 due to changes in both non-road mobile source and area source emissions

4.4.3 Relative Impacts of Urbanization due to Changes in Non-road and Area Source Emissions versus Changes in On-road Mobile Source Emissions

As shown in Table 4-18, the phase-in of new emission standards for on-road mobile sources led to reductions in area-wide maximum daily ozone concentrations for the ECT scenarios of up to 7.8 ppb which was significantly larger than the changes due only to area and non-road mobile emissions sources (Table 4-16). Table 4-19 shows the range of differences in ozone concentrations across the Austin area between the ECT Scenarios and the Basecase. ECT Scenario A showed the largest differences relative to the Basecase. In contrast to the differences in ozone concentrations due to non-road and area source emissions, the maximum decrease occurred during the daytime. It is also clearly shown that ozone concentrations increased in the morning due to titration of ozone by NOx emissions in the morning.

Figure 4-14 and 4-15 shows examples of the spatial impacts of changes in (a) non-road and area source emissions and (b) on-road mobile source emissions from ECT A and ECT D, relative to the Base Case. On-road anthropogenic emission changes resulted in afternoon decreases in ozone concentrations in some grid cells of up to -12 ppb, but increases in ozone concentrations of approximately 21 ppb at the locations where peak ozone concentrations are predicted to occur in the afternoon. As shown in Section 4.4.2, changes in ozone concentrations due to changes in non-road and area source emissions ranged from -14 to 4.1 ppb.

Table 4-18. Daily maximum 1-hour ozone concentration (ppb) for the Basecase and differences in the daily maximum ozone concentrations relative to the Basecase for the ECT Scenarios due to changes in on-road mobile source emissions

Scenario	15	16	17	18	19	20
Base Case	81.	72.	86.	86.	90.	91.
ECT A	-5.3	-2.8	-7.1	-4.3	-1.7	-7.7
ECT B	-5.7	-2.9	-7.1	-4.3	-1.7	-7.8
ECT C	-6.0	-3.0	-7.1	-4.3	-1.7	-7.8
ECT D	-6.0	-3.0	-7.1	-4.3	-1.7	-7.8

Table 4-19. Maximum and minimum differences in ozone concentrations (ppb) between the ECT Scenarios and the Basecase across the 5-county Austin area due only to changes in on-road mobile source emissions

Range of Differences in Ozone Concentrations Across the Austin Area	
ECT Scenario	'On-road'- Base Case
A	22. at 0600 on 9/20 -11. at 1400 on 9/20
B	21. at 0600 on 9/20 -11. at 1400 on 9/20
C	21. at 0600 on 9/20 -12. at 1400 on 9/20
D	21. at 0600 on 9/20 -12. at 1400 on 9/20

Note: (1) 'On-road' indicates impacts of urbanization due to changes in on-road mobile source emissions only

(a)

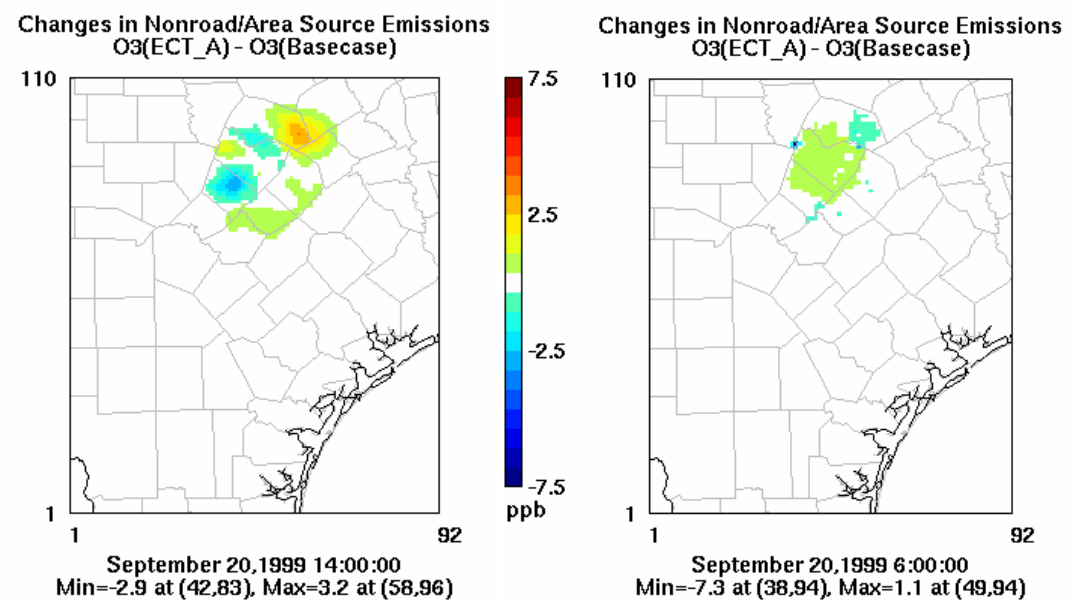

(b)

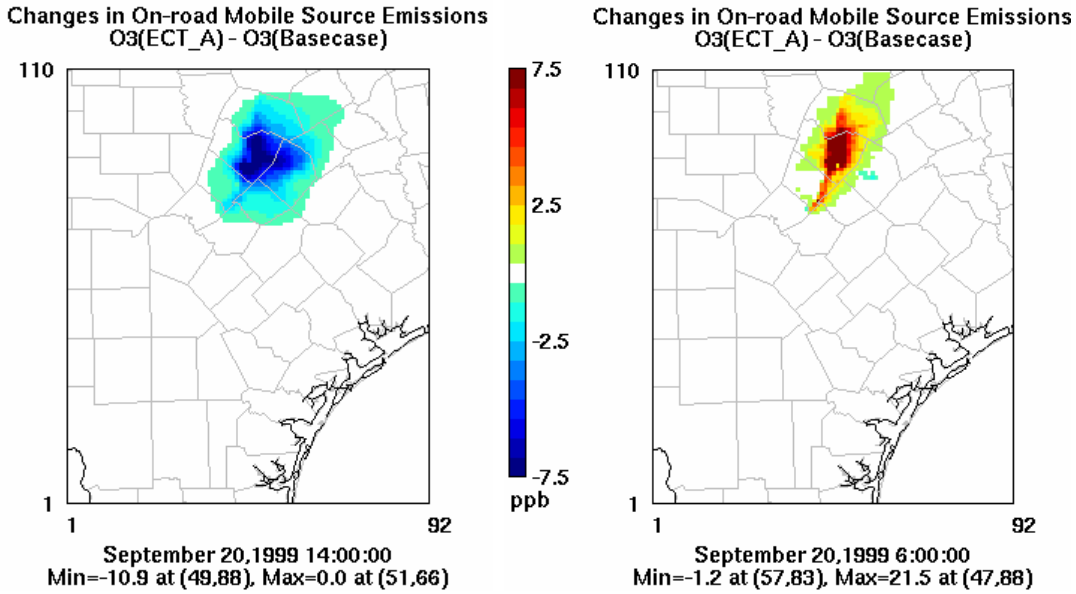

Figure 4-14. Difference in ozone concentrations between ECT Scenario A and the Base Case at 1400 and 0600 (September 20, 1999 meteorological conditions) due to changes in (a) area and non-road mobile source emissions and (b) on-road mobile source emissions

(a)

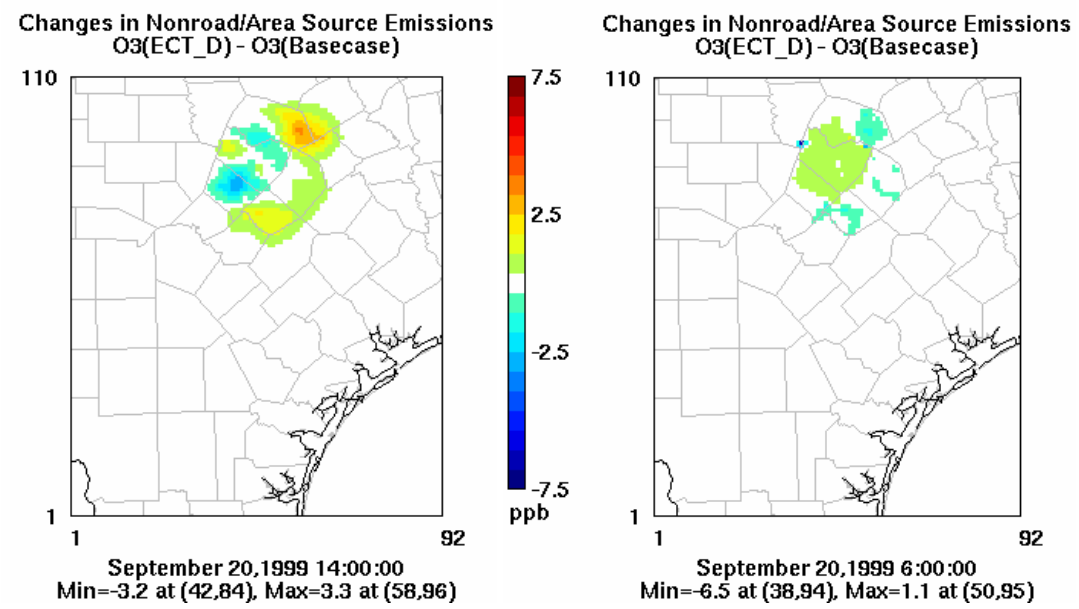

(b)

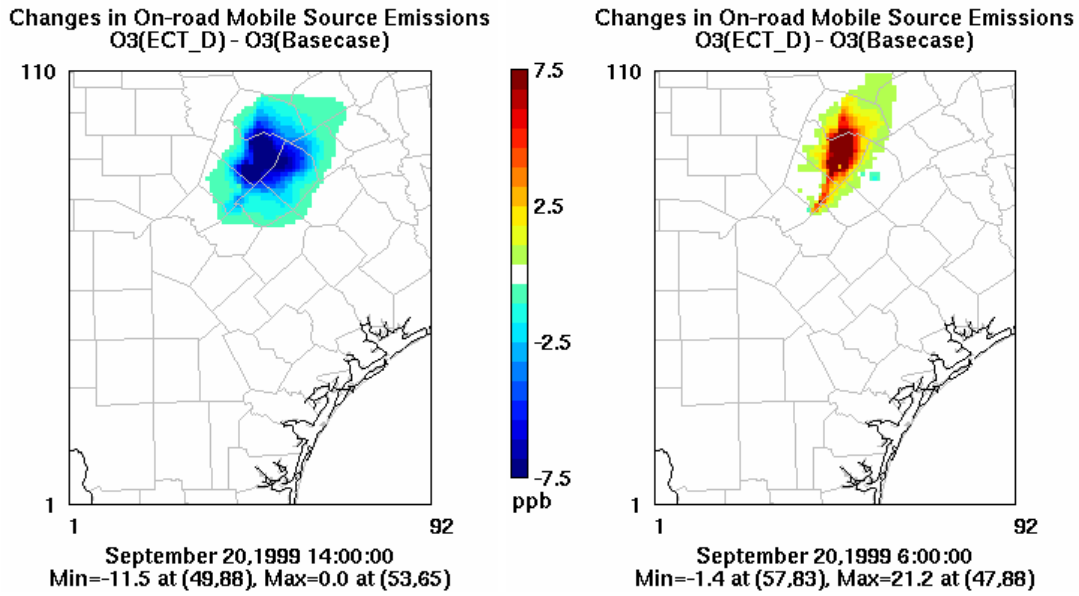

Figure 4-15. Difference in ozone concentrations between ECT Scenario D and the Base Case at 1400 and 0600 (September 20, 1999 meteorological conditions) due to changes in (a) area and non-road mobile source emissions and (b) on-road mobile source emissions

4.4.4 Relative Impacts of Urbanization due to Changes in Biogenic Emissions and Deposition versus Changes in Anthropogenic Emissions

As discussed in Chapter 3, differences in daily maximum ozone concentrations due to changes in biogenic emissions and dry deposition ranged from -0.94 ppb to 0.12 ppb with typical values of -0.15 ppb for 5-county Austin area (Table 4-20a). However, differences in daily maximum ozone concentrations due to changes in anthropogenic emissions, *i.e.*, non-road and on-road mobile source emissions and area source emissions, were far more significant, ranging from -7.0 ppb to -1.3 ppb with typical values of -4.2 ppb (Table 4-20b). ECT Scenario A showed the largest difference in the daily maximum ozone concentration. Table 21 shows the range of differences in ozone concentrations across the Austin area between the ECT scenarios and the Base Case. Ozone concentrations across the area are more influenced by changes in anthropogenic emissions versus changes in biogenic emissions and dry deposition.

Table 4-20. Daily maximum 1-hour ozone concentration (ppb) for the Basecase and differences in the daily maximum ozone concentrations relative to the Basecase for the ECT Scenarios due to changes in (a) biogenic emissions, and (b) anthropogenic emissions

(a)

Scenario	15	16	17	18	19	20
Base Case	81.	72.	86.	86.	90.	91.
ECT A	0.00	0.12	-0.11	-0.39	-0.58	-0.94
ECT B	-0.02	0.09	-0.02	-0.20	-0.21	-0.40
ECT C	-0.03	0.05	-0.03	-0.13	-0.15	-0.21
ECT D	-0.04	0.08	-0.03	-0.15	-0.15	-0.12

(b)

Scenario	15	16	17	18	19	20
Base Case	81.	72.	86.	86.	90.	91.
ECT A	-4.6	-2.1	-7.0	-4.1	-1.4	-5.9
ECT B	-4.9	-2.2	-7.0	-4.1	-1.4	-6.0
ECT C	-5.3	-2.1	-7.0	-4.1	-1.3	-5.8
ECT D	-5.3	-2.2	-7.0	-4.1	-1.3	-5.8

Table 4-21. Maximum and minimum differences in ozone concentrations (ppb) between the ECT Scenarios and the Basecase across the 5-county Austin area

Range of Differences in Ozone Concentrations Across the Austin Area		
ECT Scenario	'Bio'- Base Case	'Anthro'-Base Case
A	0.67 at 0900 on 9/15 -1.4 at 0600 on 9/19	22. at 0600 on 9/20 -14. at 0800 on 9/18
B	0.72 at 0800 on 9/19 -1.0 at 0600 on 9/19	21. at 0600 on 9/20 -12. at 0800 on 9/18
C	0.64 at 0900 on 9/15 -0.85 at 0500 on 9/19	21. at 0600 on 9/20 -13. at 1400 on 9/18
D	0.65 at 0900 on 9/15 -0.81 at 0600 on 9/19	22. at 0600 on 9/20 -12. at 1400 on 9/20

Note: (1) 'Bio' indicates impacts of urbanization due to changes in biogenic emissions and dry deposition only; (2) 'Anthro' indicates impacts of urbanization due to changes in on-road, non-road, and area source emissions only (point source emissions did not change)

Examples of the spatial differences in ozone concentrations between the ECT A, ECT D and the Base Case due to changes in biogenic emissions and dry deposition and due to changes in anthropogenic emissions are shown in Figures 4-16 and 4-17, respectively. Changes in anthropogenic emissions result in increases in ozone concentrations of up to 22 ppb due to titration of ozone by NOx emissions in the morning.

(a)

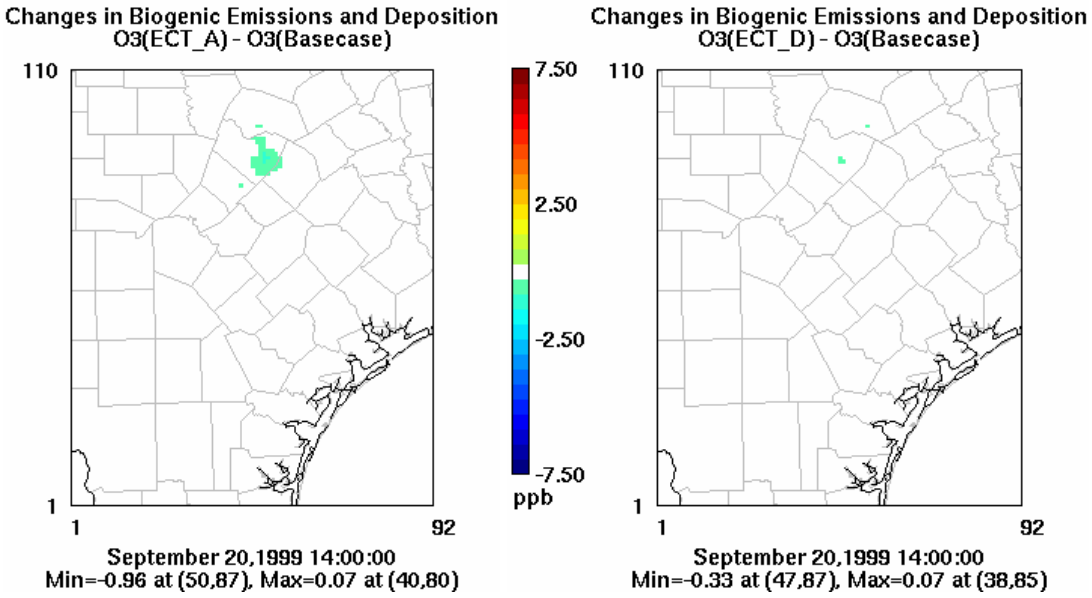

(b)

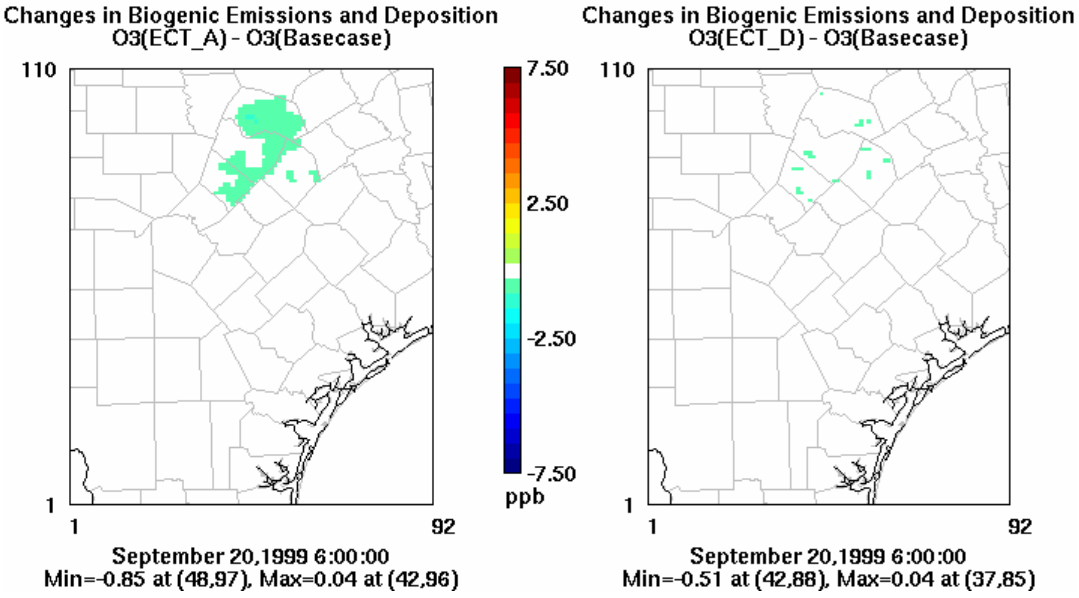

Figure 4-16. Differences in ozone concentrations between ECT A, ECT D and the Base Case due to changes in biogenic emissions and dry deposition (a) in the afternoon (1400) and (b) in the morning (0600) (September 20, 1999 meteorological conditions)

(a)

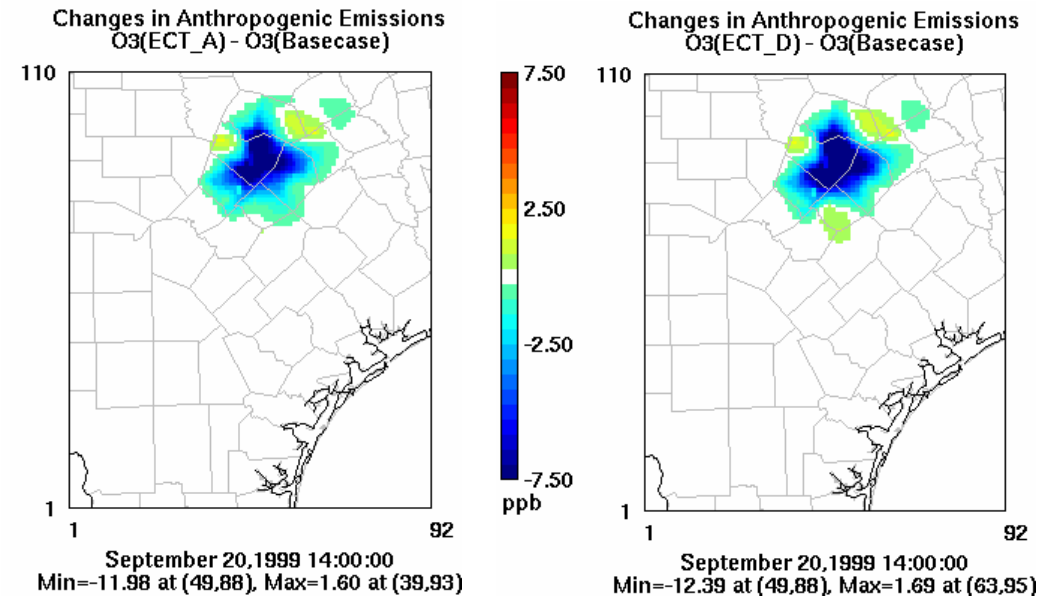

(b)

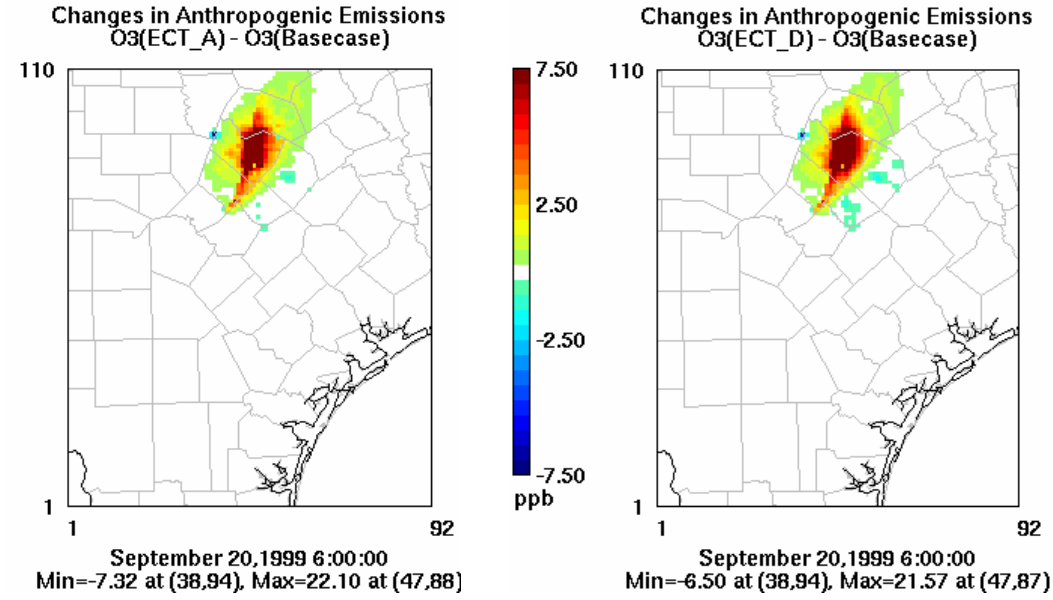

Figure 4-17. Differences in ozone concentrations between ECT A, ECT D and the Base Case due to changes in anthropogenic emissions in the afternoon (1400) and in the morning (0600) (September 20, 1999 meteorological conditions).

When changes in biogenic emissions, dry deposition, and anthropogenic emissions were all considered, the maximum differences in ozone concentrations ranged from -14 ppb to 22 ppb for the 5-county Austin area (Table 4-22). Significant increases and decreases were both associated with changes in anthropogenic emissions; the afternoon decreases were due to changes in on-road, non-road mobile source emissions and area source emissions (Figure 4-18), while the morning increases were mainly due to changes in on-road mobile source emissions (Figure 4-19).

Table 4-22. Maximum and minimum differences in ozone concentrations (ppb) between the ECT Scenarios and the Basecase across the 5-county Austin area

Range of Differences in Ozone Concentrations Across the Austin Area	
ECT Scenario	'Combined'- Base Case
A	22. at 0600 on 9/20 -14. at 0800 on 9/18
B	21. at 0600 on 9/20 -13. at 0800 on 9/18
C	21. at 0600 on 9/20 -13. at 1500 on 9/20
D	22. at 0600 on 9/20 -13. at 1400 on 9/20

Note: (1) 'Combined' indicates combined impacts of urbanization due to changes in biogenic emissions, dry deposition, and anthropogenic emissions (*i.e.*, on-road, non-road, and area source emissions)

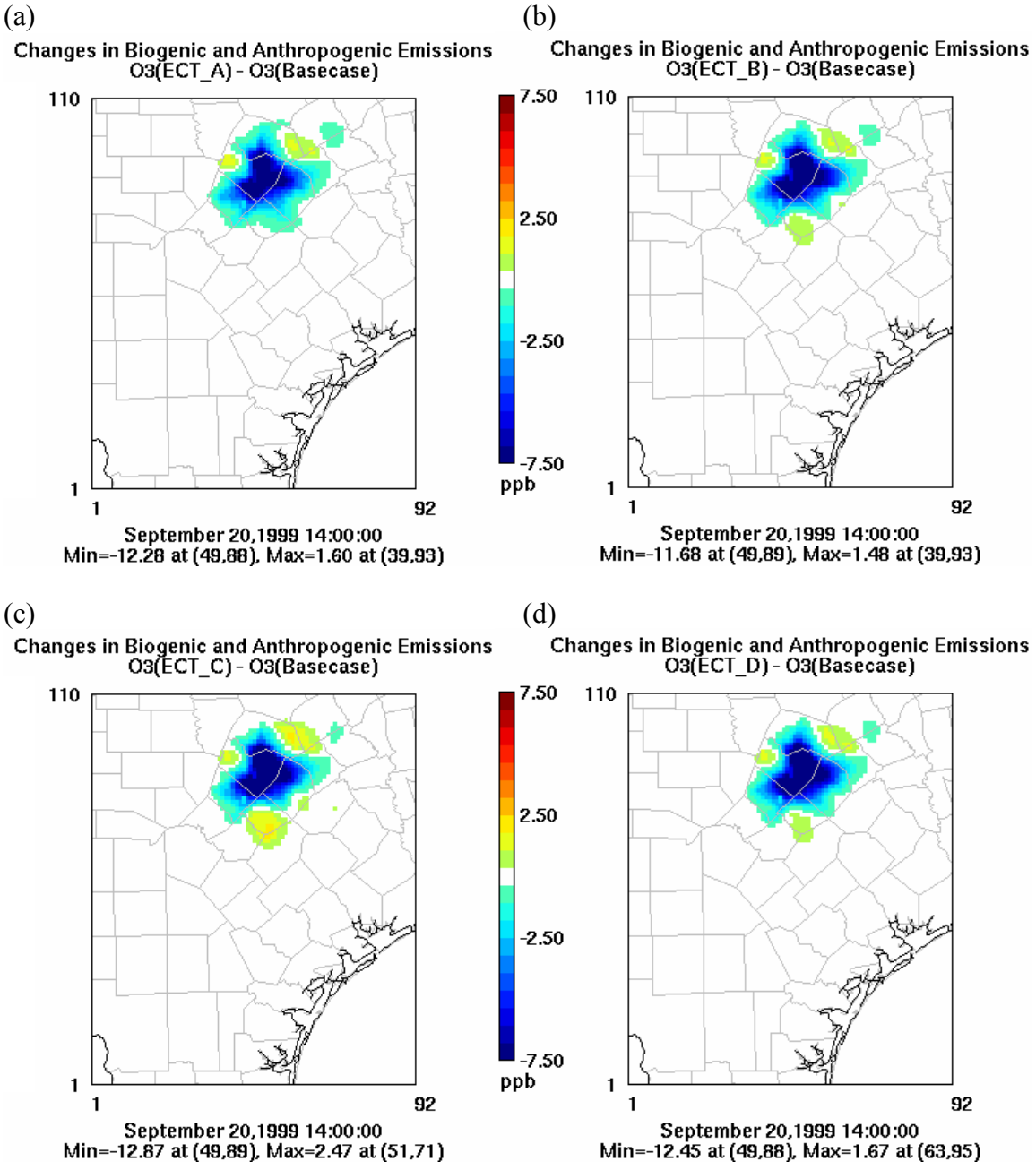

Figure 4-18. Difference in ozone concentrations between the Base Case and (a) ECT A, (b) ECT B. (c) ECT C, and (d) ECT D due to changes in biogenic emissions, dry deposition, and anthropogenic emissions at 1400 (September 20, 1999 meteorological conditions)

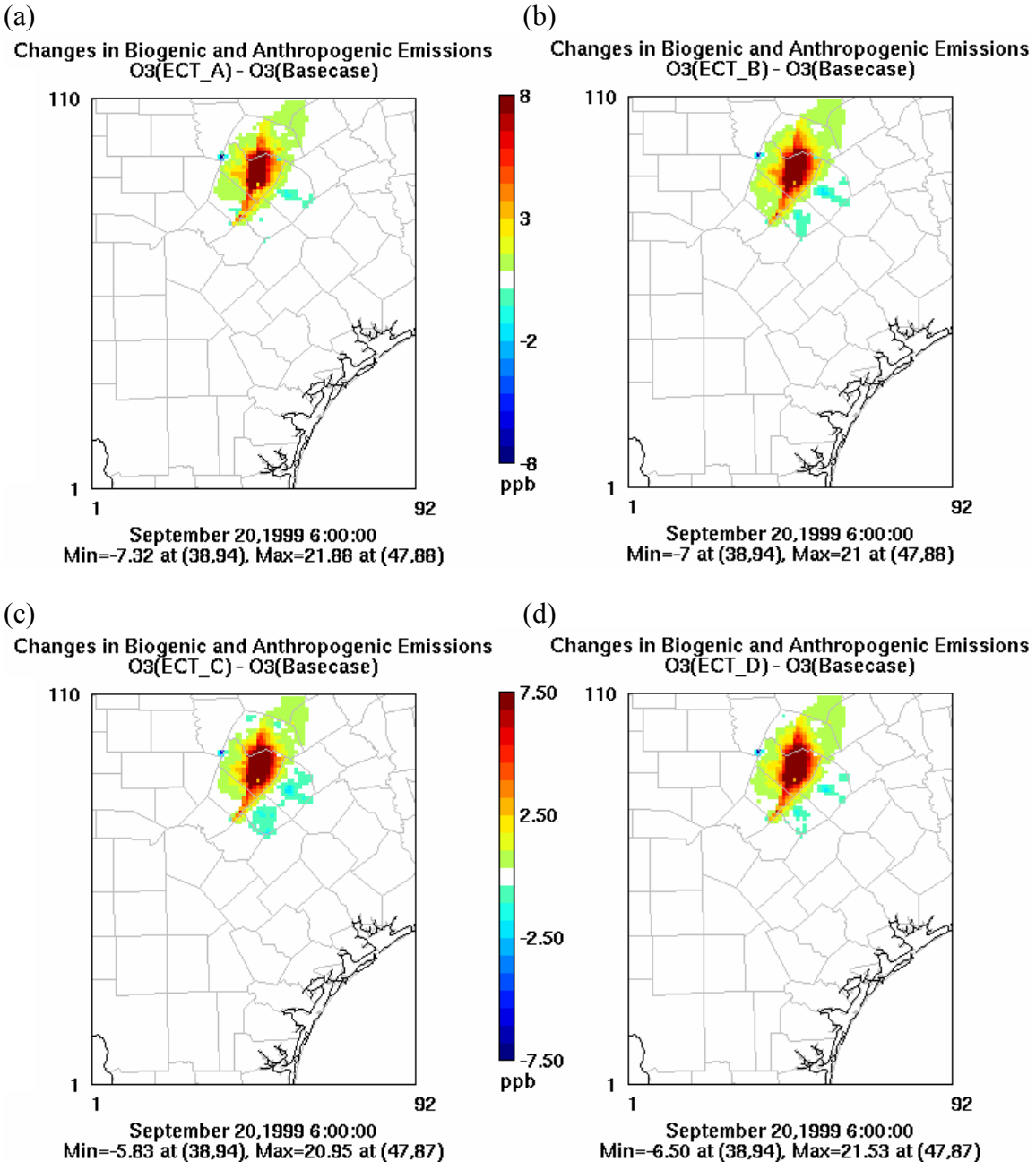

Figure 4-19. Difference in ozone concentrations between the Base Case and (a) ECT A, (b) ECT B, (c) ECT C, and (d) ECT D due to changes in biogenic emissions, dry deposition, and anthropogenic emissions at 0600 (September 20, 1999 meteorological conditions)

Figure 4-20 shows the range of changes in ozone concentrations between the ECT Scenarios and the Base Case due to changes in (a) biogenic emissions and dry deposition, (b) non-road mobile source and area source emissions, (c) on-road mobile source emissions, (d) anthropogenic emissions, and (e) biogenic emissions, dry deposition, and anthropogenic emissions. Changes in ozone concentrations only due to changes in biogenic emissions and dry deposition are relatively smaller than the changes due to changes in any anthropogenic emissions. Also, it is clearly shown that the significant increases and decreases were both associated with changes in anthropogenic emissions; the decreases were due to changes in on-road, non-road mobile source emissions and area source emissions, while the increases were mainly due to changes in on-road mobile source emissions.

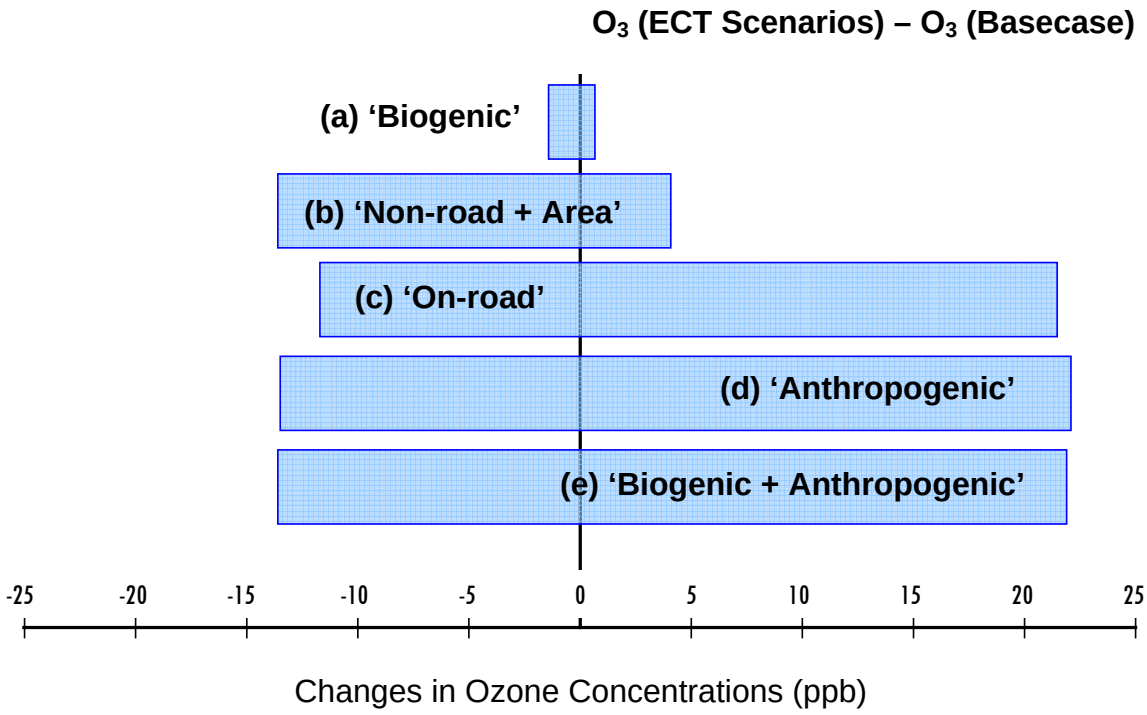

Figure 4-20. Range of changes in ozone concentrations (ppb) between the ECT Scenarios and the Basecase across the 5-county Austin area due to changes in (a) biogenic emissions and dry deposition, (b) non-road mobile source and area source emissions, (c) on-road mobile source emissions, (d) anthropogenic emissions, and (e) biogenic emissions, dry deposition, and anthropogenic emissions

These differences in ozone concentrations between the ECT Scenarios and the Base Case were much greater than the differences between the ECT Scenarios. The maximum changes between the ECT Scenarios were predicted between ECT Scenario A and C, ranging from -4.2 ppb to 3.2 ppb (see example in Figure 4-21). Since ECT Scenario A assumes a typical urban sprawl pattern which concentrates growth in the urban core, and ECT Scenario C assumes new development in new and existing towns

throughout the region, large increases in ozone concentrations occurred in the urban core, but large decreases occurred outside of the urban core.

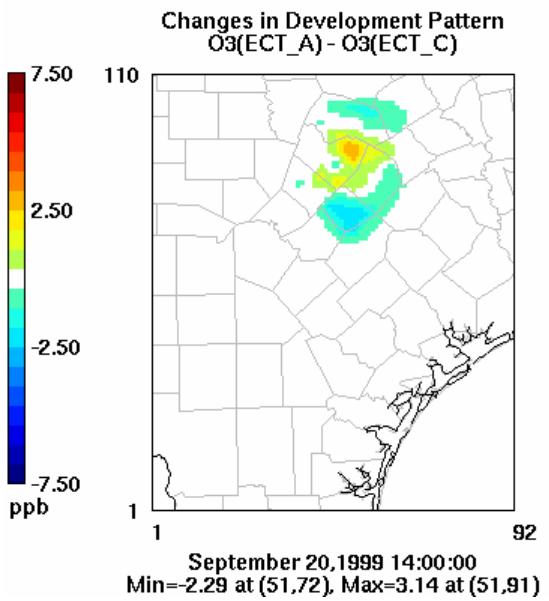

Figure 4-21. Differences in ozone concentrations between ECT Scenario A and C

Figure 4-22 shows the range of changes in ozone concentrations between the ECT Scenarios. As compared to Figure 4-20, the changes in ozone concentrations between the ECT Scenarios are much smaller than the changes in ozone concentrations between the ECT Scenarios and the Base Case. Although the magnitudes of changes in ozone concentrations are smaller, the trends of changes in ozone concentrations between the ECT Scenarios are very similar to that between the ECT Scenarios and the Base Case.

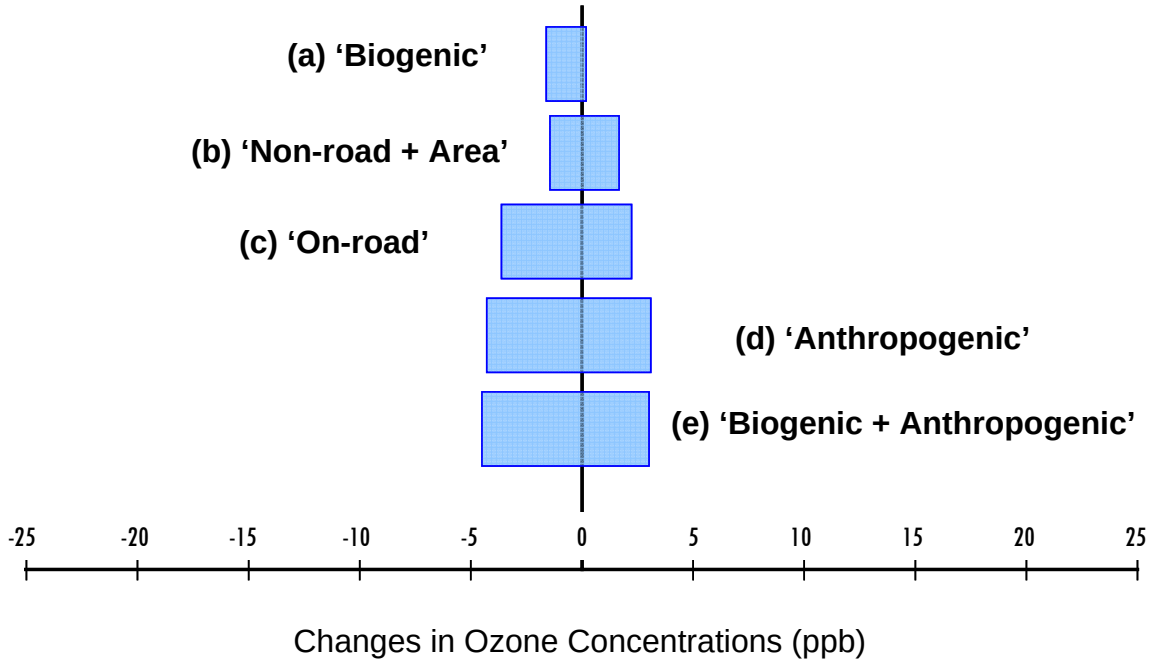

Figure 4-22. Range of changes in ozone concentrations (ppb) between the ECT Scenarios across the 5-county Austin area due to changes in (a) biogenic emissions and dry deposition, (b) non-road mobile source and area source emissions, (c) on-road mobile source emissions, (d) anthropogenic emissions, and (e) biogenic emissions, dry deposition, and anthropogenic emissions

4.4.5 Summary and Implications

Non-road and area source emission inventories were developed for four ECT Scenarios and the Base Case that included 2007 emission inventories for anthropogenic sources, emission controls adopted for Austin's Early Action Compact, and a biogenic emissions inventory and dry deposition estimates based on a land cover/land use database developed by Wiedinmyer *et al*. (2000, 2001). The photochemical modeling for the Base Case and all of the ECT scenarios used meteorology from a September 13-20, 1999 historical ozone episode that was used for Austin's Early Action Compact.

The effects of changes in non-road and area source emissions due to doubling of population were much larger than the effects of changes in biogenic emissions and dry deposition (discussed in Chapter 3). This study indicates that changes in anthropogenic emissions, especially on-road mobile source emissions, due to a doubling of population may have a large influence on ozone concentrations, as compared to the changes due biogenic emissions and dry deposition. However, even the changes due to biogenic emissions and dry deposition are comparable in magnitude to some emissions controls implemented as part of Austin's Early Action Compact. The study also indicates that the impacts of alternative development patterns are much smaller than the effects of doubling of population itself.

Urban planning initiatives rarely include the type of inter-disciplinary modeling efforts that evaluate how regional development trends affect the magnitude and spatial distribution of air pollution. Integrated modeling efforts, such as the ones described in this study, have the potential to facilitate policy decisions that support balanced growth for U.S. communities.

4.5 REFERENCES

EPA, Nonroad Engine and Vehicle Emission Study, EPA-21A-2001, November 1991.

EPA, "Regulatory Announcement: Final Emissions Standards for Locomotives." EPA420-F-97-048, December 1997. Available at http://www.epa.gov/otaq/regs/nonroad/locomotv/frm/42097048.pdf.

City of Austin. "Air Emissions Inventory, Austin-Bergstrom International Airport." Prepared by Department of Aviation, 2716 Spirit of Texas Drive, Austin, TX 78719, (512) 530-6510, August, 2002.

ENVIRON. "Final Report: Emissions Processing for the Joint CAMx Photochemical Modeling of Four Southern Texas Near Non-Attainment Areas." August 2002. 101 Rowland Way, Suite 220, Novato, CA.

Gery, M.W., Whitten, G.Z., Killus, J.P. (1989) "A Photochemical kinetics mechanism for urban and regional scale computer modeling." *Journal of Geophysical Research* **94**(12) 925-12, 956.

McDonald-Buller, E.C., Allen, D.T., Kockelman, K., Parmenter, B. (2005) "2005 Progress Report: Predicting the relative impacts of urban development policies and on-road vehicle technologies on air quality in the United States: Modeling and analysis of a case study in Austin, Texas." Submitted to EPA in 2005. Available at http://cfpub.epa.gov/ncer_abstracts/index.cfm/fuseaction/display.abstractDetail/abstract/7425/report/2005.

The Capital Area Planning Council (CAPCO). "Austin-Round Rock MSA 1999 Ozone Precursor Emissions Inventory." March 2004. Available at http://www.tceq.state.tx.us/assets/public/implementation /air/sip/sipdocs/2004-06-AUS/04086sipapd_pro.pdf.

The Capital Area Planning Council (CAPCO). "Austin/Round Rock MSA Emissions Reductions Strategies." Technical Report on behalf of The Austin-Round Rock MSA Clean Air Coalition, March 2004. Available at http://www.capcog.org/CAPCOairquality/CAAP_Apps/App5-2Austin-RR%20Emission%20Reduction%20Strategies.pdf.

The Capital Area Planning Council (CAPCO). "2007 Future Year Ozone Precursor Modeling Emissions Inventory." Technical Report on behalf of the Austin-Round Rock MSA Clean Air Coalition, March 2004. Available at http://www.tceq.state.tx.us/assets/public/implementation /air/sip/sipdocs/2004-06-AUS/04086sipape_pro.pdf.

Wiedinmyer, C., Strange, I.W., Estes, M., Yarwood, G., Allen, D.T. (2000) "Biogenic hydrocarbon emission estimates for north central Texas." *Atmospheric Environment* **34**(20), 3419-3435.

Wiedinmyer, C., Guenther, A., Estes, M., Strange, I. W., Yarwood, G., Allen, D. T. (2001) "A land use database and examples of biogenic isoprene emission estimates for the state of Texas, USA." *Atmospheric Environment* **35**(36), 6465-6477.

Chapter 5: Impacts of Climate Changes on Biogenic Emissions and Air Pollutant Concentration

5.1 INTRODUCTION

Previous chapters have examined the role that changes in patterns of urbanization have on land use, land cover and air quality. Additional changes in land cover can be expected due to the effects of changes in climate. The goal of this chapter is to estimate the effect that climate-induced changes in land cover will have on air quality (specifically, ozone concentrations) in central and eastern Texas, and to compare those impacts on air quality to the impacts predicted due to patterns of urbanization.

There have been several global and regional scale air quality studies that have investigated the sensitivity of surface ozone concentration to changes in global/regional climate (Hogrefe *et al*., 2004; Johnson *et al*., 1999; Knowlton *et al*., 2004; Leung and Gustafson, 2005; Mickley *et al*., 2004; Murazaki and Hess, 2006; Shallcross and Monks, 2000). Hogrefe *et al*. (2004) compared the contribution of regional climate change, increased anthropogenic emissions, and changes in boundary conditions to future ozone concentrations. They showed the largest changes in predicted summertime average daily maximum 8 hour ozone concentrations by 2050 are due to changes in the chemical boundary conditions. When changes in the fourth highest summertime 8 hour ozone concentration was considered, however, regional climate change was the most important contributor. The changes in climate caused changes in biogenic emissions, which, in turn, caused changes in ozone concentrations. Knowlton *et al*. (2004) also estimated changes in summer ozone concentration resulting from climate change alone and from both climate change and the changes in future anthropogenic emissions, projected to 2050. For the New York metropolitan area, climate change alone caused increases in ozone concentration of up to 4.3 ppb; climate change and changes in ozone precursor

emissions resulted in increasing ozone concentration by -3.1 to 6.0 ppb, as compared to the 1990s.

Mickley *et al*. (2004) examined the effect of changing meteorologies, due to climate change, on air pollutant concentrations. Anthropogenic emissions were held constant. For carbon monoxide and black carbon aerosol, the Northeast and Midwest U.S. showed increases in pollutant concentrations (CO and BC) of 5-10 percent, whereas other parts of the U.S. showed relatively small or no changes in pollutant concentrations.

Additional studies have examined the effect of climate changes on biogenic emissions (Constable *et al*., 1999), characteristic changes in boundary layer height, air stagnation (Leung and Gustafson, 2005), water vapor (Murazaki and Hess, 2006) and vegetation changes.

Leung and Gustafson (2005) reported climate change effects on air quality based on global-regional climate and climate-induced biogenic emission changes. For example, Texas showed decreased rainfall frequency, increased surface temperature, increased number of stagnation days, increased the boundary layer depth, and increased solar radiation during summers between 2045 and 2055, with a net increase in ozone concentrations.

Murazaki and Hess (2006) show that climate change leads to increased water vapor which leads to decreases in ozone concentration. This is also reported in other studies (Brasseur *et al*., 1998; Grewe *et al*., 2001; Johnson *et al*., 1999; Stevenson *et al*., 2005). However, the locations with high NOx emissions had higher ozone concentrations, possibly due to increases in water vapor and temperature.

All of these studies have assumed that land cover remains fixed and that changes in air quality due to climate are due to changes in meteorological variables, such as temperature, water vapor concentration, rainfall, and other parameters. There have been

few studies accounting for these effects and the effects of changes in land cover due to climate change.

Cox *et al.* (2000) showed that incorporating vegetation changes resulting from climate change have a strong impact on carbon-cycle feedbacks.

More recently, Sanderson *et al*. (2003) have calculated isoprene emissions, as well as ozone concentrations, as a result of global climate change, with vegetation changes projected from the 1990s to 2090s. Future land cover was based on the pessimistic future scenario developed by the Intergovernmental Panel on Climate Change (IPCC) and was modeled with a dynamic global vegetation model which represents land cover with a system of plant functional types (PFTs). A climate model was then coupled with future land cover to let vegetation interact with climate changes. Finally, this climate model was coupled with a Lagrangian tropospheric chemistry model (STOCHEM) to evaluate the changes in ozone concentration. STOCHEM included future anthropogenic emissions (HC and NOx) and future isoprene emissions using the algorithms given by Guenther *et al*. (1995). Results indicated the importance of incorporating vegetation changes in future air quality studies, by showing up to 10-15 ppb difference over the central US. However, the vegetation databases used by Sanderson were spatially coarse, and more regionally specific information would be useful.

This complex literature has evolved based largely on global models. The goal of this study is two-fold. A first goal is to address many of the same questions on a regional basis, and a second goal is to put the climate induced changes in landcover into context by comparing them to other changes in air quality driven by changes in landcover. Specifically, this work will examine the changes in biogenic emissions due

to land cover changes as a response to climate change. Then, the influences of biogenic emissions will be incorporated into regional air quality models.

5.2 METHODOLOGY

5.2.1 Biogenic Emission Estimation

Biogenic emission inventories were developed using two biogenic emission models; the Community Land Model version 3.0 with a dynamic phenology scheme (CLM3-DP), and the Global Biosphere Emissions and Interactions System version 3.1 (GloBEIS 3.1).

Community Land Model (CLM) version 3.0 (Bonan *et al*., 2002; Oleson *et al*., 2004) was developed to understand how natural and human change in vegetation affect climate.

CLM simulates global land biogenic emissions as follows:

$$F = \varepsilon \cdot \gamma_T \cdot \gamma_R \cdot D$$

(Levis *et al*., 2003) where F is the biogenic emission flux (μg C m^{-2} h^{-1}), ε is the species-specific emission factor (μg C g^{-1} h^{-1}) at a standard leaf temperature (T_S) of 303.15K and standard photosynthetically active radiation (PAR) flux of 1000 μmol m^{-2} s^{-1}, γ_T is the dimensionless canopy temperature scale factor, γ_R is the dimensionless PAR scale factor, and D is the foliar density of ground covered by the species (g dry mass of foliage per m^2 of land surface area). D is expressed as:

$$D = \frac{LAI}{SLA}$$

where LAI is the leaf area index (defined as one-sided, projected leaf area per amount of ground it occupies), and SLA is the specific leaf area (defined as project leaf area per unit leaf weight) from Kucharik *et al*. (2000).

Gulden and Yang (2006) employed the dynamic phenology scheme (CLM-DP) to allow biogenic emissions to respond to inter-annual variability of climate and vegetation.

Community Land Model with a dynamic phenology scheme (CLM-DP) requires data on meteorology based on MM5 outputs, land use/land cover (LULC), and species-specific emission capacities to estimate biogenic emissions. All the simulations reported in this work used the CLM3-DP model.

The study region is shown in Figure 5-1. The focus of the analysis will be on eastern Texas at a 0.1° resolution.

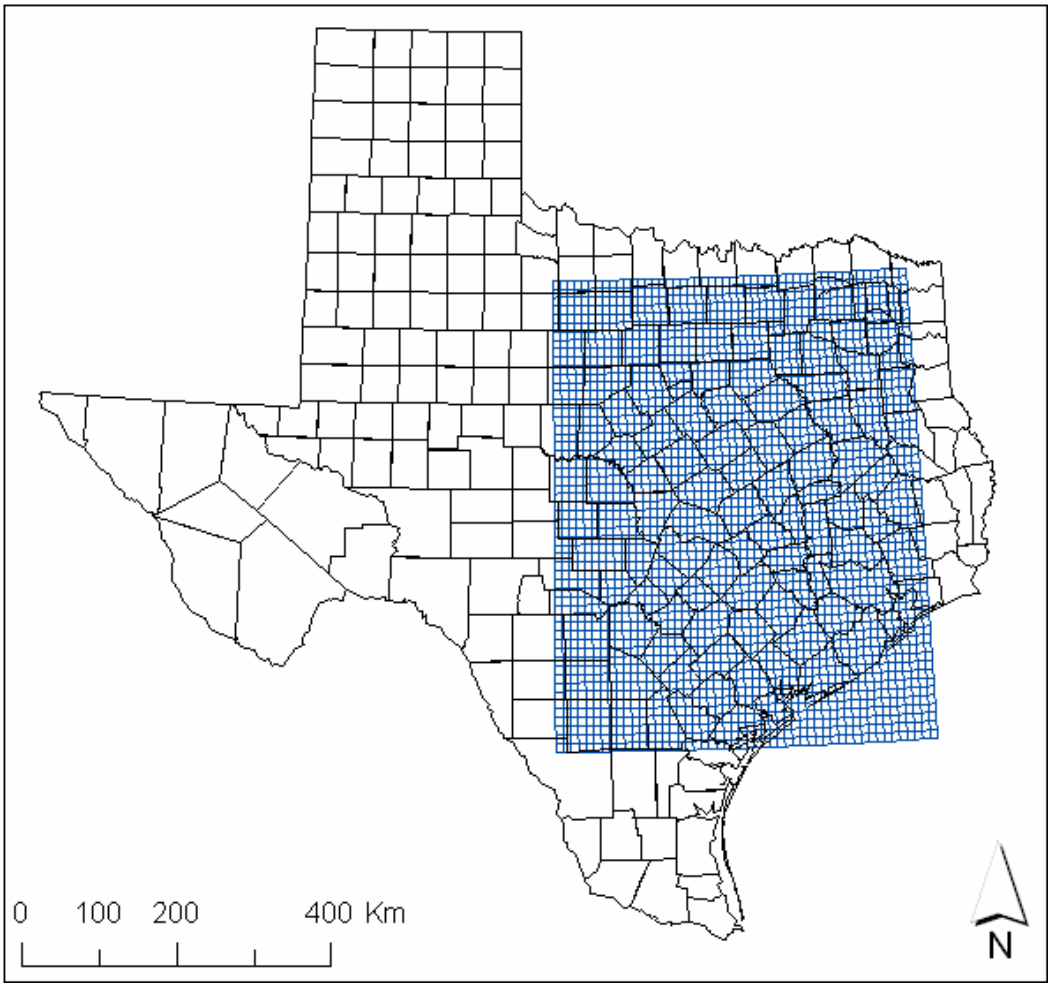

Figure 5-1. Location of study region

The LULC input data required by CLM-DP were derived from a ground referenced dataset (Wiedinmyer *et al.*, 2000, 2001). A detailed description of Wiedinmyer's dataset can be found in Chapter 3. Vegetation in CLM-DP is described in terms of plant function types (PFT) that arise from landscape differences observable from satellites. PFTs used in this study are NET (needleleaf evergreen tree), NES (needleleaf evergreen shrub), NDT (needleleaf deciduous tree), BET (broadleaf

evergreen tree), BES (broadleaf evergreen shrub), BDT (broadleaf deciduous tree), BDS (broadleaf deciduous shrub), Crop, and Grass (C_3: cool climate grasses, C_4: tropical grasses).

For each of Wiedinmyer's land cover classes, each species was assigned to one PFT according to its characteristics (Gulden and Yang, 2006). For instance, temperate evergreen coniferous shrub species in western Texas were classified as a temperate needleleaf evergreen shrub (NES). After the classification, the emission capacity of each PFT was calculated based on the information in Wiedinmyer's dataset (*i.e.*, the leaf biomass of each land cover species in Wiedinmyer's dataset).

Emission capacity of PFT with respect to a single species type, ε_x, is defined as total biogenic emission emitted by PFT_x per total leaf biomass of PFT_x per unit hour across Texas and can be calculated as:

$$\varepsilon_x = \frac{\sum_{j=1}^{n} A_j \left(\sum_{i=1}^{m_x} \varepsilon_i \cdot D_i \right)_j}{\sum_{j=1}^{n} A_j \left(\sum_{i=1}^{m_x} D_i \right)_j}$$

where n is the number of land covers in Texas, A_j is the total area in Texas covered by land cover *j*, m_x is the number of species in land cover *j* identified as PFT_x, ε_i is the emission capacity of i^{th} species identified as PFT in land cover *j*, and D_i is the leaf biomass of the i^{th} species in land cover *j*. A detailed description of developing PFT using Wiedinmyer's land cover dataset is provided in Gulden and Yang (2006).

Biogenic emissions estimated from CLM-DP as a response to climate change is a monthly average for each domain grid cell during the episode period.

The modeling episode for historical biogenic emission estimation is from 1985 to 2004. Since biogenic emissions on a typical summer day in eastern Texas dominate the overall emission inventory, the month of September was chosen as representative month. Monthly averages of September emissions for the entire domain are presented in Figure 5-2. Based on these results, 1997 was chosen as a year with high BVOC year, 1998 was chosen as a median BVOC year, and 2000 was chosen as a low BVOC year.

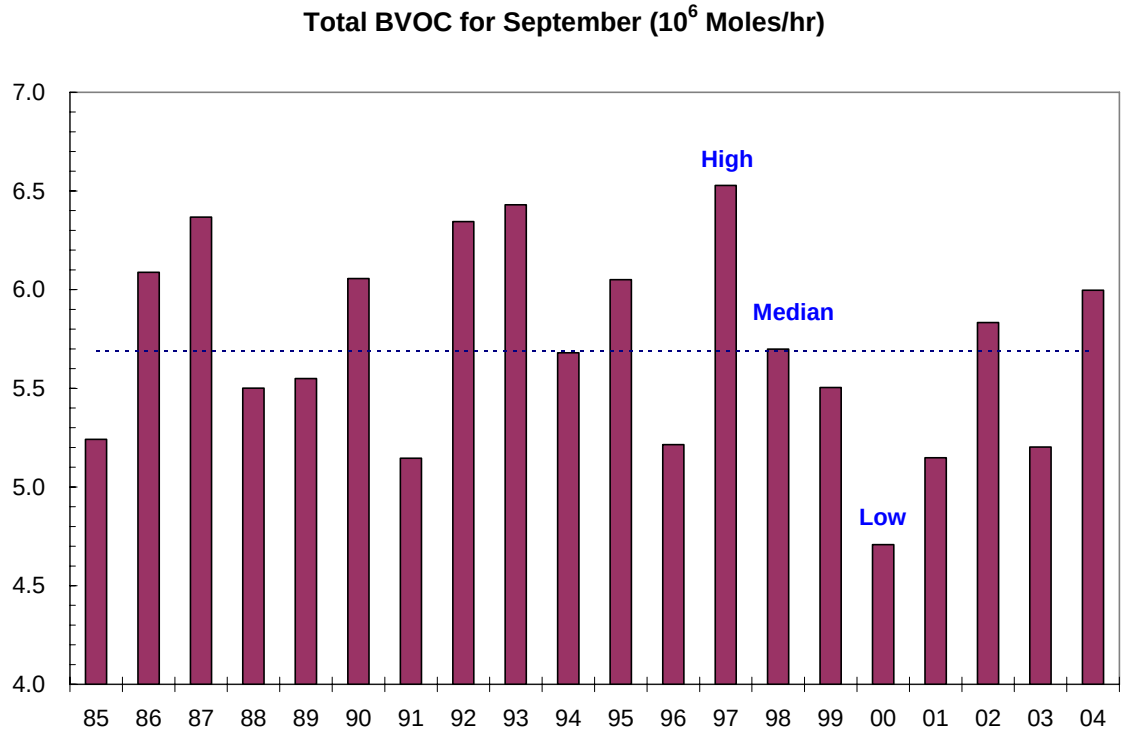

Figure 5-2. Total biogenic emissions for September from year 1985 to year 2004. 1997 is a high BVOC year; 1998 is a median BVOC year; and 2000 is a low BVOC year

As shown in Figure 5-2, inter-annual variability is larger than changes over the past 20 years over the domain of eastern Texas. During past 20 years, *i.e.*, from 1985 to 2004, the average absolute departure from the monthly mean BVOC flux is 15.1% when

dynamic phenology is employed (Gulden *et al.*, 2007), while the average absolute departure from the yearly mean BVOC flux is 5.0%. The method to estimate the average absolute departure from the monthly/yearly mean BVOC flux is shown in Appendix E. Also, Figure 5-3 shows that a long-term trend of BVOC flux is decreasing with a very gentle slope. Since inter-annual variability is much larger than a long-term variability over past 20 years, we will concern ourselves with the role of inter-annual variability in this study.

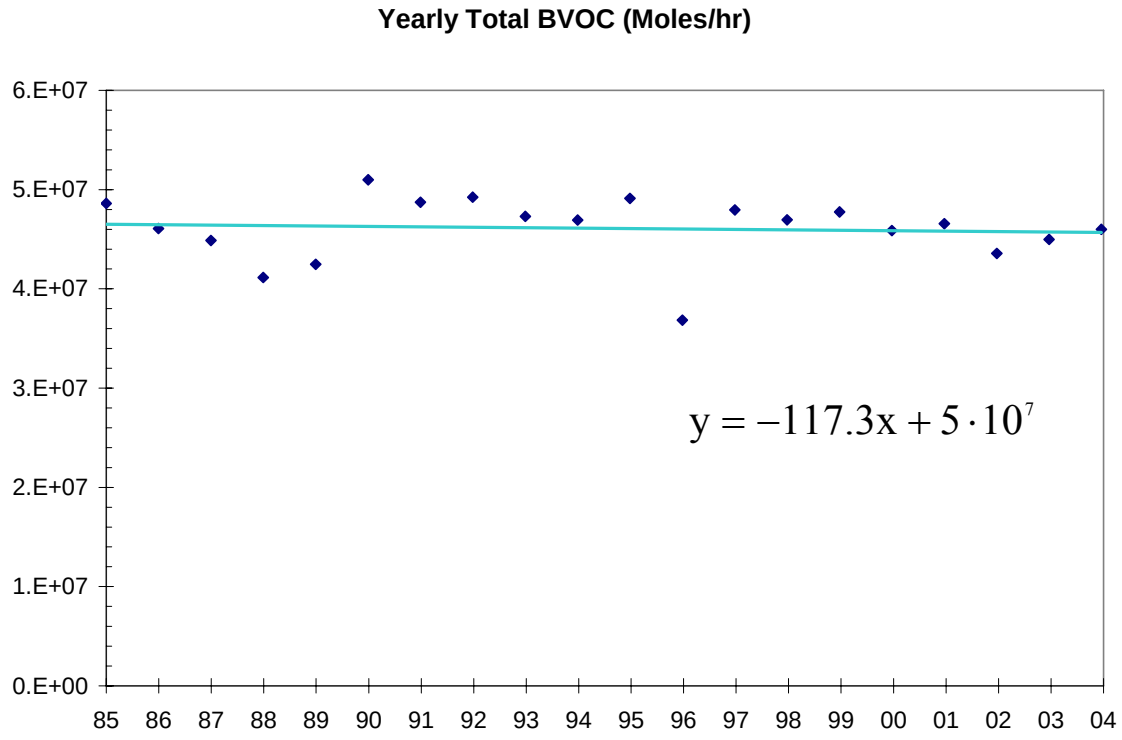

Figure 5-3. Yearly total biogenic emissions from year 1985 to year 2004

The spatial distribution of total BVOC emissions in the high BVOC emission year, 1997, is presented in Figure 5-4. As mentioned earlier, CLM-DP estimates

biogenic emissions at a 0.1° resolution. Since more spatially resolved biogenic emissions are needed in order to perform air quality modeling, the Global Biogenic Emissions and Interactions System (GloBEIS) was also used as described in the air quality modeling methods section of this chapter.

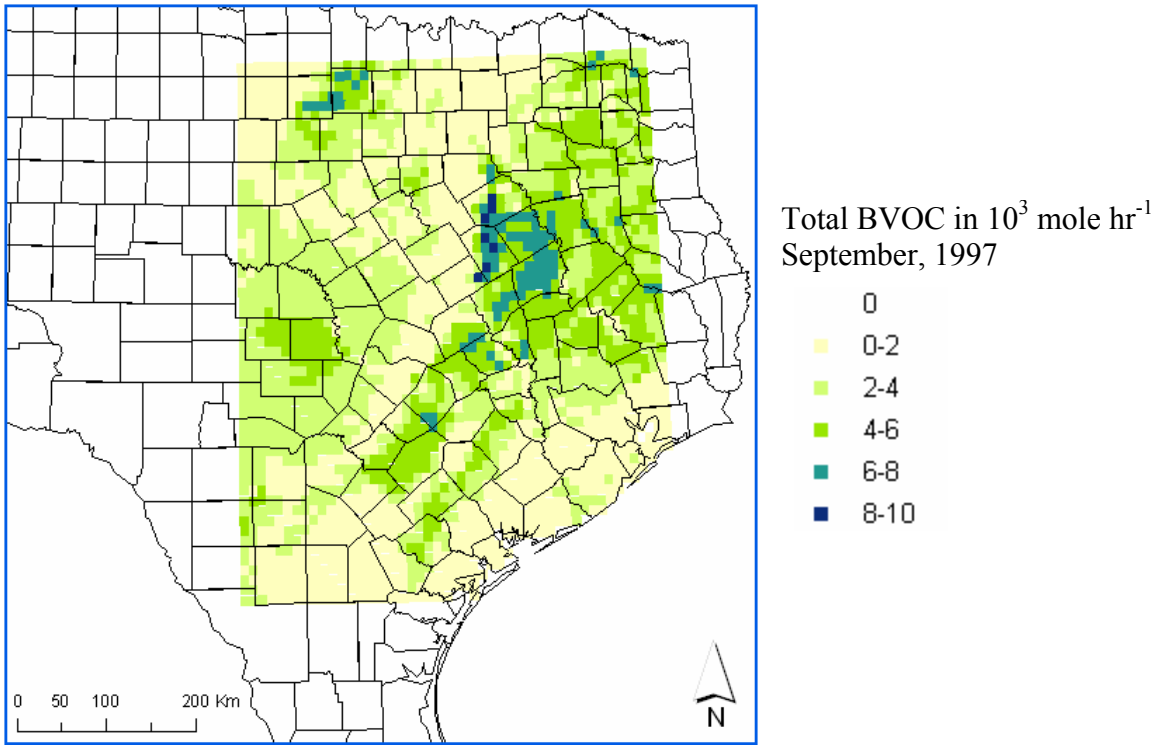

Figure 5-4. Total biogenic emissions for September in 1997. 1997 is a high BVOC year

5.2.2 Photochemical Modeling

Concentrations of air pollutants were predicted using the Comprehensive Air Quality Model, with extensions (CAMx; Environ, 2005). The modeling episodes were chosen to focus on two specific area of interest. For the Austin area, the modeling

episode is based on an episode from September 13th to September 20th, 1999. For the Houston area, modeling episode is based on an episode from August 16th to September 6th, 2000. The study region is shown in Figure 5-5.

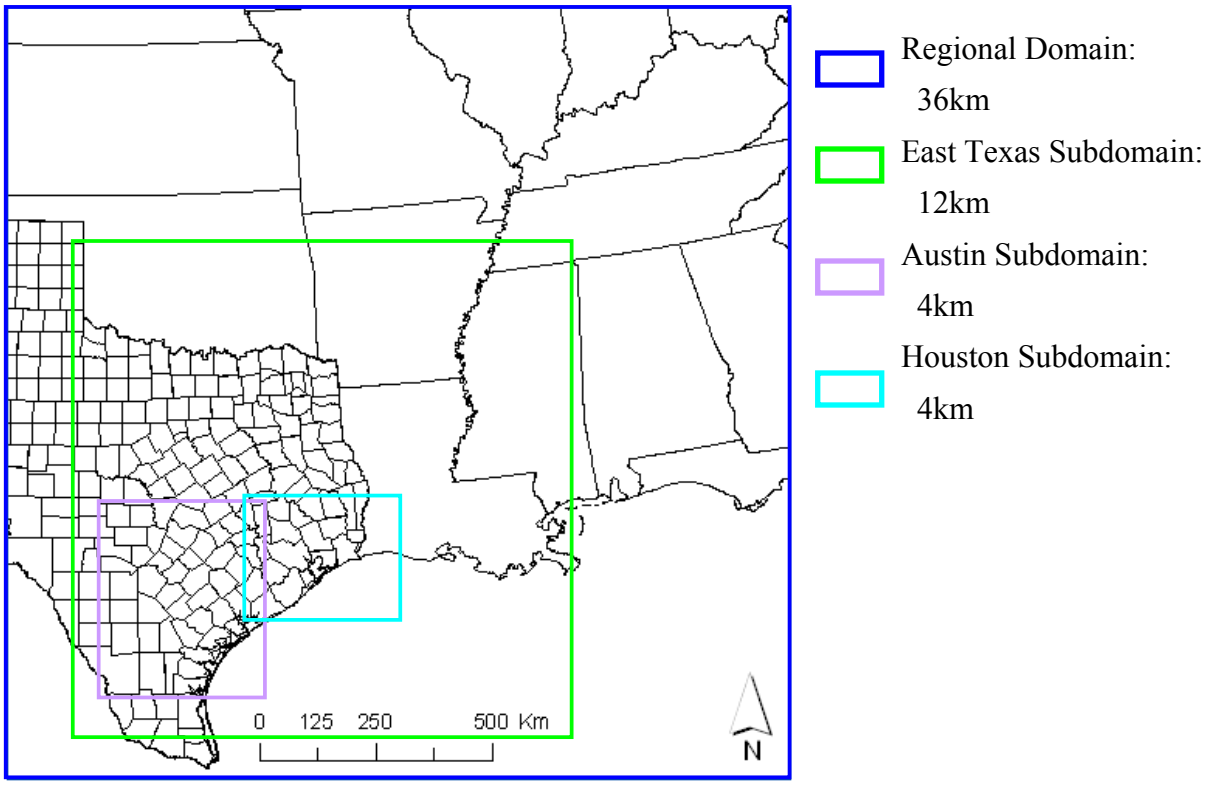

Figure 5-5. Air quality modeling domain: The domain's horizontal structure consists a coarse grid regional domain (36km by 36km resolution) and three nested fine grid subdomains; an East Texas subdomain (12km by 12km), Houston/Galveston-Beaumont/Port Arthur subdomain (4km by 4km), and Austin subdomain (4km by 4km)

For the episode which focuses on Austin area, the Regional domain (36km), East Texas subdomain (12km), and Austin subdomain (4km) were used; the episode for the Houston area shares the same domain, but the Houston subdomain (4km) was used instead of Austin subdomain. Wind field inputs were estimated for each case by the Texas Commission on Environmental Quality (TCEQ) using the MM5 meteorological model; emissions (other than biogenic emissions) were based on the emission inventories assembled by the State. Biogenic emission inventories were based on CLM3-DP and GloBEIS 3.1. Biogenic emissions for the specific episode days were calculated from GloBEIS 3.1 using day-specific meteorological data, while biogenic emissions from CLM3-DP were used as described below.

Overall, the goal of the analyses presented here is to assess the changes in air quality that might emerge due to inter-annual variability in biogenic emissions, due to inter-annual variability in climate. As indicated above, biogenic emission estimations from year 1997, 1998 and 2000, represent high, median, and low biogenic emissions, respectively, due to changes in climate. Therefore, in this work, the effect of having high, median and low biogenic emissions, were compared to the actual basecase of biogenic emission used in the two episodes. A summary of the analyses is shown in Table 5-1.

Table 5-1. Sources of biogenic emission estimation used in 1999 and 2000 modeling episode

Model	Biogenic Emissions	Modeling Episode	
		1999 Episode for Austin	2000 Episode for Houston
CLM3-DP	High case: High Biogenic Emissions	√	√
	Median case: Median Biogenic Emissions	√	√
	Low case: Low Biogenic Emissions	√	√
GloBEIS 3.1	Basecase: Basecase Biogenic Emissions	√	√

To incorporate climate based biogenic emissions into the photochemical model, some issues regarding the biogenic emissions from CLM3-DP needed to be resolved. First, domain resolutions used in CLM3-DP and CAMx are different. Outputs from CLM3-DP are in 0.1° while CAMx requires data in a smaller resolution (4km), as well as larger resolutions (12 and 36km). Modeling domains for CLM3-DP and CAMx are shown in Figure 5-6.

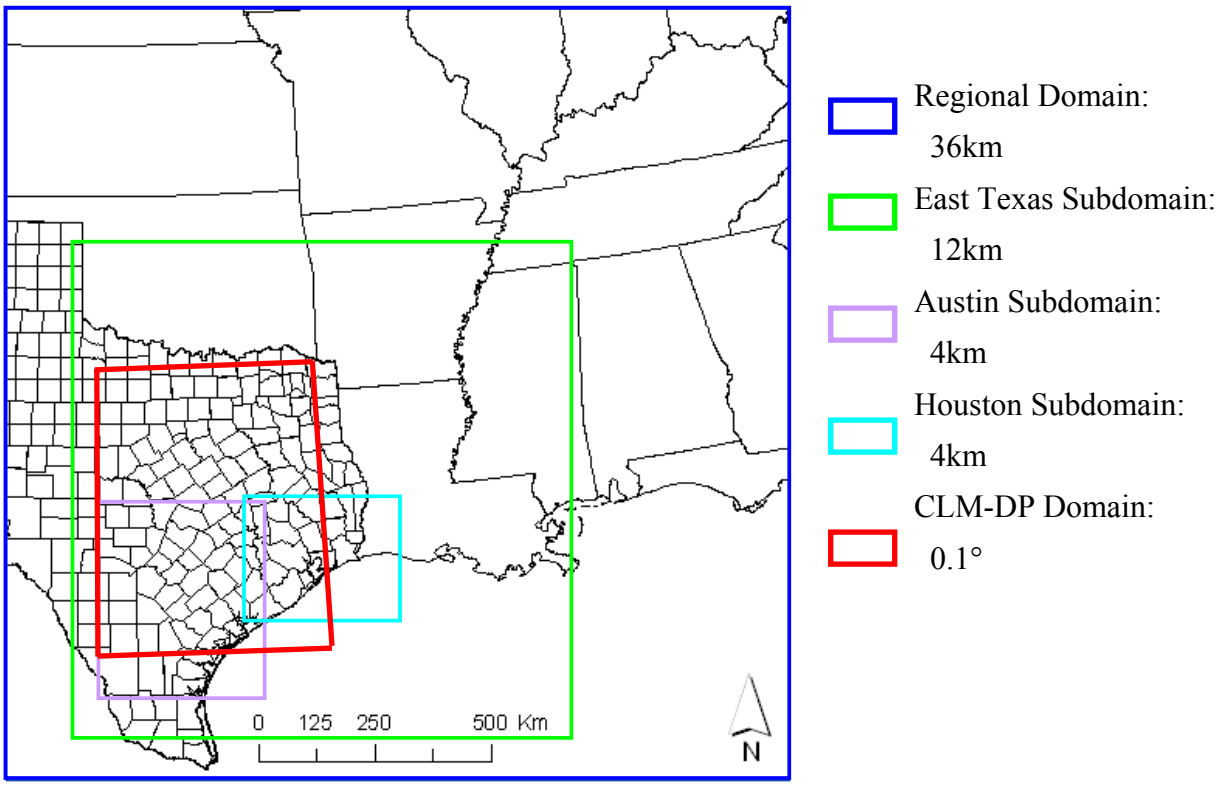

Figure 5-6. Air quality modeling domain (36km, 12km, and 4km) and Community Land Model with a dynamic phenology scheme (0.1°)

Second, CAMx requires hourly basis biogenic emissions, where CLM3-DP provides monthly average biogenic emissions; *i.e.* everyday in a specific month has same biogenic emission value.

Therefore, biogenic emission inventories for the three CLM3-DP cases (High/Median/Low) required modification. Since biogenic emissions from GloBEIS 3.1 are on an hourly basis and share the same resolution with CAMx, Basecase biogenic emissions are used but are multiplied by the ratio of biogenic emissions calculated from CLM3-DP, for the conditions of interest to the episode year ($=\frac{j_{case}}{j_{episode}}$). For example, if the condition of interest is the maximum biogenic emissions, and the emissions during the year with the maximum emissions are double the emissions in the episode year (*e.g.*, 1999 for the 1999 Austin episode), then all of the biogenic emissions in the GloBEIS model would be doubled.

For grid cells where the CAMx domain overlaps the CLM3-DP domain, biogenic emissions are increased by the ratio of emissions in the case of interest to the episode year for that specific grid cell. For the domain grid cells where the two models do not overlap, average fraction of j_{case} and $j_{episode}$ (= average of $\frac{j_{case}}{j_{episode}}$) for entire CLM-DP domain was used. In this study, modifications were done for the 4km, and 12km resolution domains. Basecase biogenic emissions were used for the 36km domain since it was not clear that the regional increases calculated for Texas would extend this far beyond the CLM-DP domain. A schematic diagram of the modification process is shown in Figure 5-7.

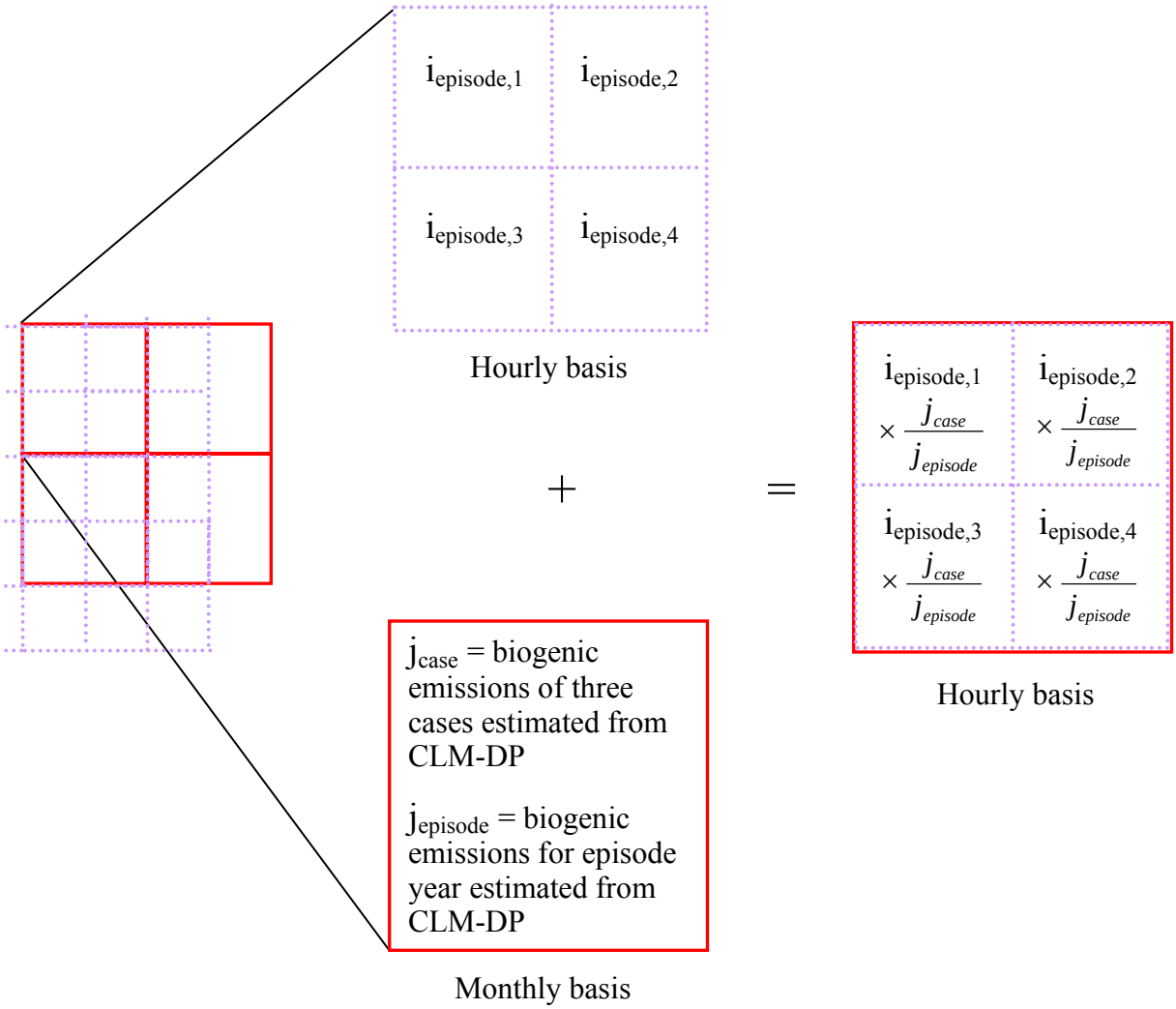

Figure 5-7. Modifications required for the cases (High/Median/Low case) and for the episodes (1999/2000 episode) to incorporate biogenic emissions from CLM3-DP into photochemical model; where purple domain indicates GloBEIS 3.1 subdomain in 4km and red domain indicates CLM3-DP domain in 0.1°. Also, *i* indicates Basecase biogenic emissions from GloBEIS 3.1 for episode year and j indicates biogenic emissions from CLM3-DP for the certain case (j_{case}) or for the certain episode ($j_{episode}$)

5.3 RESULTS

5.3.1 1999 Austin Episode

Predictions of isoprene emissions and 1-hour averaged ozone concentrations in the High, Median and Low cases were compared to predictions based on the original case, referred as the Basecase.

The domain wide changes in predicted daily isoprene emissions during episode days are presented in Table 5-2 and 5-3. Over 4km domain, isoprene emissions increased by 18.2% for the High case, but decreased by 3.1 and 22.6% for Median and Low cases, respectively (Table 5-2). Over the 12km domain, however, isoprene emissions increased by 27.1 and 1.8% for both High and Median cases, and decreased by 14.7% for the Low cases (Table 5-3).

Table 5-2. Percent difference in isoprene emissions, compared to Basecase emissions, using different CLM-DP cases over 4km domain

4km Domain	Units	Date in September, 1999						
		15	16	17	18	19	20	**Avg.**
Basecase	Mmoles day^{-1}	15.8	13.9	17.9	20.5	26.2	18.0	**18.7**
High	%	17.4	17.9	18.7	19.0	18.9	17.2	**18.2**
Median	%	-2.8	-2.9	-3.1	-3.0	-3.1	-3.4	**-3.1**
Low	%	-23.5	-23.2	-22.2	-21.6	-21.5	-23.6	**-22.6**

Note: % difference is defined as $\frac{\text{Scenario ISOP emiss - Basecase ISOP emiss}}{\text{Basecase ISOP emiss}} \times 100$

Table 5-3. Percent difference in isoprene emissions, compared to Basecase emissions, using different CLM-DP cases over 12km domain

12km Domain	Units	Date in September, 1999						
		15	16	17	18	19	20	**Avg.**
Basecase	Mmoles day^{-1}	161.1	129.2	144.1	164.2	183.6	127.4	**151.6**
High	%	27.2	27.2	27.1	27.1	27.1	26.7	**27.1**
Median	%	2.0	2.1	1.8	1.5	1.5	2.1	**1.8**
Low	%	-14.5	-14.6	-14.4	-14.5	-14.6	-15.6	**-14.7**

Note: % difference is defined as $\frac{\text{Scenario ISOP emiss - Basecase ISOP emiss}}{\text{Basecase ISOP emiss}} \times 100$

The spatial distribution of isoprene emissions, in the East Texas subdomain (12 km resolution), on September 20, 1999, is shown in Figure 5-8. Isoprene emissions increase for the High and Median cases, and decrease for the Low case.

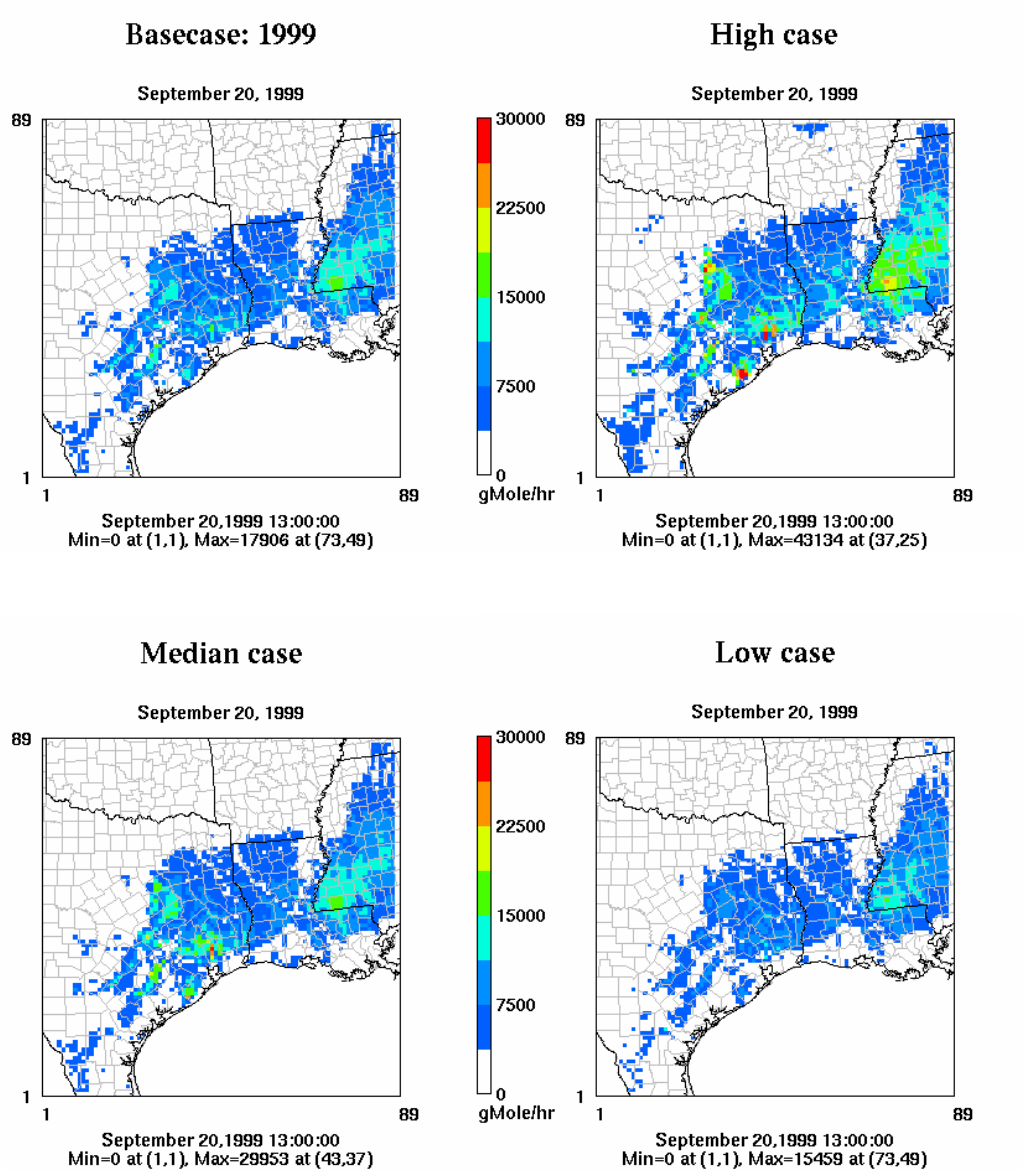

Figure 5-8. Isoprene emissions for three cases (High/Median/Low) and the Basecase

The changes in biogenic emissions due to inter-annual variability in climate led to changes in maximum ozone concentrations (Figure 5-9). Maximum changes in daily ozone concentrations, due to changes in biogenic emissions associated with inter-annual variability, ranged from +22 to -20 ppb for the East Texas area and +18 to -18 ppb for the Austin area. The largest increase in East Texas occurred in the Houston area for all cases, and largest decrease occurred in the Dallas area.

(a)

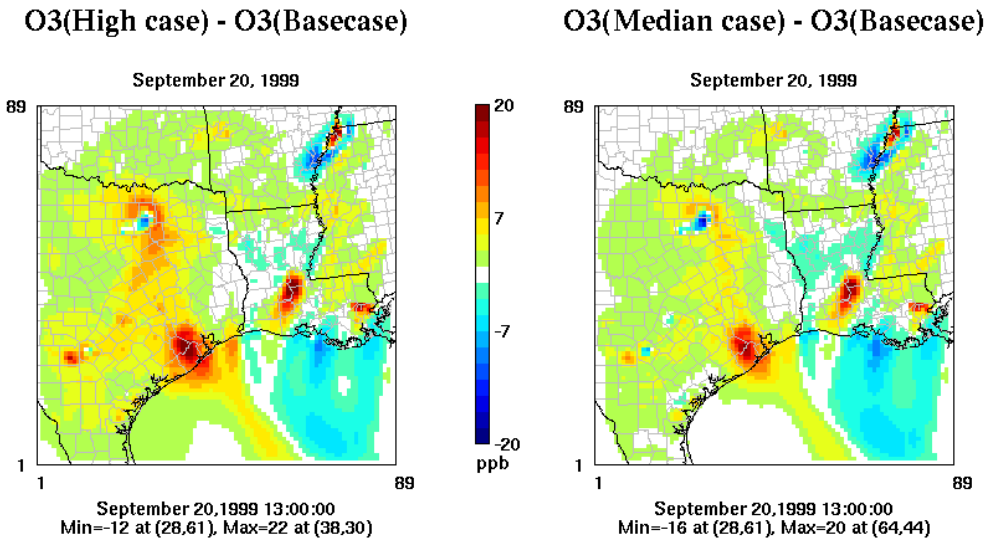
O3(High case) - O3(Basecase)
September 20, 1999
89
1
1
89
20
7
-7
-20
ppb
September 20,1999 13:00:00
Min=-12 at (28,61), Max=22 at (38,30)
O3(Median case) - O3(Basecase)
September 20, 1999
89
1
1
89
September 20,1999 13:00:00
Min=-16 at (28,61), Max=20 at (64,44)

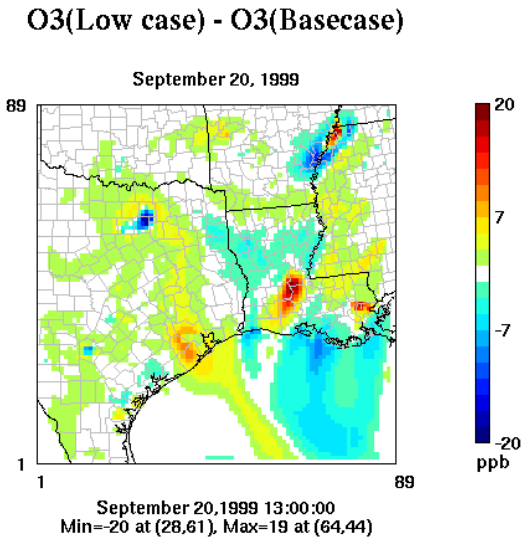
O3(Low case) - O3(Basecase)
September 20, 1999
89
1
1
89
20
7
-7
-20
ppb
September 20,1999 13:00:00
Min=-20 at (28,61), Max=19 at (64,44)

(b)

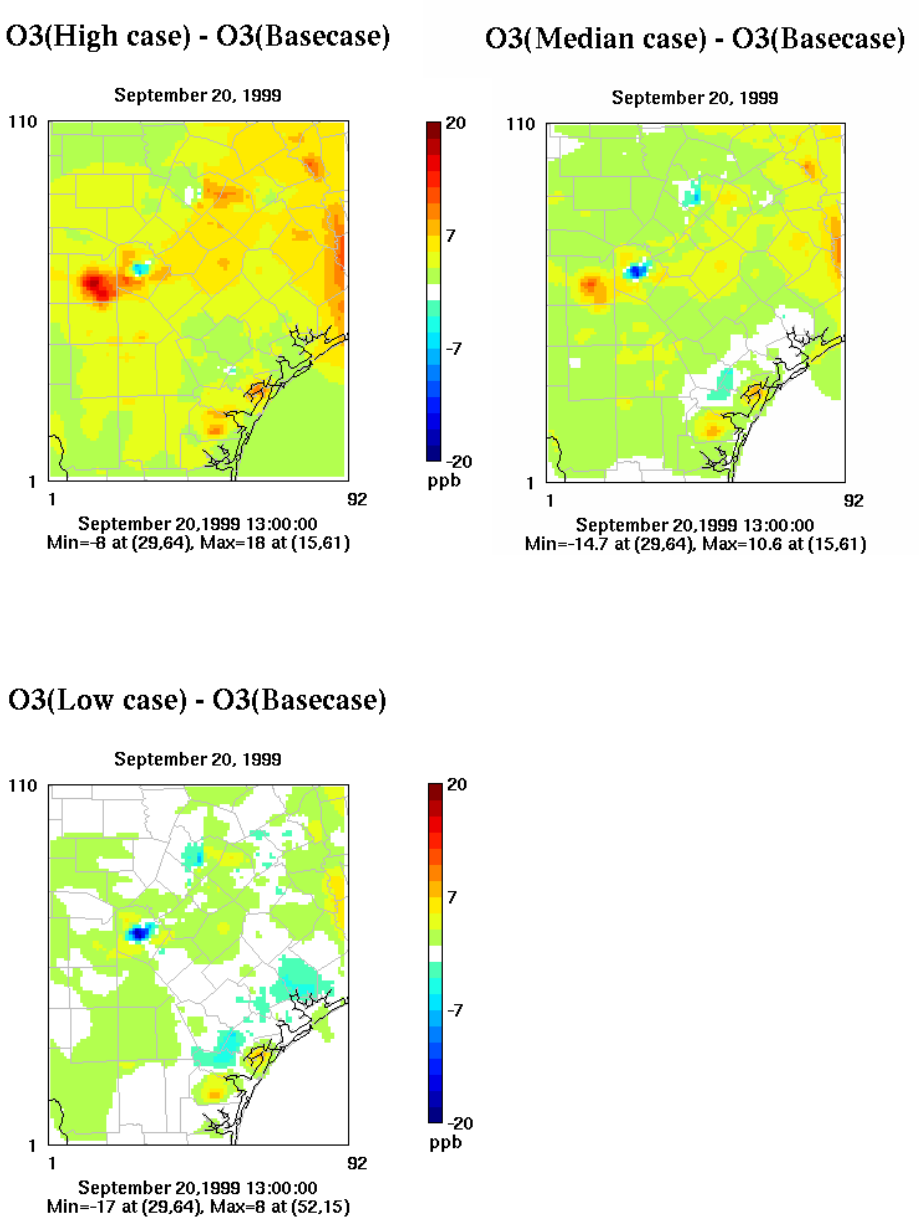

Figure 5-9. Differences in Ozone concentrations for three cases (High/Median/Low) and the Basecase: (a) East Texas subdomain (12km resolution); (b) Austin subdomain (4km resolution)

5.3.2 2000 Houston Episode

Predictions of isoprene emissions and 1-hour averaged ozone concentrations in the High and Median cases were compared to predictions based on the original case, referred as the Basecase. Since the Low biogenic emission year is the same as the episode year (2000), the Low case is excluded from the comparison.

The domain wide changes in predicted daily isoprene emissions during episode days are presented in Table 5-4 and 5-5 (Results are only shown for the high ozone days). Over 4km domain, isoprene emissions increased by 72.6% and 50.4% for High and Median cases, respectively (Table 5-4). Similarly, isoprene emissions over 12 km domain increased by 56.8 and 24.3% for both High and Median cases, respectively (Table 5-5).

Table 5-4. Percent difference in isoprene emissions, compared to Basecase emissions, using different CLM-DP cases over 4km domain

4km Domain	Units	Month-Date in 2000						
		8-25	8-30	8-31	9-01	9-02	9-03	**Avg.**
Basecase	Mmoles day^{-1}	31.1	39.2	36.7	36.7	38.6	40.0	**37.0**
High	%	71.0	72.2	72.5	73.6	73.6	72.9	**72.6**
Median	%	49.8	49.9	50.2	51.2	50.8	50.7	**50.4**

Note: % difference is defined as $\frac{\text{Scenario ISOP emiss - Basecase ISOP emiss}}{\text{Basecase ISOP emiss}} \times 100$

Table 5-5. Percent difference in isoprene emissions, compared to Basecase emissions, using different CLM-DP cases over 12km domain

12km Domain	Units	Month-Date in 2000						
		8-25	8-30	8-31	9-01	9-02	9-03	**Avg.**
Basecase	Mmoles day^{-1}	530.9	613.3	539.4	560.7	587.3	597.8	**571.6**
High	%	56.6	56.8	56.9	56.8	56.9	56.8	**56.8**
Median	%	24.0	24.3	24.5	24.4	24.3	24.4	**24.3**

Note: % difference is defined as $\frac{\text{Scenario ISOP emiss - Basecase ISOP emiss}}{\text{Basecase ISOP emiss}} \times 100$

The spatial distribution of isoprene emissions, in East Texas subdomain (12km resolution), on September 20, 1999, is shown in Figure 5-10. Isoprene emissions increase for both the High and Median cases.

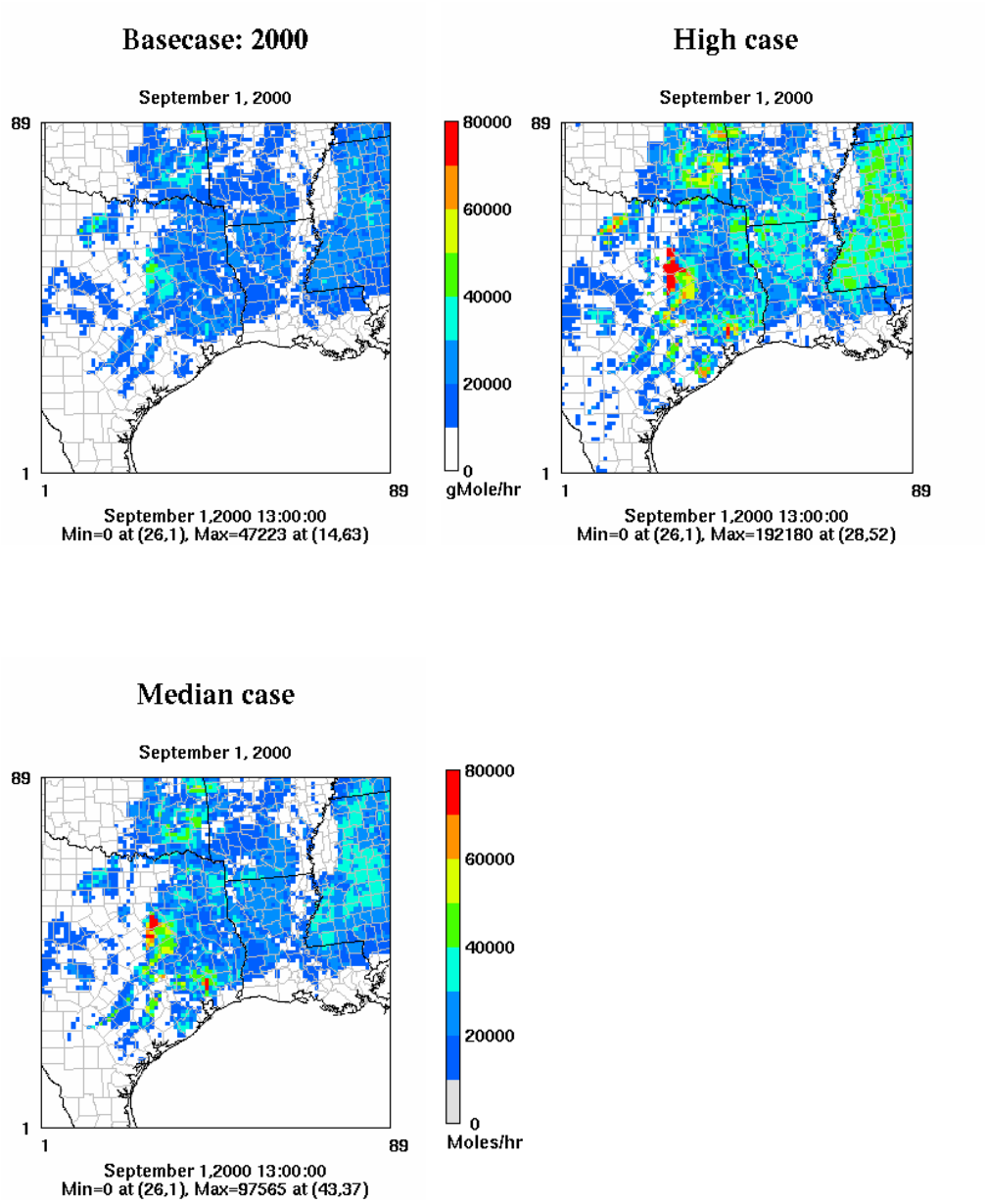

Figure 5-10. Isoprene emissions for two cases (High/Median) and the Basecase

The changes in biogenic emissions due to inter-annual variability in climate led to changes in maximum ozone concentrations (Figure 5-11). Maximum changes in daily ozone concentrations, due to increases in biogenic emissions associated with inter-annual variability, ranged from +40 to -6.0 ppb for the East Texas area and +31 to -1.0 ppb for the Houston area. For both cases, the Houston area showed increase in ozone concentrations up to 31 ppb.

(a)

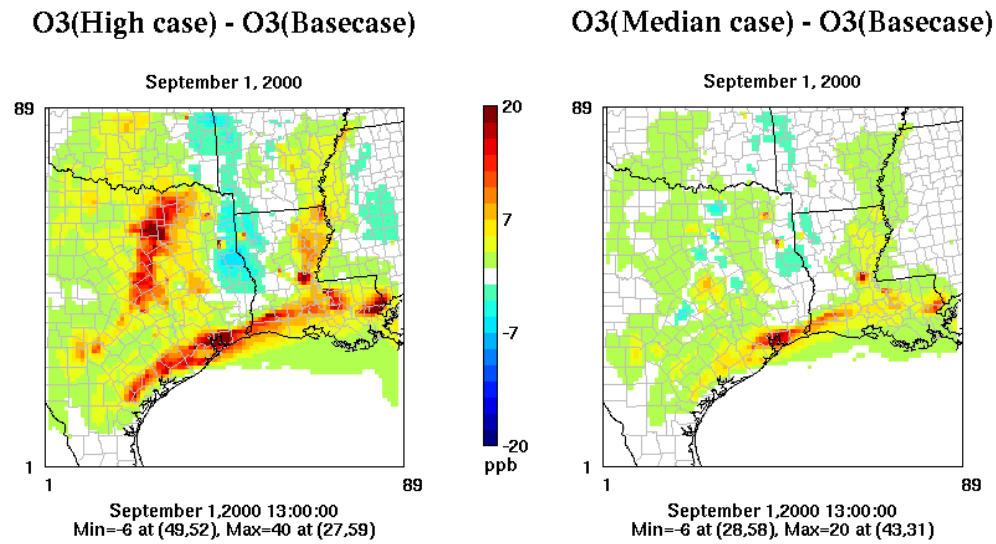

(b)

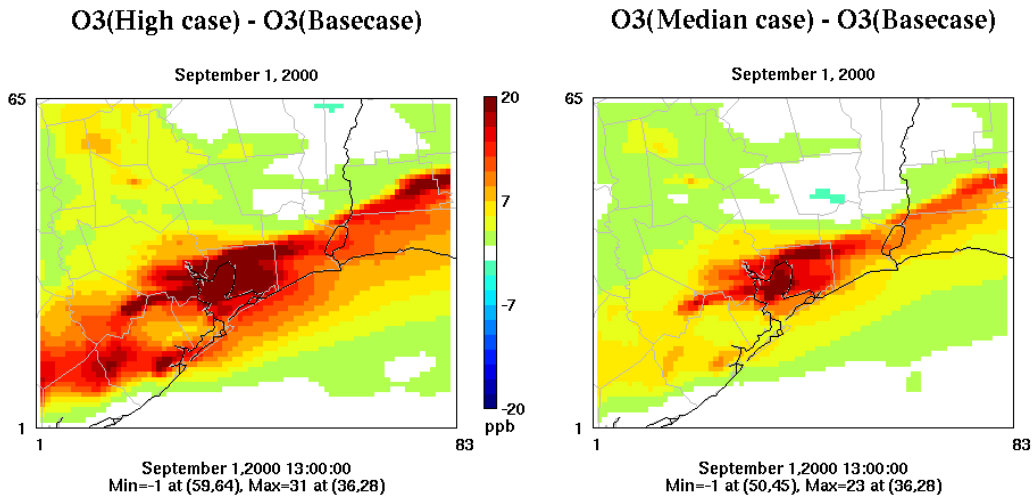

Figure 5-11. Differences in ozone concentrations for three cases (High/Median/Low) and the Basecase: (a) East Texas subdomain (12km resolution); (b) Austin subdomain (4km resolution)

With other factors remaining unchanged, changes in biomass due to changes in climate resulted in impacts of +22 to -20 ppb relative to 1999 levels, +40 to -6 ppb relative to 2000 levels on ozone concentrations in Texas. These changes are much greater in magnitude to changes due to urbanization. Doubling of population in Austin leads to -1.3 to -6.9 ppb changes in peak ozone concentrations.

5.4 REFERENCES

Bonan, G.B., Oleson, K.W., Vertenstein, M., Levis, S., Zeng, X.B., Dai, Y.J., Dickinson, R.E., Yang, Z.L. (2002) "The land surface climatology of the community land model coupled to the NCAR community climate model." *Journal of Climate* **15**(22), 3123-3149.

Brasseur, G., Kiehl, J.T., Muller, J.F., Schneider, T., Gramier, C., Tie, X., Hauglustaine, D. (1998) "Past and future changes in global tropospheric ozone: Impact on radiative forcing." *Geophysical Research Letters* **24**, 3807-3810.

Constable, J.V.H., Guenther, A.B., Schimel, D.S., Monson, R.K. (1999) "Modelling changes in VOC emission in response to climate change in the continental United States." *Global Change Biology* **5**, 791-806.

Cox, P.M., Betts, R.A., Jones, C.D., Spall, S.A., Totterdell, I.J. (2000) "Acceleration of global warming due to carbon-cycle feedbacks in a coupled climate model." *Nature* **408**(6809), 184-187.

ENVIRON International Corporation "Users Guide to the Comprehensive Air Quality. Model with Extensions (CAMx) version 4.03". Available at http://www.camx.com, 2005.

Grewe, V., Dameris, M., Hein, R., Sausen, R., Steil, B. (2001) "Future changes of the atmospheric composition and the impact of climate change." *Tellus Series B-Chemical and Physical Meteorology* **53**(2), 103-121.

Guenther, A., Hewitt, C.N., Erickson, D., Fall, R., Geron, C., Graedel, T., Harley, P., Klinger, L., Lerdau, M., Mckay, W.A., Pierce, T., Scholes, B., Steinbrecher, R., Tallamraju, R., Taylor, J., Zimmerman, P. (1995) "A global-model of natural volatile organic-compound emissions." *Journal of Geophysical Research-Atmospheres* **100**(D5), 8873-8892.

Gulden, L.E., Yang, Z.L. (2006) "Development of species-based, regional emission capacities for simulation of biogenic volatile organic compound emissions in land-surface models: An example from Texas, USA." *Atmospheric Environment* **40**, 1464-1479.

Gulden, L.E., Yang, Z.L. Niu, G-.Y. (2007) "Interannual variation in biogenic emissions on a regional scale." Submitted to *Journal of Geophysical Research-Atmospheres* in 2006.

Hogrefe, C., Lynn, B., Civerolo, K., Ku, J.-Y., Rosenthal, J., Rosenzweig, C., Goldberg, R., Gaffin, S., Knowlton, K., Kinney, P.L. (2004) "Simulating changes in regional air pollution over the eastern United States due to changes in global and regional climate and emissions." *Journal of Geophysical Research* **109**: Art. No. D22301.

Johnson, C.E., Collins, W.J., Stevenson, D.S., Derwent, R.G. (1999) "Relative roles of climate and emissions changes on future tropospheric oxidant concentrations." *Journal of Geophysical Research* **104**(D15), 18631-18645.

Knowlton, K., Rosenthal., J.E., Hogrefe, C., Lynn, B., Gaffin, S., Goldberg, R., Rosenzweig, C., Civerolo, K., Ku, J.Y., Kinney, P.L. (2004) "Assessing ozone-related health impacts under a changing climate." *Environmental Health Perspectives* **112**(15), 1557-1563.

Kucharik, C.J., Foley, J.A., Delire, C., Fisher, V.A., Coe, M.T., Lenters, J.D., Young-Molling, C., Ramankutty, N., Norman, J.M., Gower, S.T. (2000) "Testing the performance of a dynamic global ecosystem model: Water balance, carbon balance, and vegetation structure." *Global Biogeochemical Cycles* **14**, 795-825.

Leung, L.R., Gustafson, W.I. (2005) "Potential regional climate change and implications to U.S. air quality." *Geophysical Research Letters* **32**: Art. No. L16711.

Levis, S., Wiedinmyer, C., Bonan, G.B., Guenther, A. (2003) "Simulating biogenic volatile organic compound emissions in the Community Climate System Model." *Journal of Geophysical Research* **108**(D21), 4659.

Mickley, L.J., Jacob, D.J., Field, B.D., Rind, D. (2004) "Effects of future climate change on regional air pollution episodes in the United States." *Geophysical Research Letters* **31**(24): Art. No. L24103.

Murazaki, K., Hess, P. (2006) "How does climate change contribute to surface ozone change over the United States." *Journal of Geophysical Research* **111**(D5): Art. No. D05301.

Oleson, K.W., Bonan, G.B., Levis, S., Vertenstein, M. (2004) "Effects of land use change on North American climate: impact of surface datasets and model biogeophysics." *Climate Dynamics* **23**(2), 117-132.

Sanderson, M.G., Jones, C.D., Collins, W.J., Johnson, C.E., Derwent, R.G. (2003) "Effect of climate change on isoprene emissions and surface ozone levels." *Geophysical Research letters* **30**(18): Art. No. 1936.

Shallcross, D.E., Monks, P.S. (2000) "New directions: A role for isoprene in biosphere-climate-chemistry feedbacks." *Atmospheric Environment* **34**(10), 1659-1660.

Song, J., Parmenter, B., McDonald-Buller, E., Allen, D.T. (2006) "Impacts of urbanization on biogenic emissions and air pollutant deposition." In preparation of submission to *Environmental Science and Technology*.

Stevenson, D., Doherty, R., Sanderson, M., Johnson, C., Collins, B., Derwent, D. (2005) "Impacts of climate change and variability on tropospheric ozone and its precursors." *Faraday Discussion* **130**, 41-57.

Wiedinmyer, C., Strange, I.W., Estes, M., Yarwood, G., Allen, D.T. (2000) "Biogenic hydrocarbon emission estimates for north central Texas." *Atmospheric Environment* **34**(20), 3419-3435.

Wiedinmyer, C., Guenther, A., Estes, M., Strange, I. W., Yarwood, G., Allen, D. T. (2001) "A land use database and examples of biogenic isoprene emission estimates for the state of Texas, USA." *Atmospheric Environment* **35**(36), 6465-6477.

Chapter 6: Summary and Recommendations

Air quality projections typically assume that all inputs affecting air pollutant concentrations, except anthropogenic emissions, remain constant. Land cover, however, does not remain constant. As land covers change, their changes influence biogenic emissions, air pollutant dry deposition, anthropogenic emissions, and other physical parameters affecting air quality. In this study, the impacts of various factors which drive land cover to change were compared based on their influences on biogenic emissions, dry deposition rates, anthropogenic emissions, and air quality predictions. This study developed mechanisms for tracking changes in land cover and incorporating these changes in land cover into air quality models, demonstrated the importance of developing accurate land cover datasets in predicting future regional air quality; and provided the methods to quantitatively assess the effects of global climate change on regional air quality.

In this study, the uncertainties associated with the air quality model predictions were not explicitly considered; however, the entire thesis is an effective uncertainty analysis on the impact of assuming that land cover and climate remain constant. The effects of urban development on land cover were examined through a variety of mechanisms. Changes in daily maximum ozone concentrations due to the effects of urban development on biogenic emissions and air pollutant dry deposition, ranged from -0.9 to 0.1 ppb for the Austin area. The magnitude of changes in daily maximum ozone concentrations due the effects of urban development on non-road and area source emissions were similar, ranging from -0.1 to 0.8 ppb for the Austin area. However, area-wide changes in ozone concentrations due to the changes in non-road and area source emissions were larger. Ozone concentrations increased as much as 3.9 ppb in the

afternoon, but decreased as much as 13.6 ppb in the morning. This study showed that changes in anthropogenic emissions (on-road, non-road mobile source emissions and area source emissions) due to urban development have larger impacts on ozone concentrations, as compared to the changes in biogenic emissions and air pollutant dry deposition due to those same land cover changes. However, even the effects of changes in biogenic emissions and air pollutant dry deposition are comparable in magnitude to some emissions controls implemented as part of Austin's Early Action Compact (Figure 6-1).

The impacts of climate changes on biogenic emissions were also examined. Changes in daily maximum ozone concentrations, due to inter-annual variation in biogenic emissions associated with inter-annual variability in climate, ranged from -6.7 to 13.6 ppb for the Austin area and 0 to 25.2 ppb for the Houston area. These changes in daily maximum concentrations were much greater than changes due to urban development. However, area-wide changes in ozone concentrations due to urbanization and inter-annual variation in climate are comparable. For the Austin 5-county area, the changes in ozone concentrations due to urbanization ranged from -13.6 to 21.9 ppb, while the changes due to inter-annual variation in climate ranged from -21.3 to 14.0 ppb (Figure 6-1).

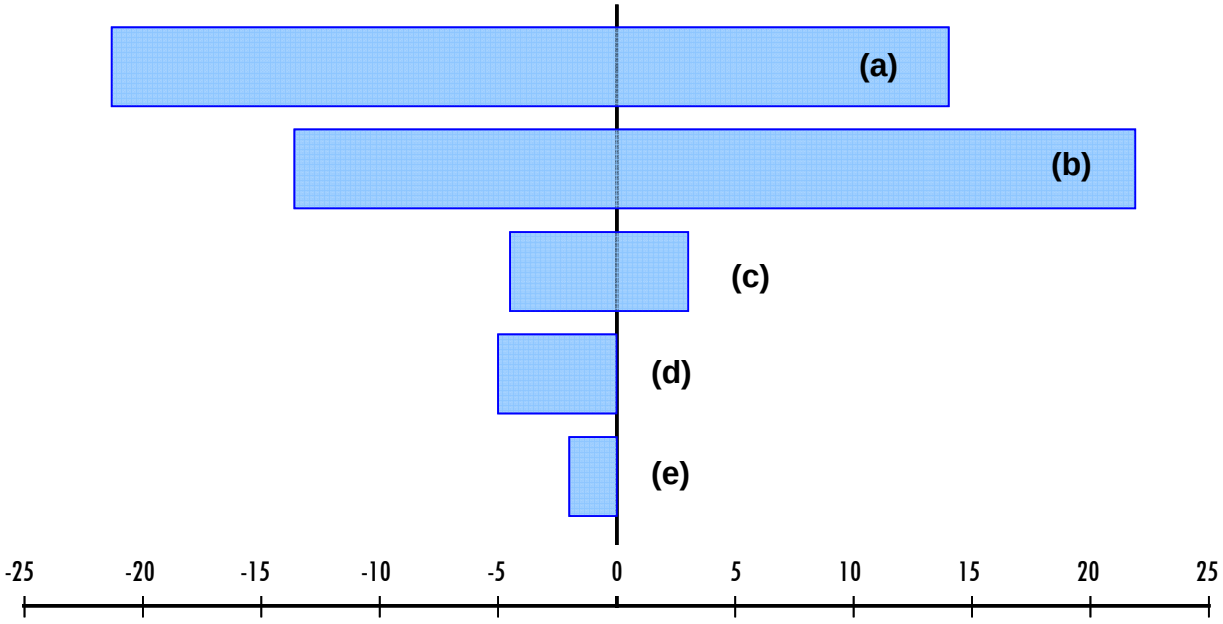

Figure 6-1. Range of changes in ozone concentrations across the 5-county Austin area due to (a) inter-annual variation in climate, (b) urbanization: effects of doubling of population, (c) urbanization: impacts of alternative development patterns, (d) emission control: reducing 50% of anthropogenic NOx emissions, and (e) emission control: reducing 50% of anthropogenic VOC emissions

It is recommended to compare the impacts of regional development scenarios on predicted human exposure patterns using a photochemical model. It is also recommended to compare the effects of changes in emissions described in this study with the impacts of emission control strategies adopted as part of Austin's Early Action Compact.

Appendix A: Impact of Development on Tree Cover

(a) (b)

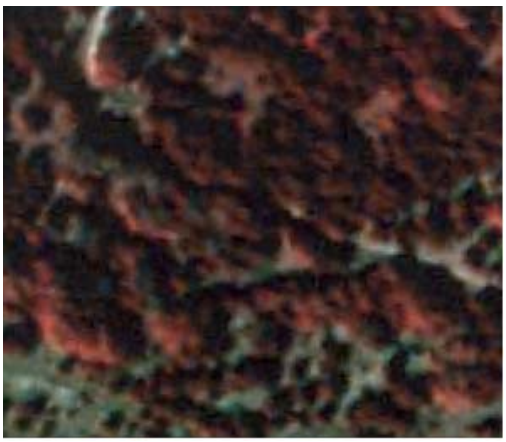

Tree coverage: 223,000 ft^2

Tree coverage: 52,000 ft^2

$$\text{Fraction of trees remaining} = \frac{\text{Tree cover before development}}{\text{Tree cover after development}} = \frac{52000}{223000} = 23\%$$

Figure A-1. Orthophotos for low density residential area in the Austin Methropolitan area; (a) Treed area before development in 1995 orthophotos, and (b) Treed area after development in 2002 orthophotos (Parmenter and Kim, 2005; Personal communication)

Appendix B: Impacts of Urbanization on Transportation and Other Anthropogenic Emissions

This work was performed by McDonald-Buller *et al*. (2005)

B.1. Transportation System Changes Due to Land Use Change in Austin, Texas

Growth scenarios for the five-county Austin area have been developed through a community visioning initiative called Envision Central Texas (ECT). All of the future scenarios are based on a doubling of population, but the scenarios assume very different types of growth. The four scenarios have transportation patterns that are consistent with their land use patterns. ECT Scenario A assumes a typical urban sprawl pattern which results in longer trips; Scenario B concentrates growth within 1 mile of transportation corridors which results in shorter average daily travel time. Scenario C assumes clustered development in new and existing towns throughout region. Additionally, new towns are built along major transportation corridors; Scenario D assumes increasing population density in existing towns and cities. Characteristics of transportation patterns in the five county region are shown in Table B-1 for each ECT scenario and the 2007 Base Case (CAMPO, 2005; ECT, 2003).

Table B-1. Characteristics of each ECT Scenario compared to the Base Case

Scenario	Daily VMT per capita	Auto trips	Transit trips	Bike and walk trips	Commuter rail and toll roads	Light rail	Bus rapid transit
	-	%	%	%	-	-	-
2007 Basecase	26.4	94	3	3	-	-	-
ECT A	34.3	92	4	4	Included	-	Included
ECT B	30.1	90	6	4	Included	Included	-
ECT C	29.0	88	4	8	Included	-	Included
ECT D	27.4	85	6	9	Included	Included	-

Note: Daily vehicle miles of travel (VMT) per capita represent the average distance traveled by a single person in one day

B.2 METHODOLOGY

Forecasts of future anthropogenic emissions from on-road mobile sources were determined through the use of a travel demand model and a mobile source emissions model. Travel demand modeling for each of the ECT scenarios was conducted by ECT planners (Smart Mobility, Inc., 2003). McDonald-Buller *et al*. (2005) conducted the mobile source emissions modeling. Their work is summarized below and provided emission estimates for investigating the impacts of urbanization due to changes in on-road mobile source emissions.

B.2.1 Travel Demand Modeling

Travel demand models are used for regional transportation planning and regional air quality analyses in the U.S. The model developed for ECT follows the standard four

step modeling framework with a number of enhancements for additional sensitivity to land use and transportation infrastructure. The standard four step modeling framework includes 1) trip generation which estimates the number of origins and destinations by trip type for each land use type, 2) trip distribution which joins the origins and destinations estimated in trip generation step to form complete trips, 3) mode choice which determines the mode for each trip, and 4) assignment which assigns vehicle trips to the roadway network. Additional enhancements include 1) an auto availability model that is sensitive to residential density and transit service, 2) a walk/bike trip model that is sensitive to residential density, employment density, and the balance between jobs and housing, 3) a mode choice model that is sensitive to land use, and 4) feedback of congested travel times to affect traveler behavior. A summary of transportation modeling process is provided in Figure B-1 (Smart Mobility, Inc., 2003).

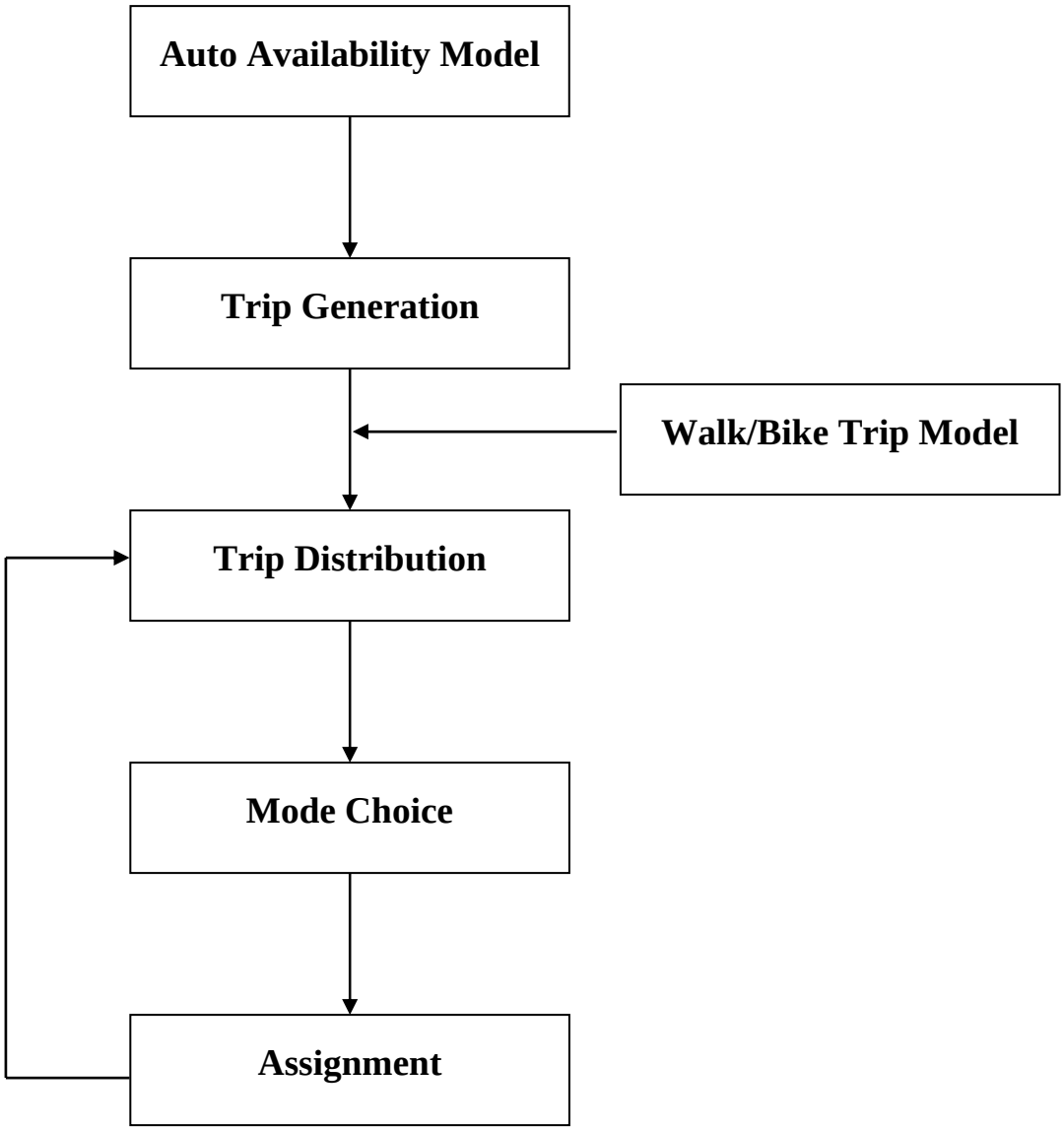

Figure B-1. Schematic diagram of travel demand model for ECT

The travel demand model requires such inputs as roadway and land use characteristics, regional demographic data (population, households, and employment), person/vehicle trip data, and travel time. As a result, the travel demand model provides estimates of VMT and average speeds for the modeling period. On-road mobile source emissions are calculated as:

$$E_{Anthro} = VMT \cdot EF$$

where E_{Anthro} is anthropogenic emissions in grams for NOx, VOC, and CO, VMT is vehicle miles of travel in miles calculated from travel demand model; EF is emission factor in grams mile^{-1} for NOx, VOC, and CO calculated from the U.S. Environmental Protection Agency's (U.S. EPA's) MOBILE 6.2 model (U.S. EPA, 2003).

B.2.2 Photochemical Modeling

The Comprehensive Photochemical Model, with extensions (CAMx) is currently being used for attainment demonstrations and air quality planning by the State of Texas (Environ, 2005). The modeling episode for Austin and Central Texas is from September 13th to September 20th, 1999. CAMx requires data on land use/land cover (LULC), meteorology, and emissions to estimate concentrations of air pollutants. The dataset developed by Wiedinmyer *et al*. (2000, 2001) was used for the LULC input data. Meteorological data were simulated using the MM5 meteorological model. Base year and 2007 future year emission inventories for the modeling domain have been developed and assembled cooperatively by the Texas Commission on Environmental Quality (TCEQ), the Capital Area Council of Governments (CAPCOG), the Alamo Area Council of Governments (AACOG), the City of Victoria, the City of Corpus Christi, the

University of Texas at Austin, ENVIRON International Corporation, the Texas Transportation Institute (TTI), and other state, local, and private sector entities (UT, 2004a, 2004b). On-road mobile source emissions for the ECT scenarios were estimated using the approach described above. In this study, a 4km resolution database was used in the photochemical modeling.

B.3 RESULTS

Predictions of on-road mobile source emissions and 1-hour averaged daily maximum ozone concentrations for the four ECT transportation patterns, referred to as the ECT Scenarios, were compared to predictions based on the current transportation pattern projected to year 2007, referred to as the Base Case for purposes of this study. Since the first two days of the modeled episode, September 13th and 14th, were used for model 'spin-up', results from these days are not included.

The daily VMT calculated from the travel demand model and emission rates of NOx, VOCs, and carbon monoxide (CO) are provided in Table B-2 (McDonald-Buller *et al.*, 2005). Emissions of NOx and VOCs from on-road mobile sources decreased by 70 to 78% and 35 to 50%, respectively, due to the phase-in of new emission standards. Although these standards focus on NOx and VOC reductions, CO emissions decreased for some of scenarios by 10 to 19%. For Scenario A, CO emissions increased slightly primarily due to the substantial increase in VMT.

Table B-2. On-road mobile source emissions in Austin

Scenario	Daily VMT	NOx	VOC	CO
	$*10^6$	tpd	tpd	tpd
2007 future case	44.5	62.1	33.7	458.3
ECT A	82.4	18.4	22.0	478.3
ECT B	72.2	15.9	19.2	413.7
ECT C	69.5	15.6	18.8	403.4
ECT D	65.9	14.4	17.0	372.9

Note: ECT scenario emissions are calculated for 2030 future year

The differences in predicted 1-hour averaged daily maximum ozone concentration during episode days are presented in Table B-3 (McDonald-Buller *et al*., 2005). Reductions in daily maximum ozone concentrations, due to decreases in NOx and VOC emissions associated with increased urbanization, ranged from 1.7 to 7.8 ppb, with typical values of 4.9 ppb for the Austin area. ECT Scenario D showed the largest differences, as compared to the Base Case. Considering that future changes in biogenic emissions and dry deposition due to urbanization resulted in impacts of -1.4 to 0.7 ppb differences on ozone concentrations and were comparable in magnitude to some emissions control strategies adopted as part of Austin's Early Action Compact (reference Chapter 3), it is clear that the impacts of urbanization due to changes associated with on-road mobile sources are significant.

Table B-3. Reductions in daily maximum 1-hour ozone concentration (ppb) in Austin, compared to the daily maximum ozone concentration from Base Case

Scenario	15	16	17	18	19	20
Base Case	80.52	71.95	85.83	86.17	90.41	90.46
ECT A	-5.28	-2.84	-7.10	-4.29	-1.68	-7.70
ECT B	-5.70	-2.94	-7.10	-4.29	-1.69	-7.82
ECT C	-6.02	-3.01	-7.10	-4.29	-1.69	-7.79
ECT D	-5.99	-3.03	-7.10	-4.29	-1.69	-7.82

B.4 REFERENCES

CAMPO. Mobility 2030 Plan, February 2005.

ENVIRON International Corporation. (2005) "User's Guide to the Comprehensive Air Quality. Model with extensions (CAMx) version 4.03." Available at http://www.camx.com.

Envision Central Texas Briefing Packet, July 2003. Available at www.envisioncentraltexas.org.

McDonald-Buller, E.C., Allen, D.T., Kockelman, K., Parmenter, B. (2005) "2005 Progress Report: Predicting the relative impacts of urban development policies and on-road vehicle technologies on air quality in the United States: Modeling and analysis of a case study in Austin, Texas." Submitted to EPA in 2005. Available at http://cfpub.epa.gov/ncer_abstracts/index.cfm/fuseaction/display.abstractDetail/abstract/7425/report/2005.

Genevieve, G. (1995) "The weakening transportation land use connection." Access. No. 6, Spring, pp. 3-11.

Smart Mobility Inc. (SMI). "Envision Central Texas Transportation Model: Technical Documentation." July 2003.

Texas Commission on Environmental Quality (TCEQ). "Austin area early action compact ozone state implementation plan revision." November 2004. Available at http://www.capcog.org/CAPCOairquality/Documents/EAC_Documents/AUS_narr_181104.pdf.

University of Texas at Austin. "Development of the September 13-20, 1999 Base Case Photochemical Model for Austin's Early Action Compact." Submitted to the Texas Commission on Environmental Quality and the U.S. Environmental Protection Agency on behalf of the Capital Area Planning Council, March 2004a.

University of Texas at Austin. "Photochemical Modeling for Austin's Early Action Compact: Development of the September 13-20, 1999 Photochemical Model with 2007 Projected Emissions and Analysis of Future 8-Hour Ozone Design Values." Submitted to the Texas Commission on Environmental Quality and the U.S. Environmental Protection Agency on behalf of the Capital Area Planning Council, March 2004b.

U.S. EPA. "User's Guide to MOBILE6.1 and MOBILE6.2: Mobile Source Emission Factor Model." August 2003.

Wiedinmyer, C., Strange, I.W., Estes, M., Yarwood, G., Allen, D.T. (2000) "Biogenic hydrocarbon emission estimates for north central Texas." *Atmospheric Environment* **34**(20), 3419-3435.

Wiedinmyer, C., Guenther, A., Estes, M., Strange, I. W., Yarwood, G., Allen, D. T. (2001) "A land use database and examples of biogenic isoprene emission estimates for the state of Texas, USA." *Atmospheric Environment* **35**(36), 6465-6477.

Appendix C: Non-road Emissions Inventory Processing for the ECT Scenarios

This Appendix summarizes the input data used to process the emissions for the ECT Scenarios. Details on the NONROAD model used to estimate non-road mobile source emissions are presented in Chapter 4. The emissions for non-road mobile sources were processed at 4km resolution.

The following tables present non-road mobile source emissions for different source categories by county. Table C-1 shows the non-road mobile source emission estimates obtained from the NONROAD model, which does not account for emissions from locomotive operations, gas cans, airport service operations, and military operations. Table C-2, C-3, and C-4 present the emissions from locomotive, airport service, and military operations and gas cans, respectively.

Table C-1. Emission estimates from the NONROAD model for the Base Case and the ECT Scenarios

Scenario	County	CO	NOx	VOC
		tpd	tpd	tpd
2007 Base Case	Bastrop	7.48	0.26	0.31
	Caldwell	4.41	0.16	0.50
	Hays	17.60	3.53	1.42
	Travis	316.32	9.36	13.73
	Williamson	72.63	2.95	3.29
	Total	418.43	16.26	19.24
ECT A	Bastrop	12.22	0.09	0.37
	Caldwell	6.46	0.05	0.38
	Hays	25.08	0.74	1.15
	Travis	438.34	3.14	13.35
	Williamson	105.59	0.89	3.36
	Total	587.68	4.91	18.62

Table C-1. (*Contd.*)

Scenario	County	CO	NOx	VOC
		tpd	tpd	tpd
ECT B	Bastrop	17.27	0.11	0.58
	Caldwell	9.67	0.08	0.37
	Hays	28.13	0.75	1.10
	Travis	453.91	3.24	13.56
	Williamson	115.74	0.97	3.66
	Total	624.73	5.14	19.27
ECT C	Bastrop	20.20	0.12	0.69
	Caldwell	12.30	0.09	0.47
	Hays	28.97	0.75	1.13
	Travis	445.07	3.21	13.22
	Williamson	117.72	0.97	3.74
	Total	624.26	5.14	19.26
ECT D	Bastrop	14.05	0.09	0.45
	Caldwell	8.24	0.06	0.44
	Hays	24.99	0.74	1.17
	Travis	432.61	3.11	13.12
	Williamson	106.82	0.90	3.40
	Total	586.71	4.90	18.58

Table C-2. Emissions from railroad operations

Scenario	County	CO	NOx	VOC
		tpd	tpd	tpd
2007 Base Case	Bastrop	0.14	0.77	0.05
	Caldwell	0.09	0.52	0.04
	Hays	0.08	0.42	0.03
	Travis	0.07	0.40	0.03
	Williamson	0.19	1.03	0.07
	Total	0.56	3.14	0.22
ECT	Bastrop	0.14	0.55	0.05
	Caldwell	0.09	0.37	0.04
	Hays	0.08	0.30	0.03
	Travis	0.07	0.28	0.03
	Williamson	0.19	0.74	0.07
	Total	0.56	2.25	0.22

Note: The ECT Scenarios have the same value

Table C-3. Emissions from residential and commercial gas cans

Scenario	County	Residential, VOC	Commercial, VOC
		tpd	tpd
2007 Basecase	Bastrop	0.05	0.02
	Caldwell	0.03	0.01
	Hays	0.10	0.03
	Travis	0.71	0.24
	Williamson	0.24	0.08
	Total	1.13	0.38
ECT A	Bastrop	0.24	0.08
	Caldwell	0.01	0.00
	Hays	0.12	0.04
	Travis	1.41	0.48
	Williamson	0.73	0.25
	Total	2.52	0.85
ECT B	Bastrop	0.33	0.11
	Caldwell	0.03	0.01
	Hays	0.12	0.04
	Travis	1.29	0.43
	Williamson	0.75	0.25
	Total	2.53	0.85

Table C-3. (*Contd.*)

Scenario	County	Residential gas cans, VOC	Commercial gas can, VOC
		tpd	tpd
ECT C	Bastrop	0.43	0.14
	Caldwell	0.04	0.01
	Hays	0.13	0.04
	Travis	1.14	0.38
	Williamson	0.80	0.27
	Total	2.53	0.85
ECT D	Bastrop	0.33	0.11
	Caldwell	0.03	0.01
	Hays	0.12	0.04
	Travis	1.26	0.42
	Williamson	0.77	0.26
	Total	2.50	0.84

Table C-4. Emissions from airport operations (Austin-Bergstrom International Airport) and military operations

Category	County	CO	NOx	VOC
		tpd	tpd	tpd
Airport Service	Total	8.22	1.06	0.75
Military	Total	4.12	1.23	0.34

Note: No growth was assumed from the Base Case to the ECT Scenarios

Table C-5 presents the weekday total non-road mobile source emissions including emissions estimated from NONROAD model and emissions from railroad service operations, airport service operations, military operations, and gas cans.

Table C-5. Weekday non-road mobile source emissions in the five-county Austin area

Scenario	County	CO	NOx	VOC
		tpd	tpd	tpd
2007 Base Case	Bastrop	7.62	1.03	0.44
	Caldwell	4.50	0.68	0.57
	Hays	17.67	3.96	1.58
	Travis	328.72	12.04	15.79
	Williamson	72.81	3.98	3.69
	Total	431.33	21.69	22.06
ECT A	Bastrop	12.36	0.64	0.75
	Caldwell	6.55	0.42	0.43
	Hays	25.16	1.04	1.34
	Travis	450.74	5.71	16.36
	Williamson	105.77	1.63	4.41
	Total	600.58	9.45	23.30

Table C-5. (*Contd.*)

Scenario	County	CO	NOx	VOC
		tpd	tpd	tpd
ECT B	Bastrop	17.41	0.66	1.08
	Caldwell	9.76	0.45	0.44
	Hays	28.21	1.05	1.29
	Travis	466.32	5.81	16.40
	Williamson	115.93	1.71	4.74
	Total	637.62	9.68	23.96
ECT C	Bastrop	20.34	0.67	1.32
	Caldwell	12.40	0.46	0.56
	Hays	29.04	1.06	1.34
	Travis	457.48	5.78	15.85
	Williamson	117.90	1.72	4.88
	Total	637.16	9.68	23.94
ECT D	Bastrop	14.18	0.64	0.95
	Caldwell	8.33	0.43	0.51
	Hays	25.07	1.04	1.36
	Travis	445.02	5.69	15.91
	Williamson	107.01	1.64	4.50
	Total	599.60	9.44	23.24

The following tables show the weekday total area source emissions by county.

Table C-6. Weekday area source emissions in the five-county Austin area

Scenario	County	CO	NOx	VOC
		tpd	tpd	Tpd
2007 Basecase	Bastrop	1.86	0.76	5.64
	Caldwell	0.95	0.67	15.84
	Hays	1.88	0.79	8.40
	Travis	9.58	4.05	58.88
	Williamson	4.27	3.84	21.90
	Total	18.55	10.12	110.66
ECT A	Bastrop	4.58	1.88	13.86
	Caldwell	2.02	1.43	33.74
	Hays	4.30	1.81	19.17
	Travis	16.00	6.77	98.36
	Williamson	9.59	8.62	49.14
	Total	36.49	20.51	214.28

Table C-6. (*Contd.*)

Scenario	County	CO	NOx	VOC
		tpd	tpd	Tpd
ECT B	Bastrop	6.29	2.58	19.04
	Caldwell	3.49	2.47	58.27
	Hays	4.45	1.88	19.85
	Travis	14.60	6.17	89.75
	Williamson	9.90	8.90	50.73
	Total	38.73	22.00	237.64
ECT C	Bastrop	8.02	3.29	24.27
	Caldwell	4.99	3.53	83.28
	Hays	4.75	2.00	21.18
	Travis	12.87	5.44	79.11
	Williamson	10.49	9.44	53.78
	Total	41.13	23.70	261.62
ECT D	Bastrop	6.28	2.57	18.99
	Caldwell	3.49	2.47	58.21
	Hays	4.47	1.89	19.95
	Travis	14.21	6.01	87.40
	Williamson	10.07	9.05	51.58
	Total	38.52	21.99	236.13

Appendix D: VOC and NOx Emissions from Non-Road and Area Sources

This Appendix presents additional figures showing differences in VOC and NOx emissions from non-road and area sources. Details on the development of the non-road and area source emission inventory are summarized in Chapter 4. The emissions for non-road and area sources were estimated at 4km resolution.

The following Figures show the maximum differences (both increases and decreases) in VOC and NOx emissions from each of the ECT scenarios relative to the Base Case due to changes in non-road and area source emissions. Figure D-1 presents maximum differences in VOC emissions from non-road mobile sources. Both maximum increases and decreases in VOC emissions occurred at 0900. Maximum differences in NOx emissions from non-road mobile sources are also presented in Figure D-2 and D-3. NOx emissions slightly increased in the morning (at 0800) for every ECT Scenarios (Figure D-2), but substantially decreased at 1300 for ECT A and B, and 1200 for ECT C and D (Figure D-3). Large reductions of NOx emissions were consistent with the regions that were classified as "urban" in EPS2.

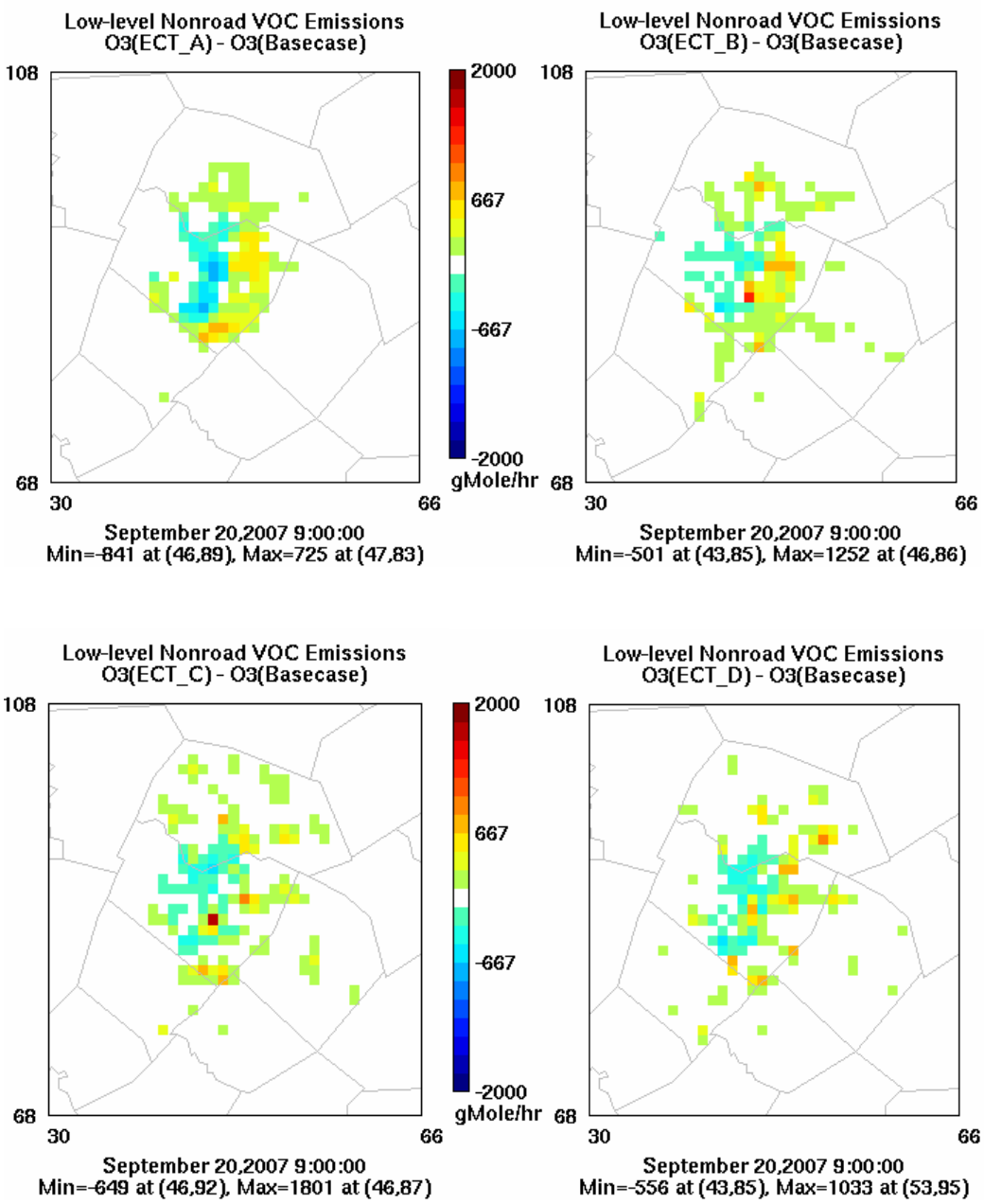

Figure D-1. Differences in VOC Emissions from non-road mobile sources between the ECT Scenarios and the Base Case at 0900

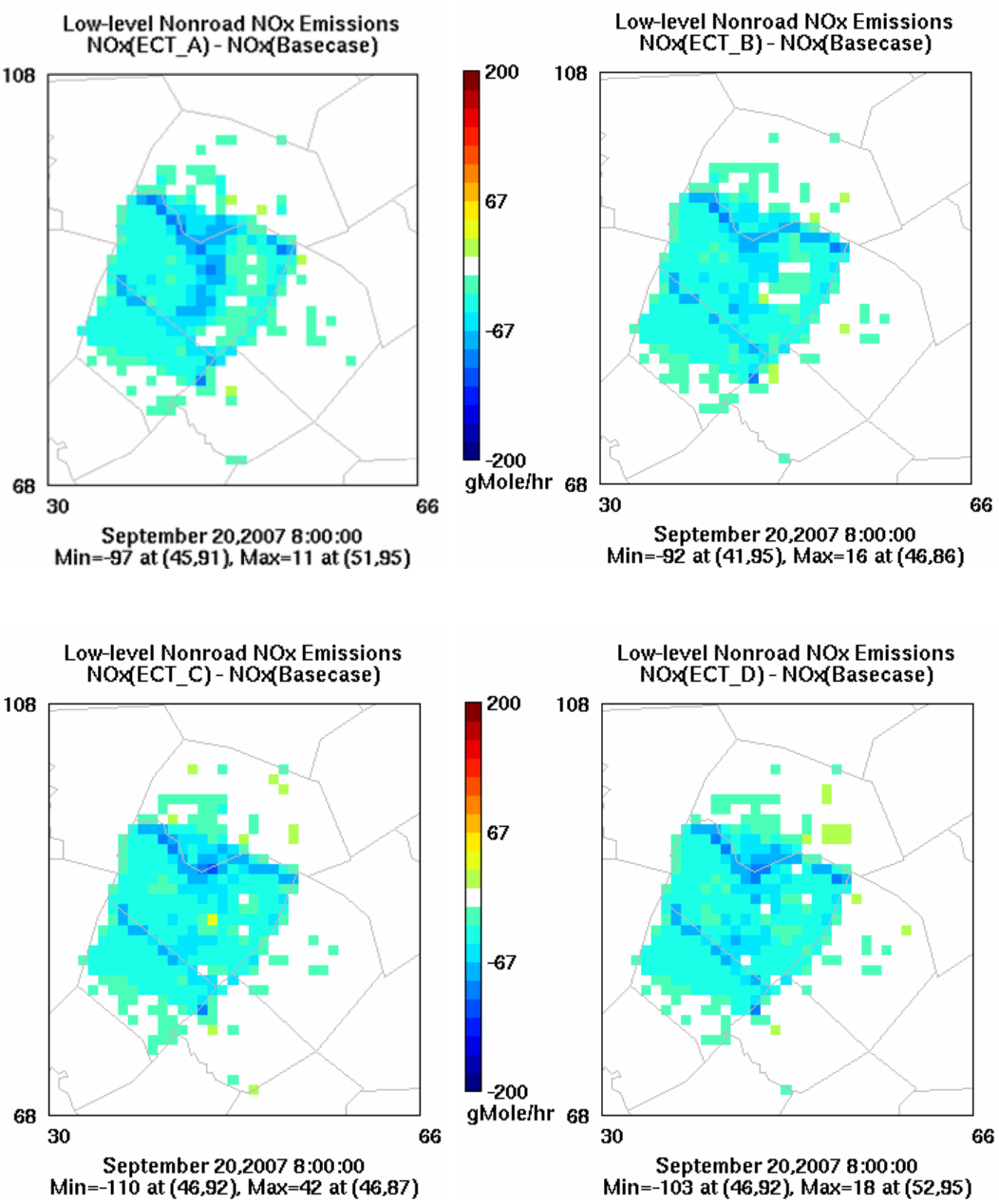

Figure D-2. Difference in NOx Emissions from non-road mobile sources between the ECT Scenarios and the Basecase at 0800

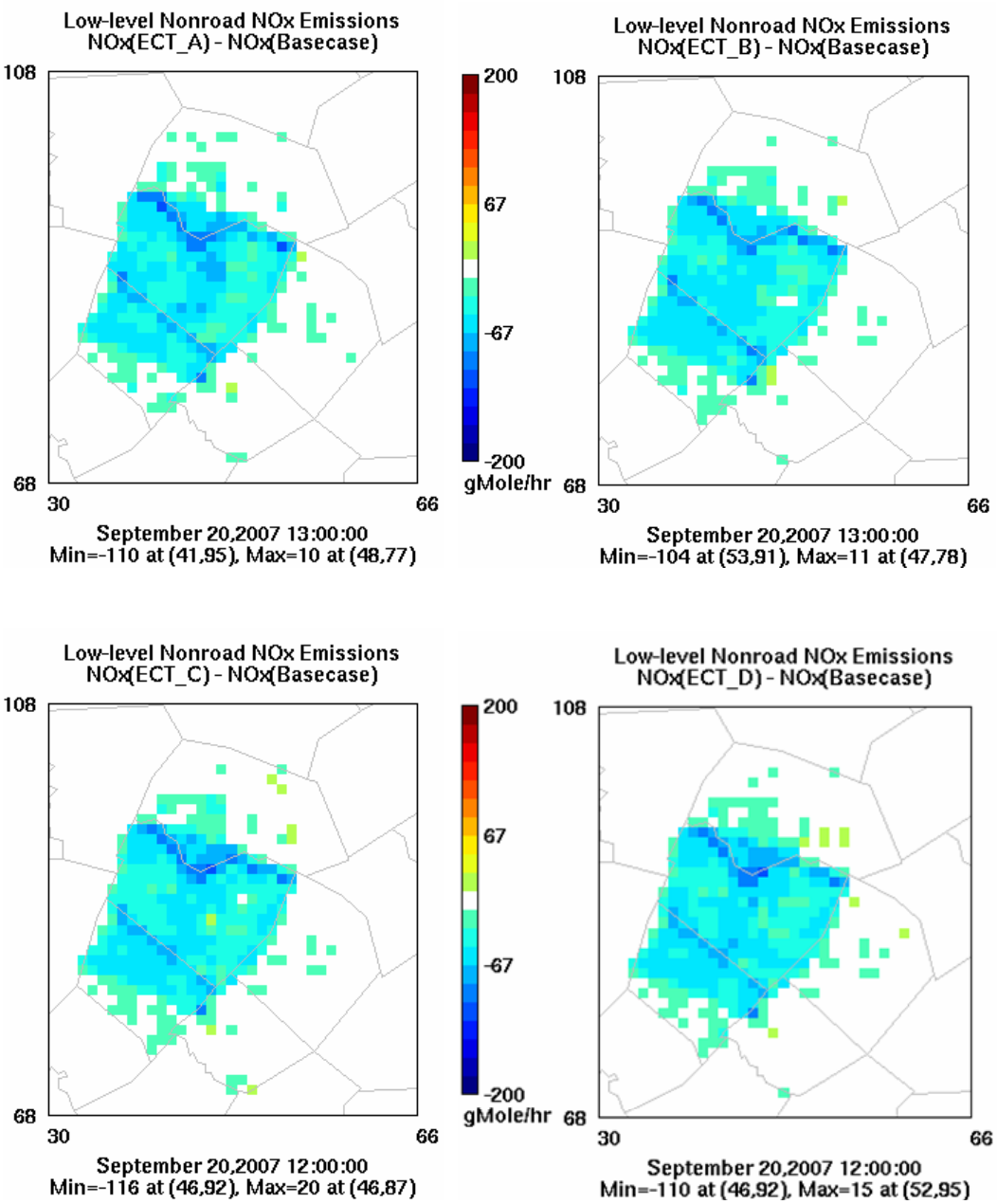

Figure D-3. Difference in NOx Emissions from non-road mobile sources between the ECT Scenarios and the Base Case at 1300 (for ECT Scenario A and B), and at 1200 (for ECT Scenario C and D)

Figures D-4 and D-5 presents the maximum difference in VOC emissions from area sources. The maximum increase in VOC emissions occurred at 0700 (Figure D-4) and the maximum decrease occurred at 1600 (Figure D-5). Maximum differences in NOx emissions from area sources are presented in Figure D-6 and D-7. The maximum increase in NOx emissions occurred at 1600 (Figure D-6) and the maximum decrease occurred at 0700 for every ECT Scenario (Figure D-7).

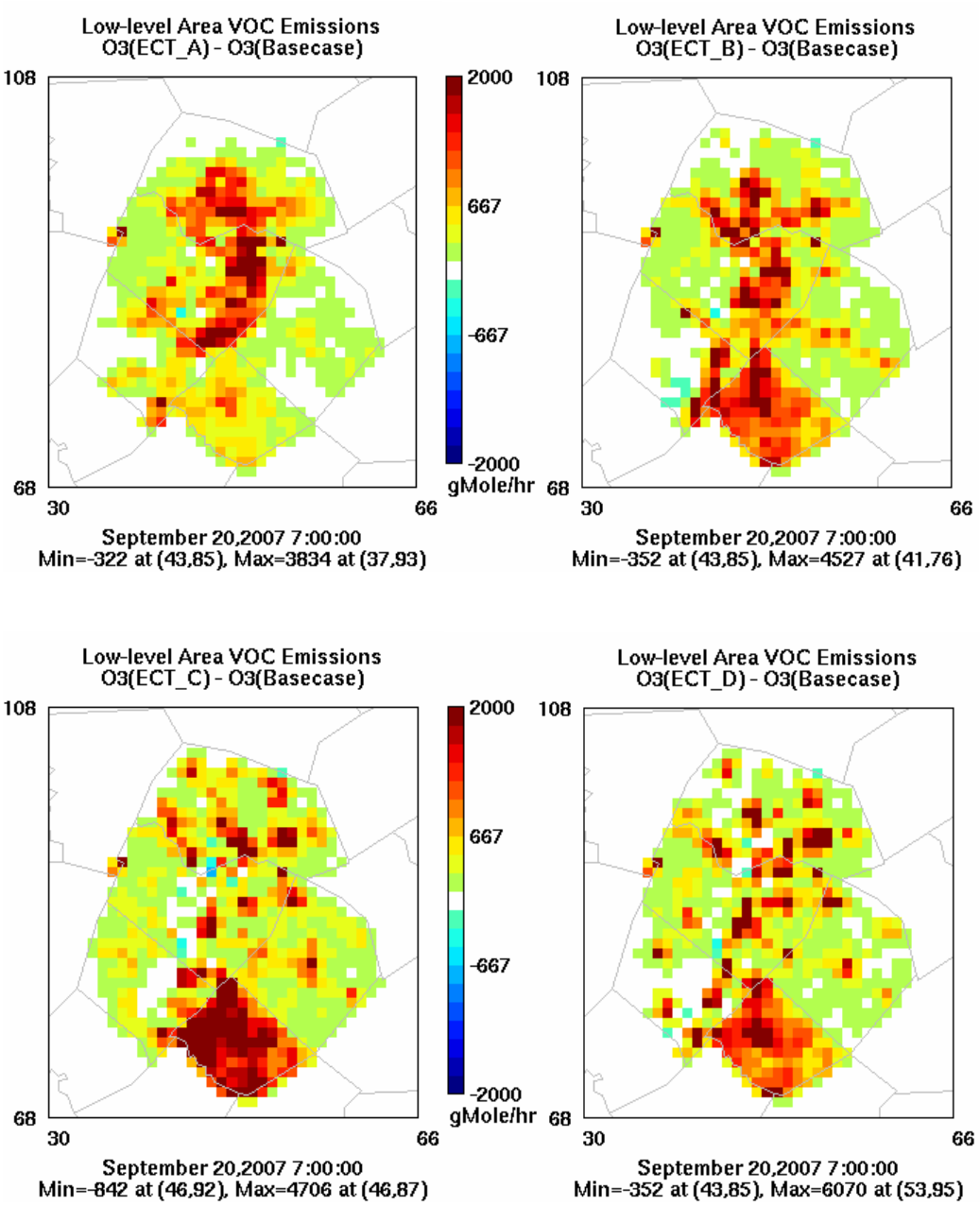

Figure D-4. Difference in VOC Emissions from area sources between the ECT Scenarios and the Base Case at 0700

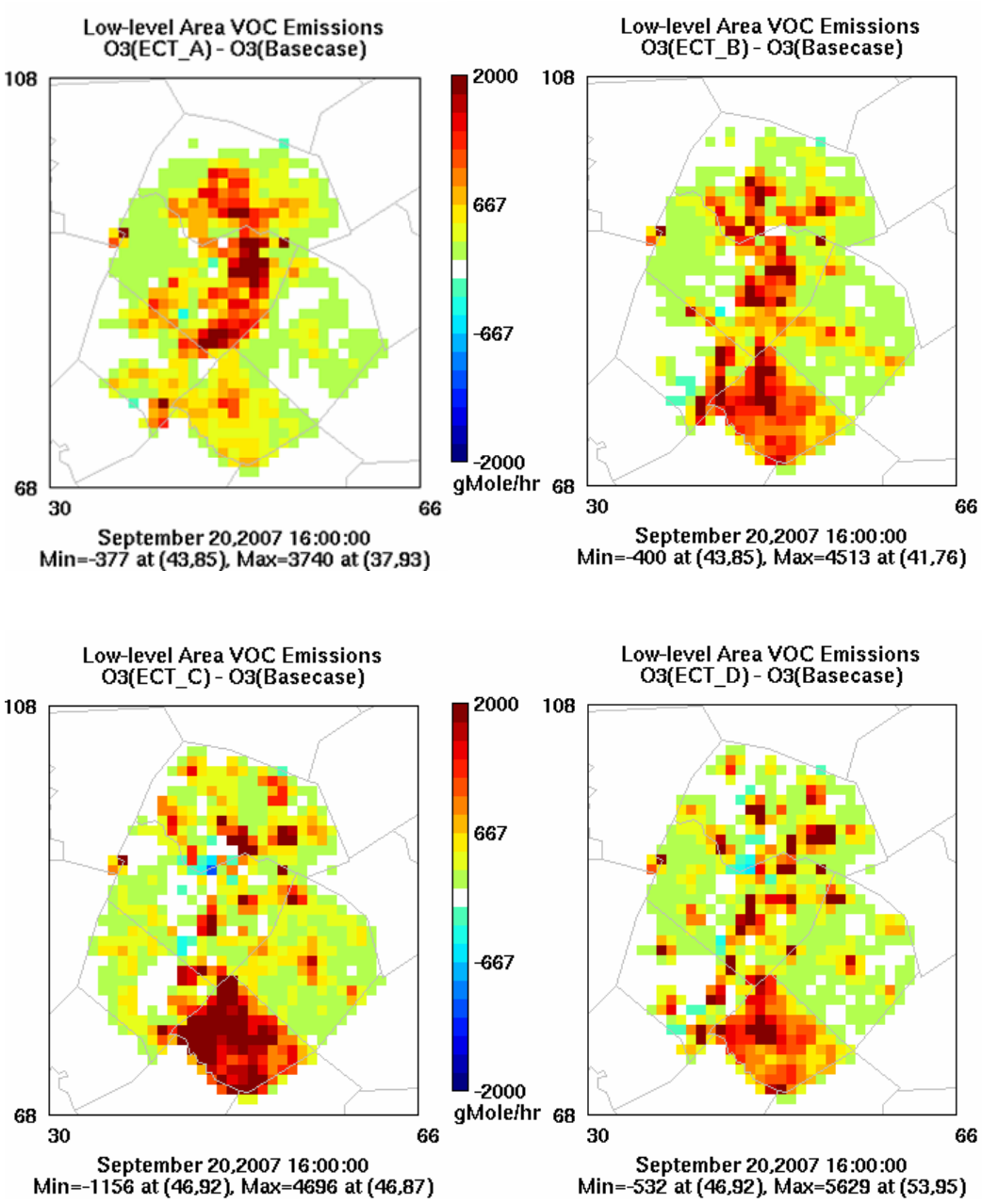

Figure D-5. Difference in VOC Emissions from area sources between the ECT Scenarios and the Base Case at 1600

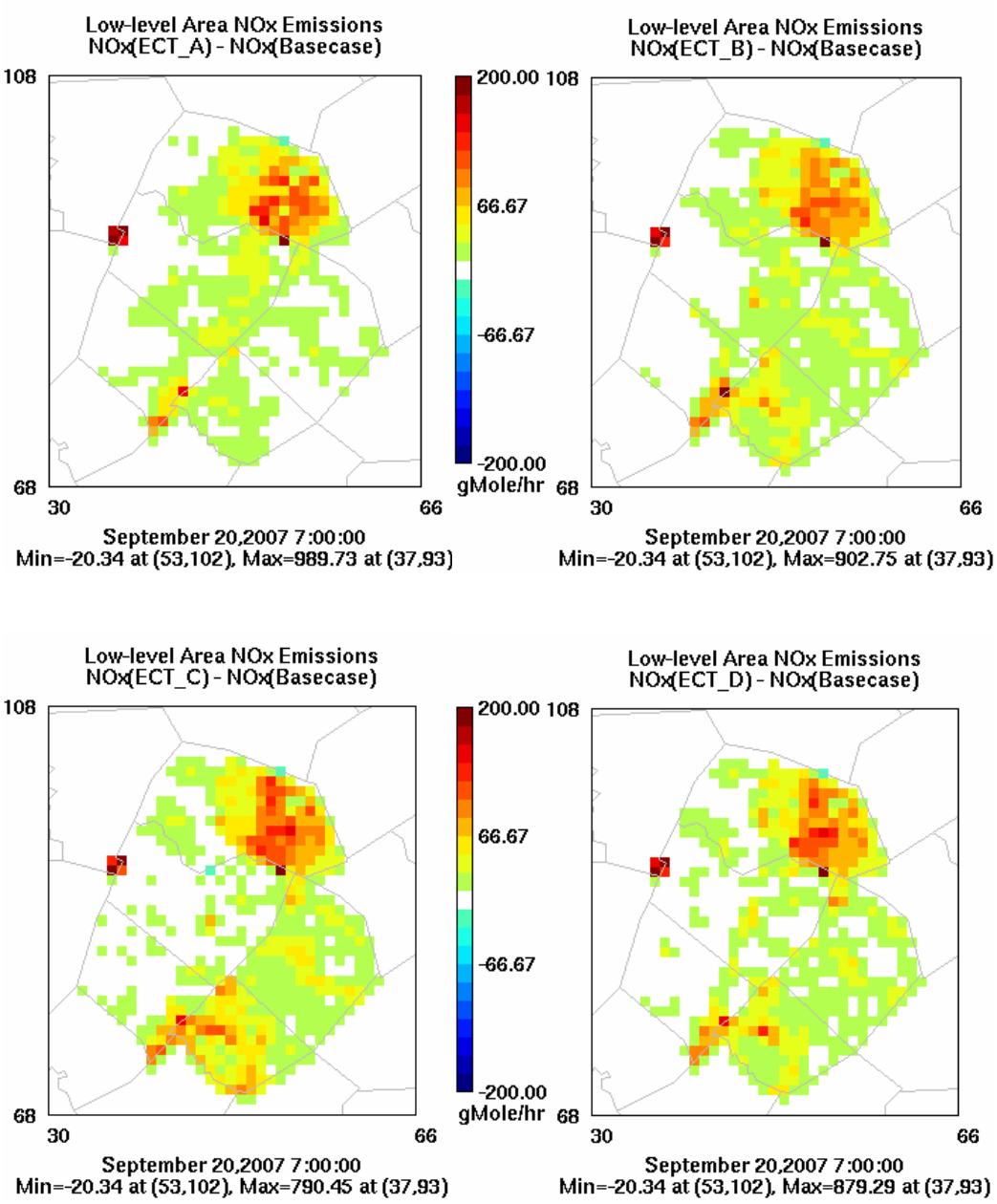

Figure D-6. Difference in VOC Emissions from area sources between the ECT Scenarios and the Base Case at 0700

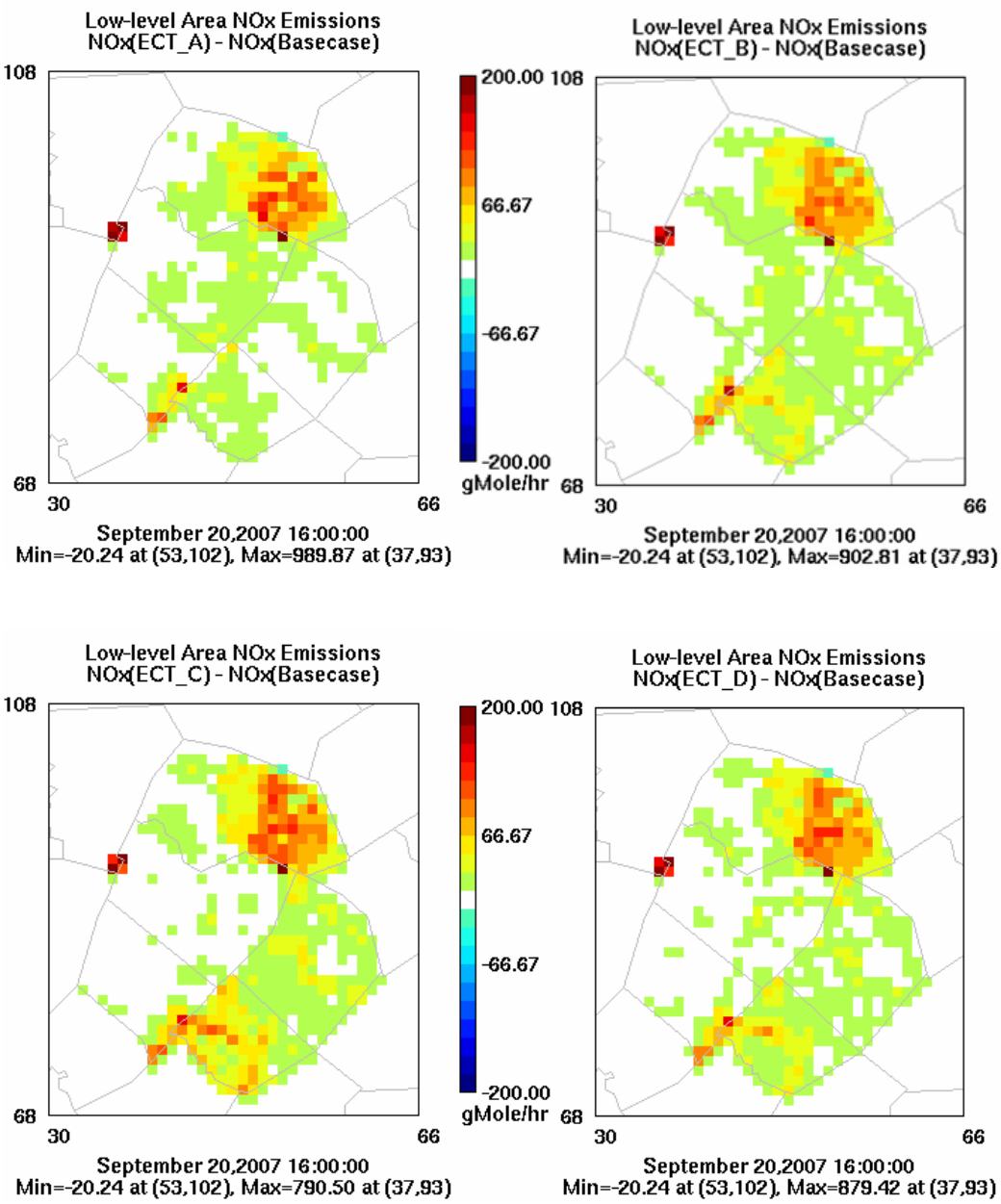

Figure D-7. Difference in VOC Emissions from area sources between the ECT Scenarios and the Base Case at 1600

Appendix E: Method to estimate the absolute departure from the monthly and yearly mean BVOC

(This method is referenced from Gulden *et al.*, 2007)

The absolute departure from the monthly mean BVOC flux is calculated as:

$$d_{y,m} = \left| \frac{BVOC_{y,m} - \overline{BVOC_m}}{\overline{BVOC_m}} \right|$$

where $\overline{BVOC_m}$ is the monthly average BVOC flux: $\overline{BVOC_m} = \frac{\sum_{y=1985}^{2004} BVOC_{y,m}}{(2004-1985+1)}$, and $BVOC_{y,m}$ is the BVOC flux for month *m* of year *y*. The average absolute departure from the monthly mean BVOC flux is then calculated by averaging $d_{y,m}$ values for each month during past 20 years.

The absolute departure from the yearly mean BVOC flux is calculated as:

$$d_y = \left| \frac{BVOC_y - \overline{BVOC_y}}{\overline{BVOC_y}} \right|$$

where $\overline{BVOC_y}$ is the yearly average BVOC flux: $\overline{BVOC_y} = \frac{\sum_{y=1985}^{2004} BVOC_y}{(2004-1985+1)}$, and $BVOC_y$ is the BVOC flux for year *y*. The average absolute departure from the yearly mean BVOC flux is then calculated by averaging d_y values for each year during past 20 years.

Bibliography

Alexandrov, V., Eitzinger, J., Cajic, V., Oberforster, M. (2002) "Potential impact of climate change on selected agricultural crops in north-eastern Austria." *Global Change Biology* **8**(4), 372-389.

Benjamin, M.T., Sudol, M., Bloch, L., Winer, A.M. (1996) "Low-emitting urban forests: A taxonomic methodology for assigning Isoprene and Monoterpene emission rates." *Atmospheric Environment* **30**(9), 1437-1452.

Betts, A.K., Ball, J.H. (1997) "Albedo over the boreal forest." *Journal of Geophysical Research-Atmospheres* **102**(D24), 28901-28909.

Betts, R.A. (2000) "Offset of the potential carbon sink from boreal forestation by decreases in surface albedo." *Nature* **408**(6809), 187-190.

Bonan, G.B., Oleson, K.W., Vertenstein, M., Levis, S., Zeng, X.B., Dai, Y.J., Dickinson, R.E., Yang, Z.L. (2002) "The land surface climatology of the community land model coupled to the NCAR community climate model." *Journal of Climate* 15(22), 3123-3149.

Brasseur, G., Kiehl, J.T., Muller, J.F., Schneider, T., Gramier, C., Tie, X., Hauglustaine, D. (1998) "Past and future changes in global tropospheric ozone: Impact on radiative forcing." *Geophysical Research Letters* **24**, 3807-3810.

CAMPO. Mobility 2030 Plan, February 2005.

Chang, C.C. (2002) "The potential impact of climate change on Taiwan's agriculture." *Agricultural Economics* **27**(1), 51-64.

City of Austin. "Air Emissions Inventory, Austin-Bergstrom International Airport." Prepared by Department of Aviation, 2716 Spirit of Texas Drive, Austin, TX 78719, (512) 530-6510, August, 2002.

Constable, J.V.H., Guenther, A.B., Schimel, D.S., Monson, R.K. (1999) "Modelling changes in VOC emission in response to climate change in the continental United States." *Global Change Biology* **5**, 791-806.

Cox, P.M., Betts, R.A., Jones, C.D., Spall, S.A., Totterdell, I.J. (2000) "Acceleration of global warming due to carbon-cycle feedbacks in a coupled climate model." *Nature* **408**(6809), 184-187.

Culf, A.D., Fisch, G., Hodnett, M.G. (1995) "The albedo of Amazonian forest and ranch land." *Journal of Climate* **8**, 1544-1554.

ENVIRON International Corporation "Users guide to the Comprehensive Air Quality. Model with Extensions (CAMx) version 4.03." Available at http://www.camx.com, 2005.

ENVIRON. "Final Report: Emissions Processing for the Joint CAMx Photochemical Modeling of Four Southern Texas Near Non-Attainment Areas." August 2002. 101 Rowland Way, Suite 220, Novato, CA.

Envision Central Texas Briefing Packet, July 2003. Available at www.envisioncentraltexas.org.

EPA, "Regulatory Announcement: Final Emissions Standards for Locomotives." EPA420-F-97-048, December 1997. Available at http://www.epa.gov/otaq/regs/nonroad/locomotv/frm/42097048.pdf.

EPA, Nonroad Engine and Vehicle Emission Study, EPA-21A-2001, November 1991.

Foster, H.L. (1989) "The influence of soil and climatic factors on groundnut production on alluvial soils in peninsular Malaysia." *Oleagineux* **44**(2), 105-111.

Fuller, D.O., Ottke, C. (2002) "Land cover, rainfall and land-surface albedo in west Africa." *Climate Change* **54**, 181-204.

Gao, F., Schaaf, C.B., Strahler, A.H., Roesch, A., Lucht, W., Dickinson, R. (2005) "MODIS bidirectional reflectance distribution function and albedo Climate Modeling Grid products and the variability of albedo for major global vegetation types." *Journal of Geophysical Research-Atmospheres* **110**(D1): Art. No. D01104.

Genevieve, G. (1995) "The weakening transportation land use connection." Access. No. 6, Spring, pp. 3-11.

Gery, M.W., Whitten, G.Z., Killus, J.P. (1989) "A Photochemical kinetics mechanism for urban and regional scale computer modeling." *Journal of Geophysical Research* **94**(12) 925-12, 956.

Giambelluca, T.W., Holscher, D., Bastos, T.X., Frazao, R.R., Nullet, M.A., Ziegler, A.D. (1997) "Observations of albedo and radiation balance over postforest land surfaces in the eastern Amazon Basin." *Journal of Climate* **10**, 919-928.

Grewe, V., Dameris, M., Hein, R., Sausen, R., Steil, B. (2001) "Future changes of the atmospheric composition and the impact of climate change." *Tellus Series B-Chemical and Physical Meteorology* **53**(2), 103-121.

Guenther, A. B., Zimmerman, P. R., Harley, P. C., Monson, R. K., Fall, R. (1993) "Isoprene and monoterpene emission rate variability: Model evaluations and sensitivity analyses." *Journal of Geophysical Research* **98**(D7), 12609-12617.

Guenther, A., Archer, S., Greenberg, J., Harley, P., Helmig, D., Klinger, L., Vierling, L., Wildermuth, M., Zimmerman, P., Zitzer, S. (1999) "Biogenic hydrocarbon emissions and landcover/climate change in a subtropical savanna." *Physics and Chemistry of the Earth Part B-Hydrology Oceans and Atmosphere* **24**(6), 659-667.

Guenther, A., Hewitt, C.N., Erickson, D., Fall, R., Geron, C., Graedel, T., Harley, P., Klinger, L., Lerdau, M., Mckay, W.A., Pierce, T., Scholes, B., Steinbrecher, R., Tallamraju, R., Taylor, J., Zimmerman, P. (1995) "A global-model of natural volatile organic-compound emissions." *Journal of Geophysical Research-Atmospheres* **100**(D5), 8873-8892.

Gulden, L.E., Yang, Z.L. (2006) "Development of species-based, regional emission capacities for simulation of biogenic volatile organic compound emissions in land-surface models: An example from Texas, USA." *Atmospheric Environment* **40**, 1464-1479.

Gulden, L.E., Yang, Z.L. Niu, G-.Y. (2007) "Interannual variation in biogenic emissions on a regional scale." Submitted to *Journal of Geophysical Research-Atmospheres* in 2006.

Henderson-Sellers, A., Wilson, M.F. (1983) "Surface albedo data for climatic modeling." *Reviews of Geophysics* **21**(8), 1743-1778.

Hogrefe, C., Lynn, B., Civerolo, K., Ku, J.-Y., Rosenthal, J., Rosenzweig, C., Goldberg, R., Gaffin, S., Knowlton, K., Kinney, P.L. (2004) "Simulating changes in regional air pollution over the eastern United States due to changes in global and regional climate and emissions." *Journal of Geophysical Research* **109**: Art. No. D22301.

Johnson, C.E., Collins, W.J., Stevenson, D.S., Derwent, R.G. (1999) "Relative roles of climate and emissions changes on future tropospheric oxidant concentrations." *Journal of Geophysical Research* **104**(D15), 18631-18645.

Kane, S., Reilly, J., Tobey, J. (1992) "An empirical-study of the economic-effects of climate change on world agriculture." *Climatic Change* **21**(1), 17-35.

Knowlton, K., Rosenthal., J.E., Hogrefe, C., Lynn, B., Gaffin, S., Goldberg, R., Rosenzweig, C., Civerolo, K., Ku, J.Y., Kinney, P.L. (2004) "Assessing ozone-related health impacts under a changing climate." *Environmental Health Perspectives* **112**(15), 1557-1563.

Kucharik, C.J., Foley, J.A., Delire, C., Fisher, V.A., Coe, M.T., Lenters, J.D., Young-Molling, C., Ramankutty, N., Norman, J.M., Gower, S.T. (2000) "Testing the performance of a dynamic global ecosystem model: Water balance, carbon balance, and vegetation structure." *Global Biogeochemical Cycles* **14**, 795-825.

Leung, L.R., Gustafson, W.I. (2005) "Potential regional climate change and implications to U.S. air quality." *Geophysical Research Letters* **32**: Art. No. L16711.

Levis, S., Wiedinmyer, C., Bonan, G.B., Guenther, A. (2003) "Simulating biogenic volatile organic compound emissions in the Community Climate System Model." *Journal of Geophysical Research* **108**(D21), 4659.

Matthews, H.D., Weaver, A.J., Meissner, K.J., Gillett, N.P., Eby, M. (2004) "Natural and anthropogenic climate change: incorporating historical land cover change, vegetation dynamics and the global carbon cycle." *Climate Dynamics* **22**(5), 461-479.

McDonald-Buller, E., Eusebi, A., Russel, M., Quigley, C., Hill, A., Allen, D. "Impacts of regional control strategies on air quality in eastern and central Texas." The Texas Natural Resources Conservation Commission Contract No. 988077600. 12100 Park 35 Circle, Austin, TX, 1999.

McDonald-Buller, E., Wiedinmyer, C., Kimura, Y., Allen, D. (2001) "Effects of land use data on dry deposition in a regional photochemical model for eastern Texas." *Journal of the Air and Waste Management Association* **51**(8), 1211-1218.

McDonald-Buller, E.C., Allen, D.T., Kockelman, K., Parmenter, B. (2005) "2005 Progress Report: Predicting the relative impacts of urban development policies and on-road vehicle technologies on air quality in the United States: Modeling and analysis of a case study in Austin, Texas." Submitted to EPA in 2005. Available at http://cfpub.epa.gov/ncer_abstracts/index.cfm/fuseaction/display.abstractDetail/abstract/7425/report/2005.

Mickley, L.J., Jacob, D.J., Field, B.D., Rind, D. (2004) "Effects of future climate change on regional air pollution episodes in the United States." *Geophysical Research Letters* **31**(24): Art. No. L24103.

Mika, J., Horvath, S., Makra, L. (2001) "Impact of documented land use changes on the surface albedo and evapotranspiration in a plain watershed." *Physics and chemistry of the Earth B-Hydrology Oceans and Atmosphere* **26**(7-8), 601-606.

Murazaki, K., Hess, P. (2006) "How does climate change contribute to surface ozone change over the United States." *Journal of Geophysical Research* **111**(D5): Art. No. D05301.

Myhre, G., Myhre, A. (2003) "Uncertainties in radiative forcing due to surface albedo changes caused by land-use changes." *Journal of Climate* **16**, 1511-1524.

Natural Resources Inventory (1997) "Land uses converted to developed land, 1987-1997." Available at http://www.nrcs.usda.gov/technical/land/meta/m5909 .html.

Olesen, J.E., Bindi, M. (2002) "Consequences of climate change for europe agricultural productivity, land use and policy." *European Journal of Agronomy* **16**(4), 239-262.

Oleson, K.W., Bonan, G.B., Levis, S., Vertenstein, M. (2004) "Effects of land use change on North American climate: impact of surface datasets and model biogeophysics." *Climate Dynamics* **23**(2), 117-132.

Parmenter, B., Kim, J.O. (2005) Personal communication.

Parry, M.L. (2000) "Assessment of potential effects and adaptations for climate change in Europe." In: M.L. Parry, Editor, The Europe ACACIA Project, Jackson Environment Institute, University of East Anglia, Norwich, UK.

Purves, D.W., Caspersen, J.P., Moorcroft, P.R., Hurtt, G.C., Pacala, S.W. (2004) "Human-induced changes in US biogenic volatile organic compound emissions: evidence from long-term forest inventory data." *Global Change Biology* **10**(10), 1737-1755.

Sanderson, M.G., Jones, C.D., Collins, W.J., Johnson, C.E., Derwent, R.G. (2003) "Effect of climate change on isoprene emissions and surface ozone levels." *Geophysical Research letters* **30**(18): Art. No. 1936.

Shallcross, D.E., Monks, P.S. (2000) "New directions: A role for isoprene in biosphere-climate-chemistry feedbacks." *Atmospheric Environment* **34**(10), 1659-1660.

Smart Mobility Inc. (SMI). "Envision Central Texas Transportation Model: Technical Documentation." July 2003.

Song, J., Parmenter, B., McDonald-Buller, E., Allen, D.T. (2006) "Impacts of urbanization on biogenic emissions and air pollutant deposition." In preparation of submission to *Environmental Science and Technology*.

Stevenson, D., Doherty, R., Sanderson, M., Johnson, C., Collins, B., Derwent, D. (2005) "Impacts of climate change and variability on tropospheric ozone and its precursors." *Faraday Discussion* **130**, 41-57.

Texas Commission on Environmental Quality (TCEQ). "Austin area early action compact ozone state implementation plan revision." November 2004. Available at http://www.capcog.org/CAPCOairquality/Documents/EAC_Documents/AUS_narr_181104.pdf.

Texas Commission on Environmental Quality (TCEQ). Houston/Galveston Air Quality Science Evaluation. Air Quality Modeling Files. CAMx Modeling Files. Files last updated December 2003. Available at http://www.tceq.state.tx.us.

The Capital Area Planning Council (CAPCO) "Austin/Round Rock MSA Emissions Reductions Strategies." Technical Report on behalf of The Austin-Round Rock MSA Clean Air Coalition, March 2004. Available at http://www.capcog.org/CAPCOairquality/CAAP_Apps/App5-2Austin-RR%20Emission%20Reduction%20Strategies.pdf.

The Capital Area Planning Council (CAPCO) "Austin-Round Rock MSA 1999 Ozone Precursor Emissions Inventory." March 2004. Available at http://www.tceq.state.tx.us/assets/public/implementation /air/sip/sipdocs/2004-06-AUS/04086sipapd_pro.pdf.

The Capital Area Planning Council (CAPCO). "2007 Future Year Ozone Precursor Modeling Emissions Inventory." Technical Report on behalf of the Austin-Round Rock MSA Clean Air Coalition, March 2004. Available at http://www.tceq.state.tx.us/assets/public/implementation /air/sip/sipdocs/2004-06-AUS/04086sipape_pro.pdf

The Capital Area Planning Council (CAPCO). "Photochemical modeling for Austin's Early Action Compact: Analysis of emission control strategies for ozone precursor." Submitted to U.S. EPA and TCEQ in March 2004a. Available at http://www.capco.state.tx.us/CAPCOairquality/Documents/eac_basecase_milestone_controlstrategy_03252004.pdf

Theurillat, J.P., Guisan, A. (2001) "Potential impact of climate change on vegetation in the European Alps: A review." *Climatic Change* **50**(1-2), 77-109.

U.S. EPA. "User's Guide to MOBILE6.1 and MOBILE6.2: Mobile Source Emission Factor Model." August 2003.

University of Texas at Austin. "Development of the September 13-20, 1999 Base Case Photochemical Model for Austin's Early Action Compact." Submitted to the Texas Commission on Environmental Quality and the U.S. Environmental Protection Agency on behalf of the Capital Area Planning Council, March 2004a.

University of Texas at Austin. "Photochemical Modeling for Austin's Early Action Compact: Development of the September 13-20, 1999 Photochemical Model with 2007 Projected Emissions and Analysis of Future 8-Hour Ozone Design Values." Submitted to the Texas Commission on Environmental Quality and the U.S. Environmental Protection Agency on behalf of the Capital Area Planning Council, March 2004b.

Vizuete, W., Junquera, V., McDonald-Buller, E., McGaughey, G., Yarwood, G., Allen, D. (2002) "Effects of temperature and land use on predictions of biogenic emissions in Eastern Texas, USA." *Atmospheric Environment* **36**(20), 3321-3337.

Walmsley, J.L., Wesely, M.L. (1996) "Modification of coded parametrizations of surface resistances to gaseous dry deposition." *Atmospheric Environment* **30**(7), 1181-1188.

Wesely, M.L. (1989) "Parameterization of surface resistances to gaseous dry deposition in regional-scale numerical-models." *Atmospheric Environment* **23**(6), 1293-1304.

Wiedinmyer, C., Guenther, A., Estes, M., Strange, I. W., Yarwood, G., Allen, D. T. (2001) "A land use database and examples of biogenic isoprene emission estimates for the state of Texas, USA." *Atmospheric Environment* **35**(36), 6465-6477.

Wiedinmyer, C., Guenther, A., Estes, M., Strange, I. W., Yarwood, G., Allen, D. T. (2001) "A land use database and examples of biogenic isoprene emission estimates for the state of Texas, USA." *Atmospheric Environment* 35(36), 6465-6477.

Wiedinmyer, C., Strange, I.W., Estes, M., Yarwood, G., Allen, D.T. (2000) "Biogenic hydrocarbon emission estimates for north central Texas." *Atmospheric Environment* **34**(20), 3419-3435.

Yarwood, G., Wilson, G., Emery, C., Guenther, A. "Development of the GloBEIS – A state of the science biogenics emissions modeling system." Final Report to the Texas Natural Resource Conservation Commission, 12100 Park 35 Circle, Austin, Texas 78753, 1999b.

Yarwood, G., Wilson, G., Shepard, S., Guenther, A. "User's guide to the Global Biosphere Emissions and Interactions System – Version 3.1." 101 Rowland Way, Suite 220, Novato, California. Available at http://www.globeis.com, 1999a.

Vita

Ji Hee Song was born in Seoul, Korea on February 2, 1980. She is the daughter of Jae Chul Song and Hyun Jeong Park-Song. After completing her work at Jinmyong High School, Seoul, Korea, in 1998, she entered Ewha Womans University in Seoul, Korea. She earned a Bachelor of Engineering in Environmental Engineering from Ewha Womans University in 2002. In September 2002, she started graduate school at the University of Texas at Austin. While in graduate school, she worked as a Graduate Research Assistant. She received a Master's of Science in Civil, Architectural, and Environmental Engineering from the University of Texas at Austin in 2004. Ji Hee started the Ph.D program in Civil, Architectural, and Environmental Engineering at the University of Texas at Austin in 2004.

Permanent address: Ramian Tower 201-601
Bangbae 3 Dong, Seo Cho Ku
Seoul, Republic of Korea

This dissertation was typed by the author.